École Polytechnique Fédérale de Lausanne

Master Thesis report

-

Optimization of the environmental impact of beams

Student: Noémie RIEZ

Academic Supervisors: Pr. Corentin FIVET & Dr. Xavier ESTRELLA

Company Supervisors: Dr. Sébastien MAITENAZ & Nicolas METGE

Acknowledgements

I would like first to thank the ISC team that welcomed me so warmly and more specifically the Conception department which integrated me and made sure my internship went smoothly.

In particular, I would like to thank Nicolas METGE for integrating me into his design office and for the close monitoring of my internship, Paul ONFROY, and Riyadh BENOSMAN for their warm welcome and their precious help on technical subjects. I would like also to thank Sébastien MAITENAZ for his daily follow-up and for the very interesting discussions on LCA, optimization, interpretation of the Eurocode 2, and so on.

Finally, I would like to thank the EPFL team who has mentored me for almost one and a half years now with one semester project, a pre-study, and the master thesis: in particular Pr. Corentin FIVET that accepted to work with me in the first place for a project on LCA calculations for an organic waste recycling center, and then on this subject of beam optimization, but also Dr. Xavier ESTRELLA for his precious help and availability during all these projects, and Dr. Jonas WARMUTH for his help on the master thesis optimization issues.

Abstract

In the European Union, building construction accounts for 40% of materials consumption, 40% of overall energy consumption, and 40% of waste production [1]. It is therefore essential to reduce the environmental impact of these structures. Various levers are available to achieve this, including better use of materials and selection of the most appropriate material for a given application.
This study focuses on isostatic beams, a simple application for identifying trends in shapes and materials to reduce their impact. By using a genetic algorithm to optimize the environmental impact of each beam typology (rectangular reinforced concrete, I-beams, or optimized, prestressed, steel and timber beams), and comparing them with one another, it was possible to select the most appropriate for a given scenario (use in a building, a bridge, most favorable and most unfavorable life-cycle analysis scenarios).
The study emphasized the fact that beams with a small width perform better environmentally and that the optimized reinforced concrete beams have great potential in reducing the environmental impact, especially for short spans.

Key-words: LCA, Optimization, reinforced concrete beam, prestressed beam, timber beam, steel beam

Résumé

Dans l'Union européenne, la construction de bâtiments représente 40% de la consommation de matériaux, 40% de la consommation globale d'énergie et 40% de la production de déchets [1]. Il est donc essentiel de réduire l'impact environnemental de ces structures. Différents leviers sont disponibles pour y parvenir, notamment une meilleure utilisation des matériaux et la sélection du matériau le plus approprié pour une application donnée.
Cette étude se concentre sur les poutres isostatiques, une application simple permettant d'identifier les leviers en matière de formes et de matériaux permettant de réduire leur impact. En utilisant un algorithme génétique pour optimiser l'impact environnemental de chaque typologie de poutre (poutre rectangulaire en béton armé, poutre en I, ou poutre optimisée, précontrainte, en acier et en bois), et en les comparant les unes aux autres, il a été possible de sélectionner la plus appropriée pour un scénario donné (utilisation dans un bâtiment, un pont, scénarios d'analyse du cycle de vie les plus favorables et les plus défavorables).
L'étude a mis en évidence le fait que les poutres avec une petite largeur sont plus performantes sur le plan environnemental et que les poutres optimisées en béton armé ont un grand potentiel dans la réduction de l'impact environnemental, en particulier pour les courtes portées.

Mots clés : ACV, optimisation, poutre en béton armé, poutre précontrainte, poutre en bois, poutre en acier

Contents

1 Problem statement

1.1 Challenges faced by the construction industry

In the European Union, building construction represents 40% of material consumption, 40 % of global energy consumption, and 40% of waste production [1]. Furthermore, among those constructions, a large majority is made out of concrete, whose main ingredient, cement, contributes to 5% of global anthropogenic CO_2 emissions [2]. There is, therefore, a strong interest in reducing emissions from the construction sector at all stages: reducing the amount of material forecast at the design stage, using materials with a reduced environmental footprint, reducing the transport distances, using less machinery or machinery with a low footprint, increasing the lifetime of the construction, decreasing the emissions related to the period of use of the construction, reducing the amount of waste, increasing their recycling rate, etc.
For example, the contributions of the different life stages for a reinforced concrete structure are represented in Figure 1. The study from which it is drawn focuses on the stages in the life of buildings that account for the greatest proportion of carbon emissions, in order to identify levers for action.

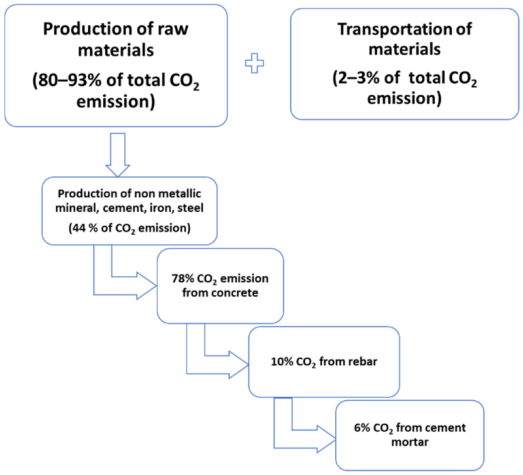

Figure 1: CO_2 emission from different phases in the construction industry [1]

1.2 Reducing the embodied footprint of constructions

Among the levers presented before, one is at stake in this study: the better use of materials at the design stage, i.e., using materials at their best not to oversize structural elements, thus reducing the global footprint of the structure.

By reducing the amount of each of the materials, the emissions associated with their production will also be reduced, as well as those associated with their transportation and likely on-site construction emissions. Furthermore, research has shown that buildings are often oversized: 50% wastage is common [3]. Figure 2 shows the increasing importance of the embodied emissions (the ones related to the construction and materials manufacturing) compared to the operational emissions (related to the use of the building). It shows that much has been done in recent years to reduce operational emissions through more efficient buildings. In the coming years, embodied emissions are the ones that will have to be reduced heavily to reduce the global impact of buildings. This is why it is important to focus on these specific emissions. Furthermore, for civil engineering works, when considering the total footprint of the construction during all its life stages, the construction phase is the most impacting phase [4][5].

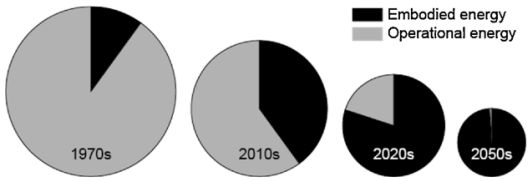

Figure 2: Increasing part of the embodied emissions for buildings (approximate data for UK built environment) [3]

Besides, the over-design of constructions (above standard values) has been proved by a study to be a real challenge to overcome since there is little demand from the client or design team to reduce embodied energy (according to 70% of a panel of engineers [3]). The cost of the structures is currently what matters the most in terms of design. But new standards arise regarding the environmental impact of buildings such as the RE2020 in France. Thus, it will become more and more important to assess and reduce the environmental impact of construction so as to meet standards. There is therefore a real interest in providing simple tools to help engineers reduce the environmental impact of their structures without losing too much time and money.

1.3 Literature review

To reduce the environmental impact of structural elements such as beams, slabs, floors, etc. two main strategies, that can be combined, have been developed. For a given use case it is possible to compare typologies and materials. It is also possible to optimize the shape, the amount of each material for composite structures, and the material mechanical properties when the typology and materials used are set.

Comparing typologies and materials A. Zeitz et al. [6] compared the impact of parking structural systems made of steel, concrete, and mass timber to assess the potential of timber to reduce the carbon footprint. Their work demonstrated that considering the best-case scenario for concrete structures, timber structures lose their advantages in terms of environmental impact. Thus, for each type of application, it is useful to compare typologies and materials with best-case and worst-case scenarios, because the results might not be the ones that are expected.

Paik and Na [7] compared different structural systems for slabs: OSS (Ordinary Slab System), FPS (Flate Plate Slab), and VDS (Voided Slab System), all three being made out of reinforced concrete. For all environmental indicators studied, they demonstrated a gain in environmental impact shifting from OSS to FPS and from FPS to VDS. Even considering a single type of material, comparing different typologies can lead to significant reductions in the global environmental impact of the structural system.

Optimizing the geometry For a given type of material and typology, it is possible to change the geometric properties of the structural system in order to find the one resulting in the least environmental impact.

Similarly, Marti et al. [8] developed a tool using a heuristic algorithm able to find the optimal shape, reinforcement, and concrete type in terms of environmental impact for precast prestressed concrete U-beam road bridges. The cost was also a criterion in the analysis. They proved that their cost-optimal and environmental-optimal designs were close to one another. Furthermore, they revealed that a reduction of one euro can save up to 4 kWh in embodied energy.

J. Fernandez-Ceniceros et al. [9] conducted a similar approach for one-way slabs in Spain. They took as input the span length, the loads applied on the slab, and its area. What was determined afterward was the optimum in terms of costs and embodied carbon by giving a combination of slab thickness, filling blocks, and type of concrete used.

B. Kwan Oh et al. [10] produced a multi-objective algorithm capable to optimize environmental impact but also cost, and vibration responses for two-way slabs in buildings. They achieved a reduction in CO_2 emissions up to 4.94%, 11.40%, and 19.96% for residential, office, and commercial buildings respectively.

S. Maitenaz [11] developed a certain typology for reinforced concrete beams. The objective is to save mass where it is not used (creating voids outside of struts and ties). It leads to a significant decrease in the environmental impact (up to 30%) only by removing matter where it does not contribute to the overall resistance of the beam.

Yeo and Gabbai [12] considered a simple rectangular reinforced concrete beam with fixed bending and shear strengths. They considered both cost and embodied energy and proved that by optimizing the shape of the beam, savings of up to 10% in embodied energy and up to 5% in cost can be achieved.

Habert and Roussel [13] proved the interest in using low-carbon concrete combined with a reduction of the amount of concrete used by considering high-resistance concrete. In France, the potential for CO_2 emissions reduction using this strategy is up to 30%.

Using both strategies at the same time It is also possible to compare, at the same time, material and typology while for each optimizing the shape of the structural member.

Miller et al. [14] compared different slab systems while varying other parameters such as concrete strength, column-to-column spacing, material properties, and geometric parameters. They demonstrated that the use of post-tensioned construction methods could lead to reductions in embodied emissions between 23.7% and 49.1%.

R. Rempling et al. [15] study is presenting the optimization of embodied carbon for bridges using Set-Based Parametric Design. They considered three types of single-span bridges: concrete-beam bridges, steel-concrete bridges with integral abutments, and concrete frame bridges. They developed a script that produces, for each type of bridge, several alternatives for a certain load and span. They demonstrated that for the three different typologies studied, the savings in CO_2 equivalent emissions go from 20 to 60%.

1.4 Room for innovation

From the literature, it can be seen that there is great potential in reducing the embodied emissions of structural systems such as slabs, beams, and parking structures. Both strategies of comparing materials, and typologies and optimizing the shape of the element studied lead to significant savings. Still, doing both at the same time was less explored and can lead to even higher savings. This study develops this strategy for the use case of beams that can be used either for buildings or for bridges.
In this study, different materials and typologies (precast beams prestressed by adhesion, reinforced concrete rectangular beams, reinforced concrete I-beams, reinforced concrete beams optimized with the strut optimization method (SOM) [11], rectangular timber beams, and steel I-beams) are studied. For each, a shape optimization is performed based on SLS and ULS design checks from the Eurocodes.

2 The Life Cycle Assessment Methodology

2.1 What is LCA ?

Life Cycle Assessment (LCA) is a methodology widely used to assess the environmental impact of products, processes, or services. It enables the comparison of different solutions and identifies action levers to reduce the impact of a given product or process [16]. It is framed by standards such as ISO 14040 and ISO 14044. It is composed of different phases (Figure 3):

- Goal and scope definition
  In this phase, the functional unit is defined. It refers to the object of the study (ex: 1 kg of cement). The study's goal and scope are also set. The scope defines the study's limits: what is considered in the calculations and what is not. For example, the "cradle to gate" approach does not take into account the lifetime and the end of life of a product, contrary to the "cradle to grave" approach that takes into account all steps from the early stages to the end of life.

- Inventory analysis
  Once the previous step has delimited the analysis, it is needed to list all inputs and outputs of the system and identify the different processes that will be used to model the process or product considered;

- Impact assessment
  Several software programs offer the possibility to perform impact assessment calculations. Among them, OpenLCA is an open-source program that performs LCA based on any database that can be added to it (such as KBOB, Ökobaudat, and Ecoinvent). This software has been used for this study to perform LCA calculations of various processes and products.

- Interpretation
  At each step presented above, it is mandatory to interpret and discuss the assumptions, and results. For example, when the source of some data or a quantity used within the global framework is not reliable, it can be useful to proceed to a sensitivity analysis. It can be done by changing the value of the data in the global framework and analyzing the impact of this change in the final results.

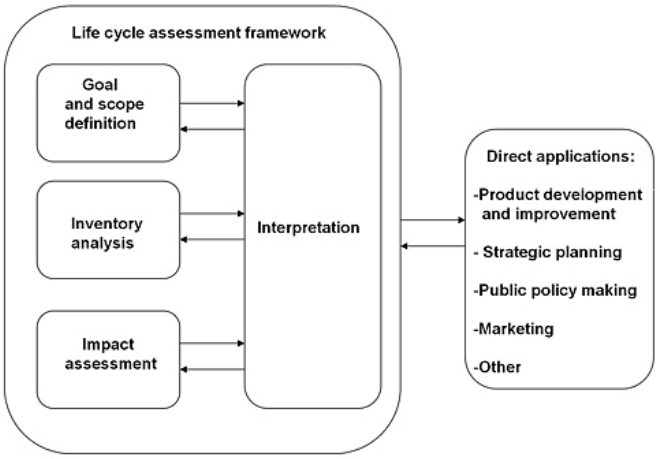

Figure 3: LCA phases according to ISO 14040:2006 [17]

The standard EN 15804 sets the rules for assessing the LCA of buildings and construction products when realizing what is called an EPD (Environmental Product Declaration). These declarations aim to provide information on the environmental impact of construction products for decision-makers when building new constructions [18].

The scope is divided into different stages referring to the life stages of the product (Figure 4).

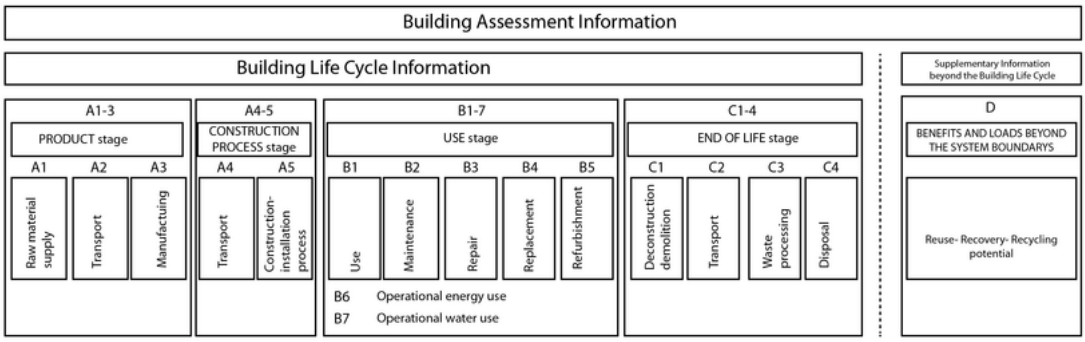

Figure 4: Scope of the EN15804 LCA Analysis for buildings [19]

Most of the LCAs in France in the construction domain are assessed using this framework. Even though Figure 4 stands for buildings, the parallel can be drawn for construction elements such as beams. The stages B1, B3, B4, B5, B6, and B7 are not relevant for this study as beams are designed for a longer or equal period of time than the building itself, and operational energy and water use are not relevant for a single beam. Within this study, the phases that will be assessed are the ones from A1 to A5 (Raw material supply, Transport, Manufacturing, Transport, Construction, and Installation process), B2 only for steel beams as the others do not require maintenance, and C1 to C4. The D part (avoided impacts from the re-use of materials for example) is not included in this study.

2.2 Choice of the database

When conducting an LCA, an important step is to gather information for the Life Cycle Inventory (LCI). This step is facilitated by the existence of LCIs that already contain information for several products and processes. There are mainly two types of databases:

- Generic databases:
  Those databases provide a large amount of data on different products and processes, some being as upstream as mining and as downstream as the construction of buildings. The main advantage of those databases is that they have data for approximately every process or product but as their scope is very large, the data is averaged and does not represent well local specifications.
  The two main generic databases are Ecoinvent and GaBi. Ecoinvent is the most used with more than 18.000 inventories and is the one used in this study.

- Specialized databases:
  On the opposite, specialized databases provide less data but are more regionalized and contextualized. For example in France, the INIES database provides data for some specific products of the construction industry in the form of EPDs [20]. DIOGEN (Données d'impact pour les Ouvrages de Génie Civil) website also provides such data [21]. These databases are very useful when a project is well-defined and the choice of products has already been done.
  At the early design stage, it might be more difficult to know exactly which product will be used and in which quantity, this is why a generic database seems more appropriate for this study. Furthermore, this is not mandatory for EPDs to provide the hypotheses on the processes that have been taken into account, which makes them difficult to use. Nevertheless, these EPDs might be of use when assessing specific products.

For this study, Ecoinvent was mostly used. Three different allocation methods are provided by Ecoinvent [22]:

- Cut-off:
  Waste is the responsibility of the producer, which is why recycled materials are available without burden. Secondary recycled materials bear only the impacts of the recycling process.

- Consequential:
  By-products are counted negatively to the input side to maintain the mass balance.

- APOS (Allocation at the point of substitution):
  The waste burden is shared between the producer of the waste and users benefiting from this waste.

In this study, the cut-off allocation method has been chosen. Thus, wastes are at the expense of the producer of the waste. Since there are many uncertainties about the end-of-life scenarios of the beam, having a cut-off allocation reduces uncertainties of the production stage as recycled materials are available burden-free. Besides, as the point of view of the study is the one of production, the cut-off allocation seems the most appropriate one.

Ecoinvent describes a product or a process using either a unit or system process. The unit process of a given product records every intermediate process and gives an outlook of all processes used to model the process studied. On the other side, the system process proceeds more like a "black box". Only the very upstream inputs can be seen when selecting a downstream process, there is no detail about the intermediate steps of calculation and the processes taken into account. This is why, for this study, the unit process has been considered to have access in Ecoinvent to every intermediate process and to see how the process or product studied was built. Furthermore, what differs between the two is mainly the computation time when conducting analyses in OpenLCA, the unit process being more time-consuming. Still, as the LCA calculations for every elementary process are performed just once, it is not a limitation for this study.

2.3 Choice of the impact assessment method

LCA cannot be narrowed to the calculation of the carbon footprint, it is only one indicator among many others. There exist two types of indicators [18]:

- Midpoint indicators:
  These indicators are the ones directly linked to the emissions of different substances in the environment. They reflect the impact of substance emissions on the environment. These impacts can take the form of various effects such as for example global warming potential, freshwater acidification, human toxicity, mineral resource use, etc. [23].

- Endpoint indicators:
  Endpoint indicators assess the impact at the areas of protection level (Human health, Ecosystem, and Resources). It is calculated via weighting factors for each midpoint indicator. As there are only a few of them, these indicators are mostly used when a difference has to be made between one product or another. It is then useful for decision-makers when a choice needs to be done between alternatives.

The calculations from the release of chemical components to the midpoint indicators and from the midpoint indicators to the endpoint indicators rely on relations and weightings that have been studied in detail. Different relations and models have been proposed by the scientific community over the years. Among these impact assessment methods, the most used and recent ones are Recipe 2016 [24] and IMPACTWorld+ (2019) [25] but many others have been used over the years. IMPACTWorld+ has been chosen for this study as it is the most recent one, thus includes the most advanced models for the analysis of impact pathways, and includes both endpoint and midpoint indicators. The list of the indicators used in this methodology can be seen in Figure 5.

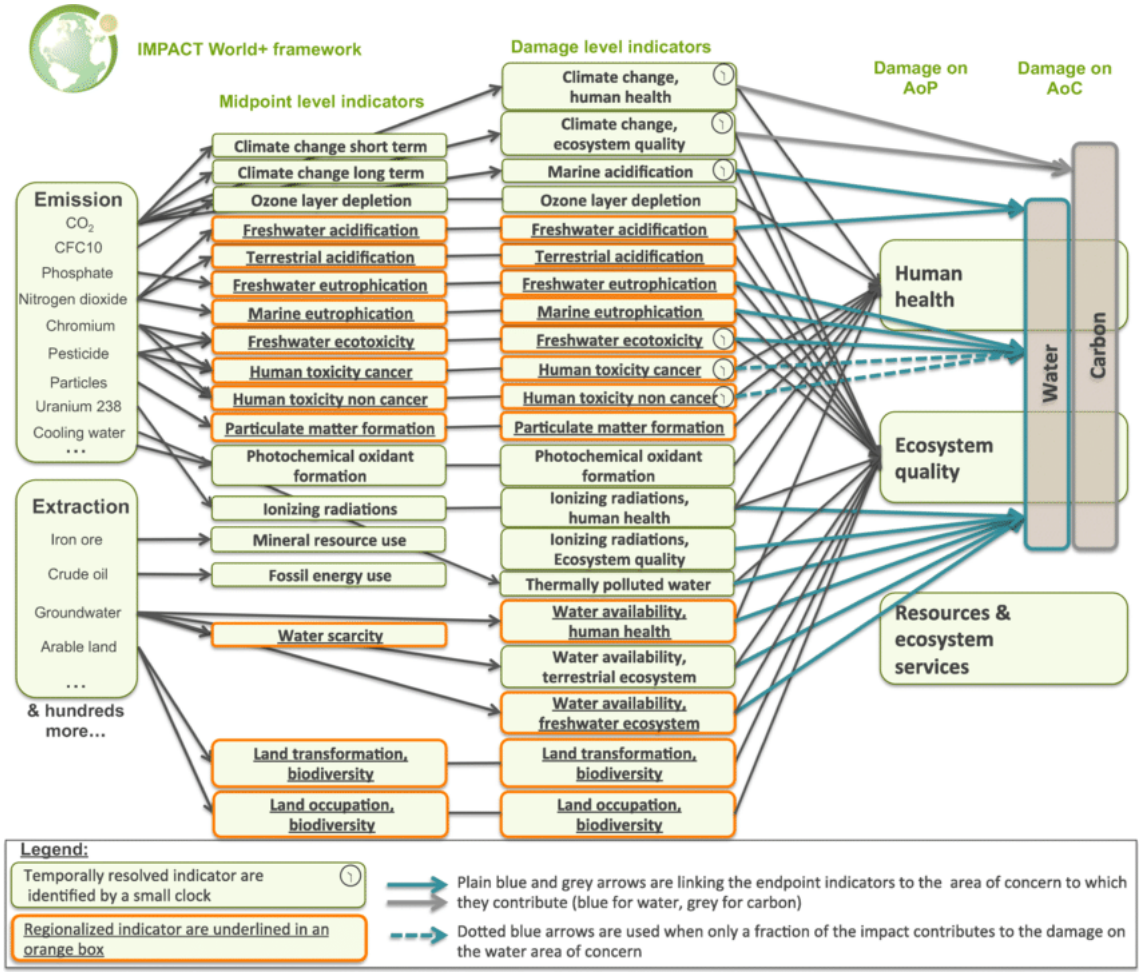

Figure 5: IMPACTWorld+ Framework [25]

Presentation of different midpoint level indicators Among the indicators used within the IW+ methodology, some are of higher interest as will be seen in the coming parts.

- Midpoint indicators
  - Climate change long and short-term ($kgCO_{2,eq}$)
    Climate change is related to the emissions of Green House Gases (GHG), which increase the radiative forcing on Earth and leads to effects such as temperature changes, higher frequency of natural disasters, etc. The midpoint indicators for climate change are separated into two timelines (long and short-term) as defined by the Intergovernmental Panel on Climate Change (IPCC). The long-term indicator corresponds to the Global Temperature Potential for a 100-year time horizon (GTP100) and the short-term indicator to the Global Warming Potential for a 100-year time horizon.

To give an order of magnitude, one m3 of conventional C30/37 concrete used for buildings corresponds to $287 kgCO_{2,eq}$ and $291 kgCO_{2,eq}$ for climate change long- and short-term respectively and one m3 of glue laminated timber to $131 kgCO_{2,eq}$ and $137 kgCO_{2,eq}$.

- Water scarcity ($m^3_{world,eq}$)
  This midpoint indicator reflects, at the endpoint level, the impact that can cause a lack of water on human health and the quality of ecosystems.
  The same concrete corresponds to $102 m^3_{world,eq}/m^3$, and the same timber to $81.91 m^3_{world,eq}/m^3$.
- Freshwater ecotoxicity (CTU_e)
  This indicator expresses the impact on the aquatic environment, for example, caused by the release of chemicals in rivers. The pollution of freshwater can lead to a decrease in biodiversity but can also cause damage to human health. It is expressed in Comparative Toxic Units (CTUe) per unit mass of emitted chemicals.
  The same concrete corresponds to $7.11.10^5 CTU_e/m^3$, and the same timber to $1.27.10^6 CTU_e/m^3$.
- Human toxicity cancer (CTU_h)
  Human health can be affected by the release of toxic components into the air and water that can be either breathed, eaten, or drunk. It is measured in Comparative Toxic Units (CTU_h) per unit mass of chemical emitted, which corresponds to the increase in deaths due to the emissions of chemicals.
  The same concrete corresponds to $6.97.10^{-6} CTU_h/m^3$, and the same timber to $1.59.10^{-5} CTU_h/m^3$.
- Particulate Matter Formation ($kgPM2.5_{eq}$)
  This impact represents the release of fine particles in the environment. Fine particles are those with a diameter of less than 2.5 μm. When breathed, they can lead to respiratory and cardiovascular problems. They mostly come from the combustion of certain materials or fuels.
  The same concrete corresponds to $4.39.10^{-2} kgPM2.5_{eq}/m^3$, and the same timber to $2.37.10^{-1} kgPM2.5_{eq}/m^3$.

- Endpoint indicators

  - Human health ($DALY$=Disability Adjusted Life Years)
    This endpoint indicator stands for the sum of the years of life lost and the years lived with disability. It takes into consideration several midpoint indicators that have an impact on human health (climate change, human toxicity, particulate matter formation, and others) as a weighted sum. The relation that leads to the calculation of the human health indicator is based on scientific research for all the midpoint indicators considered.
    The same concrete corresponds to $1.19 * 10^{-3} DALY/m^3$, and the same timber to $1.04 * 10^{-3} DALY/m^3$.
  - Ecosystem quality ($PDF.m^2.yr$, PDF= Potentially Disappeared Fraction of species)
    The ecosystem quality indicator represents the loss of biodiversity due to several midpoint indicators (freshwater ecotoxicity, climate change, land occupation, etc.). For example, 10 $PDF.m^2.yr$ stands either for:
    -$10 m^2$ has lost all its species in a year's time
    -$100 m^2$ has lost 10% of its species in a year's time
    -$10 m^2$ has lost 10% of its species in 10 year's time
    The same concrete corresponds to $726\, PDF.m^2.yr/m^3$, and the same timber to $899\, PDF.m^2.yr/m^3$.

Among the eighteen indicators provided by the IW+ methodology, only some will be studied, as studying every one of them is complex and irrelevant. The choice of the relevant indicators is based on the methodology proposed by K. Mam in his Ph.D. [26]. The endpoint indicators are calculated via the midpoint indicators via weighting factors. Thus, midpoint indicators do not contribute in the same proportion as endpoint indicators. So, for each endpoint indicator, the contribution of the midpoint indicators has been analyzed to put into light the ones that have the biggest impact with a hurdle at 5%.

2.4 Allocation methods for by-products

When assessing the environmental impact of by-products, the proportion of the impact that goes to one by-product or the other has to be defined. For example, during the production of pig iron, blast furnace slag is also produced. One does not come without the other. Then, it is difficult to know which part of the impact of the production of pig iron goes for the pig iron itself and for the slag.
ISO 14044 [17] recommends a three-step procedure for choosing an appropriate allocation:

- The allocation should be avoided when possible by dividing the process into subprocesses or by expanding the system boundary to include the additional functions of co-products
- Allocation should be done in a way that reflects an underlying causal physical relationship (ex: mass allocation)
- Other relationship (ex: economic allocation)

As it is difficult for many processes such as the production of pig iron to divide the global process into different subprocesses, a choice has to be made to use the appropriate allocation method. Two will be presented in the following paragraphs: the mass and economic allocations.

Mass allocation This allocation splits the environmental impact of the main product and co-products based on the mass proportion of each in the global process.

$$LCI_j = \frac{m_j}{\sum_{0 \leq i < n} m_i} LCI_{tot}$$

where :
-LCI_j is the life cycle inventory of by-product j
-LCI_{tot} is the life cycle inventory of the process producing all by-products
-m_j is the mass of by-product j
-m_i are the masses of all by-products i

Economic allocation This allocation splits the environmental impact of the by-products based on the price of each by-product and their mass.

$$LCI_j = \frac{p_j m_j}{\sum_{0 \leq i < n} p_i m_i} LCI_{tot}$$

where :
-LCI_j is the life cycle inventory of by-product j
-LCI_{tot} is the life cycle inventory of the process producing all by-products
-m_j is the mass of by-product j
-m_i are the masses of all by-products i
-p_j is the price per mass of by-product j
-m_i are the prices per mass of by-products i

Choice of the allocation method The two methods presented above are the ones the most used in the scientific community, but there is still debate about the one that is best to use.
The mass allocation has the advantage of being stable in time and relies only on physical processes. It is consistent with other processes that are purely physical and that do not involve co-products. But, when considering supplementary cementitious materials (SCM) used in concrete, the mass allocation gives an important impact on them, while they still remain co-products of a bigger industry (pig iron production for ground granulated blast furnace slag (GGBFS), Silicon for Silica Fume (SF), Electricity produced with coal for Fly ashes (FA)). Thus, it seems far-fetched to attribute such a great impact to products that are waste [27].
This is why the economic allocation can be an alternative to the mass allocation in the way that it takes into account the economic value of co-products and reflects more the status of waste of SCMs [28][29].
Besides, as the DHUP (Direction de l'Habitat de l'Urbanisme et des Paysages : Housing, Urban Planning and Landscapes Department) [30] has chosen the economic allocation and acts as a reference in France, this allocation has been chosen in this study. Still, it has to be kept in mind that the economic allocation relies on data (prices of products) that are not very reliable as their scatter is very large and as they depend significantly on time and on the geographical context.

Economic allocation for SCMs So as to proceed to the economic allocation of SCMs, a collection of data from previous studies and from actors of the sector has been made (Table 1).

Reference	Year	GGBFS (€/t)	Steel (€/t)	FA (€/t)	Electricity (€/kWh)	SF (€/t)	Silicon Metal (€/t)
Collepardi et al. [31]	2004			25		250-500	
Habert et al. [32]	2011	45		25			
Teixeira et al.[33]	2016			21			
Chen et al.[34]	2010	40	400	20	0.1		
Van Den Heede[28]	2014	40		35		400-750	
Chen[27]	2007	80	370	35	0.07	400	1200
US geological Survey[35]	2020	48					2100
Dreveton[36]	2020	95-150	400-500				
Henan Superior[37]	2021					160-650	
Argus[38]	2021						1520-2250
Arcelor Mittal[39]	2016-2020		591				
Kelwatt [40]	2022				0.206		
HSA Material [41]	2022					186-858	
DHUP [30]	2022	20	410				
Boral [42]	2016			23-70			
MineralInfo [43]	2018						2107
UHPFC Factory in France	2023	90				650	
Chosen values		50	410	30	0.21	500	2100

Table 1: Collection of prices for SCMs and their related primary products

Data regarding the mass of each by-product produced during the studied processes have been collected in Table 2.

Reference	GGBFS (kg/kg pig iron)	FA (kg/kWh)	Hard coal (kg/kWh)	SF (kg/kg silicon)
Chen et al [34]	0.24	0.052	0.367	
Chen [27]	0.34	0.052		0.15
Worlsteel [44]	0.28			
Ecoinvent [22]		0.046	0.424	
Fidjestol et al. [45]				0.4-0.5/0.2-0.25
ACI Committee [46]				0.3
MineralInfo [47]				0.4
Condesil [48]				0.3
DHUP [30]	0.275			
Chosen values	0.275	0.046	0.424	0.4

Table 2: Masses of co-products relative to their related primary product

Then, it is possible to calculate the mass and economic allocation based on the tables presented above. The results are presented in the table 3.

Product	Mass allocation	Economic allocation
Steel	78.43%	96.76%
GBFS	21.57 %	3.24 %
Electricity	90.21 %	99.35 %
FA	9.79%	0.65 %
Silicon Metal	71.43 %	99.99%
SF	28.57 %	0.01 %

Table 3: Economic and mass allocation of SCMs

As discussed before, it can be seen in Table 3 that the mass and economic allocations differ considerably. In fact, mass allocation gives more impact on SCMs compared to economic allocation as the production of each primary product creates in mass up to approximately 30% of SCM. On the other hand, economic allocation gives a low impact on SCMs, which can also be controversial.

So as to understand the impact of the allocation method chosen on concrete global impact, a sensitivity analysis was conducted for two given concrete recipes (C30/37 for use in buildings and in bridges). The increase of the global footprint going from economic to mass allocation in terms of the midpoint indicators of the IW+ framework is presented in Figure 4.

	C30/37 Bridge	C30/37 Building
Human toxicity non cancer	37%	20%
Terrestrial acidification	42%	36%
Freshwater eutrophication	15%	21%
Ionizing radiations	9%	4%
Photochemical oxidant formation	79%	69%
Freshwater ecotoxicity	26%	22%
Mineral resources use	2%	33%
Land transformation, biodiversity	11%	31%
Climate change, long term	37%	13%
Land occupation, biodiversity	21%	112%
Fossil and nuclear energy use	46%	46%
Particulate matter formation	84%	91%
Water scarcity	4%	5%
Freshwater acidification	42%	37%
Ozone Layer Depletion	21%	28%
Marine eutrophication	44%	32%
Climate change, short term	39%	15%
Human toxicity cancer	52%	51%

Table 4: Increase of the impact of concrete for the eighteen midpoint indicators for two use cases going from economic to mass allocation

What can be seen is that the increase of impact in terms of the different indicators is not negligible at all when going from economic to mass allocation. In fact, when considering the economic allocation for climate change, the impact of slag is quite low (127 $kgCO_{2,eq}/t$) while it becomes more than three times higher when considering mass allocation (429 $kgCO_{2,eq}/t$), which becomes more comparable to the impact of Portland Cement CEM I (854 $kgCO_{2,eq}/t$). This is why it seems inappropriate to choose the mass allocation for co-products such as GGBFS. The mass allocation does not take into account the fact that GGBFS is waste: GGBFS would never be produced for itself. When using the mass allocation SCMs do not provide a great advantage compared to Portland cement. This is why, for this study, the economic allocation has been chosen even if it has some drawbacks.

2.5 Assessing LCA for beams - Hypotheses

2.5.1 Transport of construction materials and prefabricated beams

Transport of materials is present at different steps during the life cycle of a beam. For example, when considering a prefabricated beam in reinforced concrete, transport appears when gathering concrete constituents and reinforcing bars at the prefabrication location, and when transporting the beam from the prefabrication site to the construction site.

Concrete Concrete constituents are transported from the place where they are produced or mined to the prefabrication plant where the concrete is produced. Table 5 lists the data collected from various references.

Reference	Travel	Type of transport	Interval (km)	Chosen value (km)
Maitenaz S. [11]	SCM - Prefabrication Plant	Road	500-700	600
Maitenaz S. [11]	Fine limestone - Prefabrication Plant	Road	70-200	100
Maitenaz S. [11]	Sand - Prefabrication Plant	Road	22	22
		Waterway	22.25	22.25
Maitenaz S. [11]	Aggregates - Prefabrication Plant	Road	22	22
		Waterway	22.25	22.25
Maitenaz S. [11]	Cement - Prefabrication plant	Road	123.8	123.8
		Rail	18.2	18.2
		Waterway	26	26

Table 5: Transport distances used for the concrete constituents

For heavy goods trucks, the Ecoinvent process was created from the distribution in the French fleet of trucks according to the Euro standards [49] (Table 8).

Process	Ecoinvent process	Region	Quantity	Unit
Transport Euro 3	transport, freight, lorry 16-32 metric ton, EURO3	RER	0.1	tkm
Transport Euro 4	transport, freight, lorry 16-32 metric ton, EURO4	RER	0.6	tkm
Transport Euro 5	transport, freight, lorry 16-32 metric ton, EURO5	RER	7.8	tkm
Transport Euro 6	transport, freight, lorry 16-32 metric ton, EURO6	RER	91.5	tkm
Truck Euro			T_E	tkm

Table 6: Share of trucks for each Euro standard

Furthermore, if the beam is cast on-site, the transport of concrete between the concrete factory to the construction site has to be taken into account. Based on EPDs for concrete products, this distance was taken at 20km.

Reinforcing steel The distances considered in the study for the reinforcing steel are presented in Table 7. The primary steel is produced at the steel factory while the secondary use steel must be transported from the collection point to the steel factory.

Reference	Travel	Type of transport	Interval (km)	Chosen value (km)
Ecoinvent	Recycled steel - Steel factory	Road	206	206
		Rail	190	190
		Waterway	20	20
		Sea	440	440
Maitenaz S. [11]	Rebars- Prefabrication Plant	Road	185-525	250

Table 7: Transport distances used for reinforcing steel

If the beam is built on site, first the steel bars are assembled into a rebar cage in a factory and then transported as a rebar cage to the construction site. Based on a benchmark of the factories building rebar cages, the distance between the construction site and those factories was taken as 150km.

Prestressing steel As will be discussed more in the paragraph concerning the LCA of strands, prestressing steel was assumed to come from Italy and from the Netherlands. The maximum distance from the Italian factory to a construction site in France is 2000km. A distance of 1300km was considered for the LCA calculations.
The Dutch factory is at a maximum distance from the South of France of 1400km with a distance of 800km. So as to gather further information, Virginie Perier, assistant to the head of the Cerema South-West Structures Monitoring Group was contacted. She emphasized that for prestressed steel, the main mean of transport is by truck. The distribution of Euro Trucks was used as described by table 8.

The transport distance between the steel mills and the prestressed rebar factories must also be considered. V. Perier calculated a distance of 500km as an average value for the factories registered at the ASQPE. This value has been considered for both factories.

Timber As two types of timber beams were considered, a benchmark for factories producing solid finger-jointed wood and glued laminated wood in France has been conducted as can be seen in Figure 6.

For glue-laminated timber, the maximum distance between a factory and a construction site in France is 260km and an average distance of 160 km was found.

For solid finger-jointed wood, the maximum distance between a factory and a construction site in France is 400km and an average distance of 250 km was found.

The benchmark has been conducted by searching for sawmills producing either glue-laminated or solid timber on Google Maps with a double check on Google Search. The density of those factories is higher in the Auvergne-Rhône Alpes region as a website (https://www.boisdici.org/entreprises/) has a register of the factories in this region.

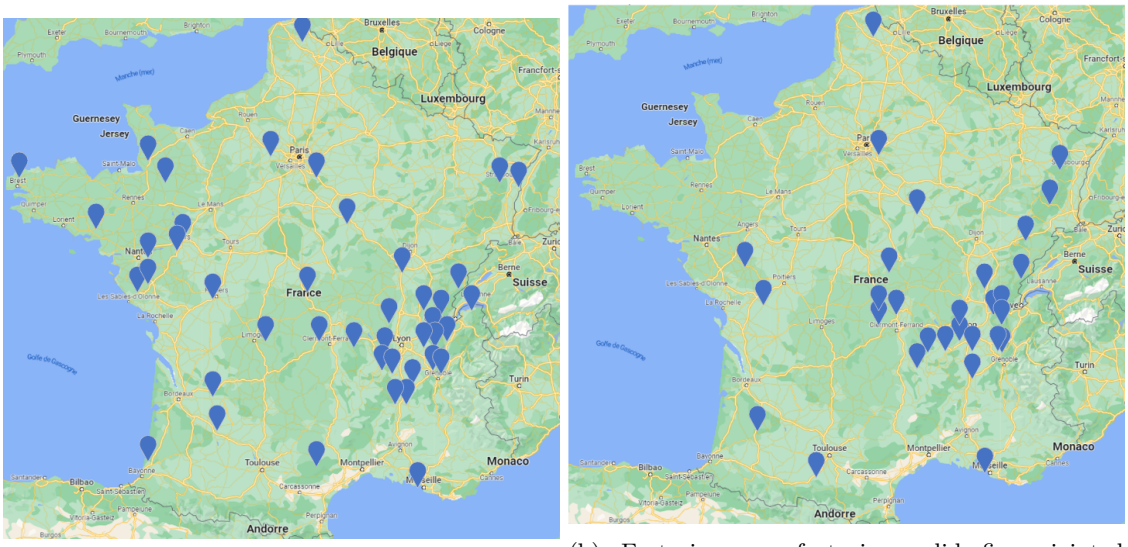

(a) Factories manufacturing glued-laminated beams

(b) Factories manufacturing solid finger-jointed beams

Figure 6: Benchmark for timber beams factories

The beams were supposed to be transported by lorry. Thus, the Euro mix from Table 8 has been used as the transport remains in France.

Construction Steel The distance considered from the production site of the beam to the construction site is based on the EPD from the CTICM (Centre Technique Industriel de la Construction Métallique) [50]. The CTICM's EPD takes into account the French average transport distances collected from the various actors in the sector and is therefore representative of the French context. The values considered are the following:

- Lorry: 593 km
- Barge: 14 km

The Euro mix of lorries described in Table 8 has been used.

Process	Ecoinvent process	Region	Quantity	Unit
Transport by lorry	Truck Euro	FR	593*T_s	tkm
Transport by barge	market group for transport, freight, inland waterways, barge	GL	14*T_s	tkm
Steel profiles transport			T_s	tkm

Table 8: Ecoinvent processes used for the transport of construction steel

Transport of the entire beam If the beam is prefabricated off-site, it needs to be transported to the construction site. Depending on the type of beam the factories are not located in the same place and do not cover the French territory equally. This is why different values have been considered depending on the type of beam. For the timber beams, the transport of the entire beam is the same as the one from the sawmill to the construction site. The Euro mix from Table 8 has also been used for lorries.

Type of beam	Reference	Travel	Type of transport	Interval (km)	Chosen
PBPA	Benchmark + Cerib	Prefabrication factory - Construction site	Road	100-170	150
RC I	Benchmark + Cerib	Prefabrication factory - Construction site	Road	100-140	120
RC Rect	Benchmark + Cerib	Prefabrication factory - Construction site	Road	100-140	120
Optimized RC beam	S. Maitenaz [11]	Prefabrication factory - Construction site	Road	100-140	120

Table 9: Transport distances used for the LCA of the beams

2.5.2 Concrete

As discussed above, assessing the environmental impact of concrete can be difficult due to the choice of the allocation method for the SCMs and the collection of the data required. Furthermore,

there exist concretes for every application with formulas that differ in the type and quantity of cement and SCM, in the ratio of water over cement, in the amount of sand, aggregates, and other products such as superfluidifiers. These recipes rely on the concrete strength, the exposure classes, and the type of pouring (vibrated or self-compacting, on-site or off-site). Thus, it is necessary to formulate appropriate concrete recipes for each case study and strength class sought.

Concrete recipes have been formulated for two main applications:

- beams for bridges with exposure classes XD1, XF2, XC3 for spans from 12 to 30m and strengths from $fck = 30MPa$ to $fck = 60MPa$
- beams for buildings with exposure class XC1 for spans from 5 to 12m and strengths from $fck = 20MPa$ to $fck = 60MPa$

These recipes can be found in Appendix 1. They are based on formulations used for Vinci construction sites.
For each strength class and application, two scenarios have been created: a pessimistic one with concrete containing only CEMI and an optimistic one for what can be called low-carbon concrete with the addition of GGBFS.
There is no clear definition of what is low-carbon concrete. A document from a collaboration of actors in the construction sector defined a table to categorize concretes [51] as can be seen in Figure 7b. This table does not provide a classification for concretes of strength above $fck = 45MPa$. This is why the table that has been used is the one from Exegy, a solution for low-carbon concretes within Vinci [52] (Figure 7a).

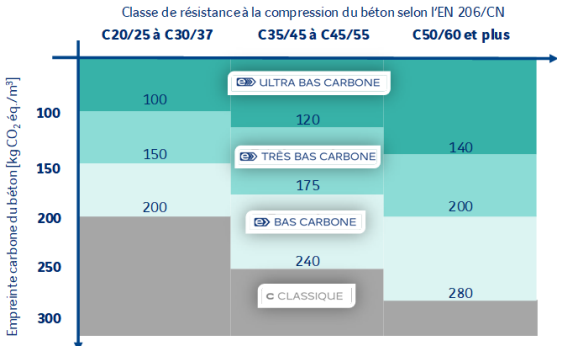

(a) Exegy classification for classic- low - very low - ultra-low-carbon concrete [52]

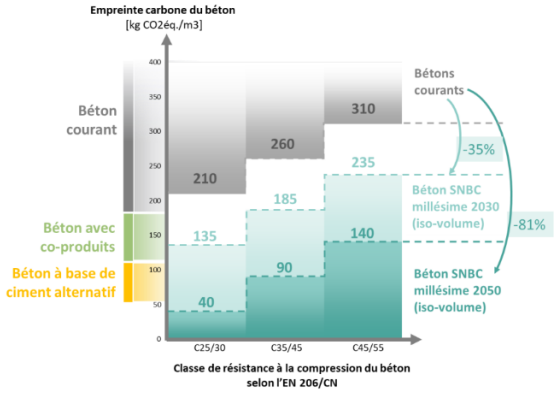

(b) Table from the collaboration of actors [51]

Figure 7: Two scales to determine what is a low-carbon concrete

According to this table, all concretes considered for the optimistic scenario are low-carbon concretes (not very low or ultra-low) and the ones from the pessimistic scenario are conventional concretes.

2.5.3 Reinforcing Steel

The process to produce steel is well known and the data on the environmental impact of steel from the electrical or primary steel industry are reliable. Still, what is challenging for its assessment is to know the proportion of steel used for reinforcing bars that come from recycled steel (electric production).
According to M. Chiappini [53], all rebars made in France come from secondary steel. Still, it does not mean that all rebars used in France come from recycled materials depending on their production location. No data has been found on the origin of steel used in France.
This is why, as for concrete, a pessimistic and an optimistic scenario have been drawn based on the European context [11]. The optimistic scenario is based on 100% of secondary steel and the pessimist one is based on 44% of secondary steel 10. The transport of secondary steel considered comes from the Ecoinvent process: market for steel, low-alloyed (RoW). The economic allocation envisaged for steel and GGBFS was also taken into account, leading to a coefficient of 0.97 for primary steel.

Reference	Scrap (%)	Region
Reinforcing steel production, Ecoinvent 3.7.1 [22]	25	World
FDES: Plancher Dalle Bois-Béton de 20 cm d'épaisseur [20]	100	
LCI - Steel Rebar [11]	44	Europe
	34.8	World
	23.1	Asia

Table 10: Share of recycled steel for rebars production [11]

Process	Ecoinvent process	Region	Quantity	Unit
Secondary Steel Production	steel production, electric, low-alloyed	RER	$0.44S_{r44}$	kg
Primary Steel Production	steel production, converter, low-alloyed	RER	$0.56*0.97*S_{r44}$	kg
Hot rolling	hot rolling, steel	RER	S_{r44}	kg
Transport of secondary steel to the steel factory	market group for transport, freight train	GLO	$0.44*190*S_{r44}*10^{-3}$	tkm
Transport of secondary steel to the steel factory	market group for transport, freight, inland waterways, barge	GLO	$0.44*20*S_{r44}*10^{-3}$	tkm
Transport of secondary steel to the steel factory	market group for transport, freight, lorry, unspecified	GLO	$0.44*206*S_{r44}*10^{-3}$	tkm
Transport of secondary steel to the steel factory	market for transport, freight, sea, bulk carrier for dry goods	GLO	$0.44*441*S_{r44}*10^{-3}$	tkm
Reinforcing steel with 44% secondary steel			S_{r44}	kg

Table 11: Ecoinvent processes for reinforcing steel with 44% of secondary steel

Process	Ecoinvent process	Region	Quantity	Unit
Secondary Steel Production	steel production, electric, low-alloyed	RER	S_{r100}	kg
Hot rolling	hot rolling, steel	RER	S_{r100}	kg
Transport of secondary steel to the steel factory	market group for transport, freight train	GLO	$190*S_{r100}*10^{-3}$	tkm
Transport of secondary steel to the steel factory	market group for transport, freight, inland waterways, barge	GLO	$20*S_{r100}*10^{-3}$	tkm
Transport of secondary steel to the steel factory	market group for transport, freight, lorry, unspecified	GLO	$206*S_{r100}*10^{-3}$	tkm
Transport of secondary steel to the steel factory	market for transport, freight, sea, bulk carrier for dry goods	GLO	$441*S_{r100}*10^{-3}$	tkm
Reinforcing steel with 100% secondary steel			S_{r100}	kg

Table 12: Ecoinvent processes for reinforcing steel with 100% of secondary steel

2.5.4 Prestressing steel

So as to gather information about strands used in PBPA (Precast Beams Prestressed by Adhesion), Miklos TOTH, a research engineer from Freyssinet was reached. Freyssinet is a subsidiary of Vinci, historically specialized in prestressed structures.
Most of the strands used by them are manufactured in the Far East or in Central Europe. The percentage of recycled steel used to produce the strands is very hard to know. Even the providers of strands have little information. They usually provide numbers from 0 to 50%. Furthermore, the providers do not know the exact location of the factories producing the strands.
V. Perier referred to the factories registered by the ASQPE (Association pour la Qualification de la Précontrainte et des Equipements des Ouvrages de Génie Civil) that gathers the factories providing strands for construction sites in France. Most of those factories are in Europe (Italy, Portugal, Spain, Hungary, Netherlands, and France). Some others are farther away: Thailand, South Africa, Tunisia, and Saudi Arabia. Among them, only a few declare the percentage of recycled steel used to manufacture the strands in their EPD (SIW in Thailand: 43% of scrap, Nedri Spanstaal in the Netherlands: 51% of scrap). The other EPDs have a higher environmental impact for the same products, so one can infer that no recycled steel is used for them.

In order to assess the environmental impact of beams using strands, two scenarios were considered:

- First Scenario:
  Strands are made from 51% of scrap steel and come from the Netherlands (Nedri Spanstaal Bv)

- Second Scenario:
  Strands are entirely made from primary steel and come from Italy near Rome (Siderurgica Latina Martin S.p.A.)

Both scenarios have been implemented in OpenLCA.

Process	Ecoinvent process	Region	Quantity	Unit
Secondary Steel Production	steel production, electric, low-alloyed	RER	$0.51S_n$	kg
Primary Steel Production	steel production, converter, low-alloyed	RER	$0.49*0.97*S_n$	kg
Hot rolling	hot rolling, steel	RER	S_n	kg
Transport of secondary steel to the steel factory	market group for transport, freight train	GLO	$0.51*190*S_n*10^{-3}$	tkm
Transport of secondary steel to the steel factory	market group for transport, freight, inland waterways, barge	GLO	$0.51*20*S_n*10^{-3}$	tkm
Transport of secondary steel to the steel factory	market group for transport, freight, lorry, unspecified	GLO	$0.51*206*S_n*10^{-3}$	tkm
Transport of secondary steel to the steel factory	market for transport, freight, sea, bulk carrier for dry goods	GLO	$0.51*441*S_n*10^{-3}$	tkm
Transport from the steel mill to the rebar factory	Truck Euro	FR	$0.49*500*S_n*10^{-3}$	tkm
Transport to the prefabrication factory	Truck Euro	Fr	$800*S_n*10^{-3}$	tkm
Prestressing steel Netherlands recycled			S_n	kg

Table 13: Ecoinvent processes for prestressing steel from the Netherlands

Process	Ecoinvent process	Region	Quantity	Unit
Primary Steel Production	steel production, converter, low-alloyed	RER	$0.97*S_i$	kg
Hot rolling	hot rolling, steel	RER	S_i	kg
Transport from the steel mill to the rebar factory	Truck Euro	FR	$500*S_i*10^{-3}$	tkm
Transport from the rebar factory to the prefabrication factory	Truck Euro	FR	$1300*S_i*10^{-3}$	tkm
Prestressing steel Italy			S_i	kg

Table 14: Ecoinvent processes for prestressing steel from Italy

2.5.5 Timber

Biogenic carbon Timber is what is called a bio-product. It captures CO_2 during its growth and releases it at the end of its life (decomposition, energy recovery), this carbon is called biogenic carbon. There are mainly two ways of accounting for biogenic carbon in LCAs.
The first approach considers that all the stored carbon will be re-emitted at some point; thus, there is no need to consider it in the LCA calculations. This method is called 0/0: 0 carbon is taken into account at the production stage and 0 is released at the end of life.
The second approach is called -1/+1. At the production stage, a negative value of carbon is taken into account to consider the stored carbon in timber, which will be released (+1) at the end of life. This is the approach that is used for EPDs as described by EN15804. This approach allows considering that at the end-of-life stage of the timber product, only some of the wood will be burned as energetic valorization. The other part will still store CO_2 in the form of other timber products (re-use for the production of furniture for example). This method can thus lead to negative emissions of timber products, and the impacts depend heavily on the end-of-life scenario chosen for the product.
The two scenarios are based on the assumption that logging is sustainable because if fewer trees are planted than are cut down the impact of using timber for a product can not be considered as zero with the first approach and can not be negative for the second.
As described in the article from the website of the French Ministry of Agriculture [54], forests managed by the ONF (Office National des Forêts) are not felled more than their natural growth rate, meaning that their management is sustainable.

These considerations led to the emergence of dynamic LCA. This new method for LCA considers the time at which carbon was released to better capture the reality of the emissions for timber products. The time of observation of the global system and the time horizon of each emission is considered as described in [55] that offers a new model for calculating Global Warming Potential with a dynamic approach. What can be observed is that the time at which the carbon is stored or emitted has an impact on the results. It is possible to consider either that the carbon stored corresponds to the tree used for the timber construction or to the tree planted to replace the tree used for the construction. For the second assumption, the time that the carbon is released is compensated by the growth of a new tree, this carbon will contribute to the Global Warming Potential and its impact can not be taken as zero. This consideration led to a new indicator called the GWP_{bio} that considers this additional contribution and the dynamic approach of LCA for bio-products [56].

As a recap, Figure 8 explains the different approaches to account for the impact of bio-products.

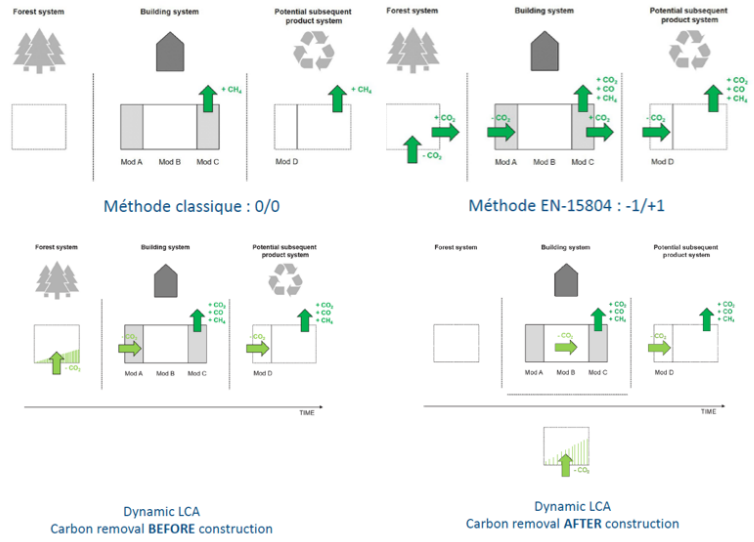

Figure 8: Different approaches for the LCA of bio-products [57]

In conclusion, the LCA calculations of bio-products depend heavily on the method chosen for the consideration of the stored carbon and the dynamic of the emissions. Thus, making hypotheses on the end-of-life of the product, the time of growth of the tree, and the time when it grows as well as choosing the appropriate temporal horizon are mandatory steps to implement a dynamic LCA.

As this study is based on a cradle-to-site approach, the end-of-life of the beam is out of scope. It therefore seems inappropriate to consider a dynamic LCA approach for timber, especially since a large number of assumptions have to be made and it is difficult to know how accurate they are for the dynamic approach. This is why the 0/0 approach has been implemented for this study. The processes used were the ones from the Ecoinvent database both for glued laminated or solid timber. For solid timber, two different processes were used depending on the drying percentage so as to see the impact that it has on the global results.

Process	Ecoinvent process	Region	Quantity	Unit
GL24h & GL28h	glued laminated timber production, average glue mix	Europe without Switzerland	GL	m^3
Glued laminated timber			GL	m^3

Table 15: Glued laminated timber Ecoinvent process

Process	Ecoinvent process	Region	Quantity	Unit
Solid timber dried 10%	planing, beam, hardwood, u=10% — sawnwood, beam, hardwood, dried (u=10%)	Europe without Switzerland	ST_{10}	m^3
Solid timber 10% dried			ST_{10}	m^3

Table 16: Solid timber dried 10% Ecoinvent process

Process	Ecoinvent process	Region	Quantity	Unit
Solid timber dried 20%	planing, beam, hardwood, u=20% — sawnwood, beam, hardwood, dried (u=20%)	Europe without Switzerland	ST_{20}	m^3
Solid timber 20% dried			ST_{20}	m^3

Table 17: Solid timber dried 20% Ecoinvent process

Steel connections Steel connections are used to connect the timber members with each other. The total amount of steel varies mainly according to the load to which the beam is subjected.
So as to evaluate the amount of steel used for connections in general, an engineer from a construction design office specialized in timber structures (Gustave) was contacted. Most of the projects require 50 to 200 kg/m^3 of steel connections for beams.
The project of the Arcueil-Cachan train station, designed by ISC, was also studied. For this particular project, the ratio was $100kg/m^3$ which confirms the range of values. Thus, it was decided to conduct a sensitivity analysis on this parameter so as to see the influence that it has on the global

emissions to switch from a $50kg/m^3$ ratio to a $200kg/m^3$ one. The amount of recycled steel used to produce the connections is around 10% [26]. It has been modeled in OpenLCA as described in Table 18.

Process	Ecoinvent process	Region	Quantity	Unit
Secondary Steel Production	steel production, electric, low-alloyed	RER	$0.1S_c$	kg
Primary Steel Production	steel production, converter, low-alloyed	RER	$0.9*0.97*S_c$	kg
Hot rolling	hot rolling, steel	RER	$1S_c$	kg
Transport of secondary steel to the steel factory	market group for transport, freight train	GLO	$0.1*190*S_c*10^{-3}$	tkm
Transport of secondary steel to the steel factory	market group for transport, freight, inland waterways, barge	GLO	$0.1*20*S_c*10^{-3}$	tkm
Transport of secondary steel to the steel factory	market group for transport, freight, lorry, unspecified	GLO	$0.1*206*S_c*10^{-3}$	tkm
Transport of secondary steel to the steel factory	market for transport, freight, sea, bulk carrier for dry goods	GLO	$0.1*441*S_c*10^{-3}$	tkm
Zinc coating	zinc coating, pieces	RER	0.00653	m^2
Transport to the construction site	Truck Euro	FR	$200*S_c*10^{-3}$	tkm
Steel connections			S_c	kg

Table 18: Ecoinvent processes for steel connections for timber beams

2.5.6 Construction steel

So as to assess the environmental impact of steel beams, four main pieces of information need to be known: the percentage of primary and secondary steel used for the production of the beam, the amount of steel for the connections, the type of corrosion protection, and the type of fire protection.

Use of secondary steel A benchmark based on European EPDs has been carried out in order to gather information on the amount of recycled steel used to produce steel profiles. The data collected are presented in the table 19.

Reference	% of secondary steel in steel beams
EPD ArcelorMittal XCarb [58]	100
EPD Bauforumstahl e. V. [59]	75
EPD Duferdofin [60]	75
EPD Özkan [61]	100
EPD Siderurgica Balboa [62]	85
EPD WOST SA [63]	100
EPD CTICM [50]	67
EPD CELSA Barcelona [64]	100

Table 19: Use of secondary steel in European steel beams

Based on this benchmark, two boundary values were considered to perform a sensitivity analysis, the first one of 70% secondary steel and the other of 100%.

Process	Ecoinvent process	Region	Quantity	Unit
Secondary Steel Production	steel production, electric, low-alloyed	RER	$0.7S_{p70}$	kg
Primary Steel Production	steel production, converter, low-alloyed	RER	$0.3*0.97*S_{p70}$	kg
Hot rolling	hot rolling, steel	RER	S_{p70}	kg
Transport of secondary steel to the steel factory	market group for transport, freight train	GLO	$0.7*190*S_{p70}*10^{-3}$	tkm
Transport of secondary steel to the steel factory	market group for transport, freight, inland waterways, barge	GLO	$0.7*20*S_{p70}*10^{-3}$	tkm
Transport of secondary steel to the steel factory	market group for transport, freight, lorry, unspecified	GLO	$0.7*206*S_{p70}*10^{-3}$	tkm
Transport of secondary steel to the steel factory	market for transport, freight, sea, bulk carrier for dry goods	GLO	$0.7*441*S_{p70}*10^{-3}$	tkm
Steel Profile 70% recycled			S_{p70}	kg

Table 20: Ecoinvent processes for steel profiles made of 70% secondary steel

Process	Ecoinvent process	Region	Quantity	Unit
Secondary Steel Production	steel production, electric, low-alloyed	RER	S_{p100}	kg
Hot rolling	hot rolling, steel	RER	S_{p100}	kg
Transport of secondary steel to the steel factory	market group for transport, freight train	GLO	$190*S_{p100}*10^{-3}$	tkm
Transport of secondary steel to the steel factory	market group for transport, freight, inland waterways, barge	GLO	$20*S_{p100}*10^{-3}$	tkm
Transport of secondary steel to the steel factory	market group for transport, freight, lorry, unspecified	GLO	$206*S_{p100}*10^{-3}$	tkm
Transport of secondary steel to the steel factory	market for transport, freight, sea, bulk carrier for dry goods	GLO	$441*S_{p100}*10^{-3}$	tkm
Steel Profile 100% recycled			S_{p100}	kg

Table 21: Ecoinvent processes for steel profiles made of 100% secondary steel

Consideration of steel connections Steel connections are also included in this study as a steel beam has to be connected to the rest of the structure via screws, bolts, and plates. The percentage depends on the type of structure and the loads applied to the beam.

ArcelorMittal declares in its EPD a ratio from 1.15 to 4.5% [58] and the CTICM a ratio of 2.06% in mass [50]. Those values apply mostly to building cases.

For engineering structures such as bridges, the ratio is more from 5 to 15% based on Vinci's engineers' experience. A sensitivity analysis for bridges based on the two values 5 and 15% will be performed.
For buildings, it was chosen to set the value to 3%. No sensitivity analysis was performed as the range of values found is narrower.

Steel connections were considered as being made of the same steel as the beam itself, thus using the Ecoinvent processes described above.

Corrosion and fire-protection Steel is subjected to corrosion that alters its mechanical properties over time. Different methods are used to protect steel from being corroded: zinc coating (galvanization), anti-corrosion paint, or powder-coated paint application. When the environment is aggressive, a combination of these technologies can be used. For example, it is common to use either anti-corrosion or powder-coated paint on zinc-coated pieces.
An average scenario has been considered for which the beams are galvanized with two additional layers of anti-corrosion paint. The process used in Ecoinvent is described in Tables 22 and 23. The values for the anti-corrosion paint are based on the EPODUX ZINC 62-208 paint from Julien Anticorrosion, which is a paint certified by the ACQPA (Association pour la Certification et la Qualification en Peinture Anti-Corrosion: Association for Certification and Qualification in Anti-Corrosion Painting) [65]. No transport for the painting has been considered as it had a very low impact on the global results (based on 200km by truck). The density of this paint is $2580 kg/m^3$ and one liter can cover theoretically $15 m^2$ for one layer.

Process	Ecoinvent process	Region	Quantity	Unit
Galvanization	zinc coating, pieces	RER	Z_c	m^2
Zinc coating			Z_c	m^2

Table 22: Ecoinvent process for galvanization

Process	Ecoinvent process	Region	Quantity	Unit
Zinc	market for zinc — zinc	GLO	$0.07AC$	kg
Epoxy resin	market for epoxy resin, liquid	RER	$0.93AC$	kg
Anti-corrosion Paint			AC	kg

Table 23: Ecoinvent process for anti-corrosion paint

Steel is a material that is very sensitive to heat. It loses its resistance quickly when it is subjected to high temperatures. Thus, in the case of buildings, beams are often protected to ensure resistance to fire. For bridges, when there is a risk of a fire, steel will not be used by engineers as the main material of the structure. Thus, no fire protections were considered for bridge applications.
To prevent heat to alter steel properties, three main technologies exist: cladding with plasterboards, covering with fire-resisting flocking, or intumescent paint. Intumescent paint is very expensive and is used only in cases where there is an architectural will to leave the profiles visible.
Otherwise, flocking is preferred for housing applications and plasterboard cladding for office applications as there are almost always false ceilings in the offices.

As there was no data in Ecoinvent for intumescent paint and flocking, the beams used in buildings for this study were considered clad with plasterboards (Table 24). A density for plasterboards of $700 kg/m^3$ has been considered with a thickness of $14mm$. It was assumed that the plasterboard box was covering three of the four faces of the beam (sides and bottom).

Process	Ecoinvent process	Region	Quantity	Unit
Plasterboard production	market for gypsum plasterboard — gypsum plasterboard	GLO	P_c	kg
Plasterboard cladding			P_c	kg

Table 24: Ecoinvent process for fire protection

2.5.7 Fabrication of the beam

PBPA Information about the construction of PBPA beams was collected from the Spanish company Tierra Armada which manufactures prestressed and precast T and U-beams. The different stages of the production and their corresponding contribution are described in Table 25. An additional process for bending and cutting the stirrups was also considered.

Process	Subprocess	Power	Time (min)	Consumption	Ecoinvent process
Cube Gantry crane	Lifting	25 kWh	2	0.093 kWh/m3	market for electricity, medium voltage - FR
	Gantry crane translation	8 kWh	20	0.296 kWh/m3	market for electricity, medium voltage - FR
	Trolley translation	3 kWh	1	0.00556 kWh/m3	market for electricity, medium voltage - FR
Gantry crane for steel	Lifting	25 kWh	4	1.67 kWh/beam	market for electricity, medium voltage - FR
	Gantry crane translation	14 kWh	40	9.33 kWh/beam	market for electricity, medium voltage - FR
	Trolley translation	3 kWh	4	0.200 kWh/beam	market for electricity, medium voltage - FR
Gantry crane for the beam	Lifting	25 kWh	4	1.67 kWh/beam	market for electricity, medium voltage - FR
	Gantry crane translation	14 kWh	40	9.33 kWh/beam	market for electricity, medium voltage - FR
	Trolley translation	3 kWh	4	0.200 kWh/beam	market for electricity, medium voltage - FR
Concrete cart	Gasoil	2L/h	60	0.222 L/m3	market for diesel—diesel - Europe without Switzerland
Rebar cage construction [11]	Cutting and bending stirrups	-	-	0.013 kWh/m	market for electricity, medium voltage - FR

Table 25: Construction stages of the PBPA

Reinforced concrete beams For rectangular RC beams, the rebar cage fabrication needs to bend and cut the stirrups as for PBPAS (0.013 kWh/m) and also to cut longitudinal rebars (0.09 kWh/m) [11]. The last stage of fabrication is pouring concrete (0.92 kWh/m [11]).

Process	Ecoinvent process	Region	Quantity	Unit
Bend and cut stirrups	market for electricity, medium voltage	FR	$0.013RC_c$	kWh/m
Cut longitudinal rebars	market for electricity, medium voltage	FR	$0.09RC_c$	kWh/m
Pouring concrete	market for electricity, medium voltage	FR	$0.92RC_c$	kWh/m
RC beam construction			RC_c	kWh/m

Table 26: Ecoinvent processes for the construction of RC beams

The optimized RC beams are built the same way as RC rectangular beams, with the same consumption of machinery. The only additional impact is when the beam is cast in situ, the impact of the formworks used to make the voids in the beam is taken into account as they will not be used many times. For these formworks, plywood is used. Three scenarios were considered depending on whether the forms were used 1 or 10 times. The amount of plywood used is based on the perimeter of the voids in the beam and a thickness of $18mm$.

Process	Ecoinvent process	Region	Quantity	Unit
Formworks for holes	Plywood production	FR	Ply	m^3
Plywood			Ply	m^3

Table 27: Ecoinvent processes for plywood

For the rectangular and optimized RC beams, the exterior formwork is not taken into account as both off-site or in-situ these formworks will be used many times (over 10 years approximately according to Vinci construction sites) so their impact in the entire process is negligible. The I-beams are considered to be built the same way as PBPAs (with the same impacts). One just needs to add the cutting of the longitudinal rebars (0.09 kWh/m [11]).

Timber beams No additional processes than the ones described in the timber section are needed.

Steel beams No additional processes than the ones described in the steel section are needed.

All of the beams For all of the beams considered, a last stage is common and involves the crane used on-site to put the beam into its definitive location. This involves an electricity consumption of 0.16 kWh/m [11].

2.5.8 End-of-life

For the end-of-life scenarios, it was chosen not to consider the avoided impacts of re-using the wastes produced by the demolition of the beams (for example using steel scrap to make new steel elements avoids the use of primary steel). This choice was made in order to be consistent with the cut-off allocation method chosen for this study.

Concrete So as to consider the end-of-life of concrete in LCA calculations, several EPDs have been considered among which the ones from the CERIB (Centre d'Etudes et de Recherches de l'Industrie du Béton) [66] [67]. They act as references for reinforced concrete elements in France. The scenario considered is the same for all their EPDs :

- 70% of concrete waste is sent to a sorting center and crushed for material recovery
- 30% of concrete waste is eliminated in a waste storing installation
- Recycled concrete covers a distance of 30km
- Waste concrete covers a distance of 30km

The value regarding the carbonation rate for concrete elements was found on the Infociments website [68]. The value is close to what can be found in EPDs when considering the volume of the beams.

The deconstruction process was taken from an EPD for a timber beam [69] (15 mins/m^3 of heavy machinery).

Process	Ecoinvent process	Region	Quantity	Unit
Carbonation	Carbon dioxide — Resource in air	-	37.5*C_{EoL}	kg
Transport of disposed waste	Truck Euro	FR	0.001*30*0.3*C_{EoL}	tkm
Transport of recycled waste	Truck Euro	FR	0.001*30*0.7*C_{EoL}	tkm
Concrete landfilling	treatment of waste concrete, inert material landfill (Avoided waste)	Europe without Switzerland	-2500*0.3*C_{EoL}	kg
Concrete crushing for gravel use	treatment of waste concrete gravel, recycling (Avoided waste)	RoW	-2500*0.3*C_{EoL}	kg
Deconstruction Machinery	market for machine operation, diesel, ≥ 74.57 kW, generators	GLO	15*C_{EoL}	min
End of Life - Concrete			C_{EoL}	m3

Table 28: End-of-life scenario for concrete

Reinforcing and Prestressing steel The values considered for prestressing and reinforcing steel also come from the EPD from the CERIB [66] [67] [70]. The deconstruction process is already taken into account in the waste processes for steel, this is why no additional process was considered.

Process	Ecoinvent process	Region	Quantity	Unit
Transport of disposed waste	Truck Euro	FR	0.001*30*0.06*RS_{EoL}	tkm
Transport of recycled waste	Truck Euro	FR	0.001*100*0.94*RS_{EoL}	tkm
Steel disposal	treatment of waste reinforcement steel, collection for final disposal (Avoided waste)	RoW	-0.06*RS_{EoL}	kg
Steel recycling	treatment of waste reinforcement steel, recycling (Avoided waste)	RoW	-0.94*RS_{EoL}	kg
End of Life - Reinforcing and Prestressing steel			RS_{EoL}	kg

Table 29: End-of-life scenario for reinforcing and prestressing steel

Steel beams End-of-life scenarios for steel beams were based on the EPD from the CTICM [50], knowing that the same assumptions also stand in the EPD from Arcelor Mittal [58] :

- 88% of steel is recycled and covers a distance of 375km
- 11% of steel is reused on site
- 1% of steel is landfilled and covers a distance of 150 km

Furthermore, maintenance has been considered for bridge applications. In fact, the anti-corrosion paint must be renewed every 10 years, which over a 100-year lifespan (equal to that of the EPDs of construction products), corresponds to 8 renewals. Each time, two layers of the paint already considered for the construction phase are added to the steel surface.

Process	Ecoinvent process	Region	Quantity	Unit
Transport of disposed waste	Truck Euro	FR	0.001*150*0.01*SB_{EoL}	tkm
Transport of recycled waste	Truck Euro	FR	0.001*345*0.88*SB_{EoL}	tkm
Steel disposal	treatment of waste reinforcement steel, collection for final disposal (Avoided waste)	RoW	-0.01*SB_{EoL}	kg
Steel disposal	treatment of waste reinforcement steel, recycling (Avoided waste)	RoW	-0.88*SB_{EoL}	kg
End of Life - Steel Profiles			SB_{EoL}	kg

Table 30: End-of-life scenario for steel beams

Timber beams The end-of-life scenario for timber elements is based on the one from the EPD of the FNB (Fedération Nationale du Bois) [69] :

- Transport to sorting facility: 30km
- 57.2% of timber is recycled
- 17.3% of timber is landfilled
- 25.5% of timber is burned for energy recovery
- $1m^3$ of timber requires 15mins of diesel consumption of a demolition machine
- 0.030 kWh/kg_{timber} electricity for crushing and sorting
- 0.0437 MJ/kg_{timber} of diesel for material handling ($46MJ/kg_{diesel}$)
- 210 $kgCO_2/m^3_{timber}$ of biogenic carbon stored in timber

A density of $420kg/m^3$ for timber was considered.

Process	Ecoinvent process	Region	Quantity	Unit
Transport of waste	Truck Euro	FR	0.001*420*30*T_{EoL}	tkm
Diesel for material handling	market group for diesel	RER	0.0437/46*420*T_{EoL}	kg
Electricity for crushing and sorting	market for electricity, medium voltage	FR	0.03*420*T_{EoL}	kWh
Deconstruction Machinery	market for machine operation, diesel, $\geq$ 74.57 kW, generators	GLO	15*T_{EoL}	min
Biogenic carbon stored in re-used products	Carbon dioxide - Resource in air	-	0.572*210*T_{EoL}	kg
End of Life - Timber			T_{EoL}	m^3

Table 31: End-of-life scenario for timber beams

As can be seen in Table 31, stored biogenic carbon for recycled timber was considered. It has to be underlined that this process does not change the final LCA results for the Impact World + methodology. But, as another methodology might be used for other studies, it is important to write it down for the processes taken into account.

Steel connections The end-of-life scenario for steel connections used in timber beams was also included in FNB's EPD:

- 95% of steel is recycled
- 5% of steel is landfilled
- Both recycled and landfilled steel cover a distance of 30km

Process	Ecoinvent process	Region	Quantity	Unit
Transport of waste	Truck Euro	FR	0.001*30*SC_{EoL}	tkm
Steel disposal	treatment of waste reinforcement steel, collection for final disposal (Avoided waste)	RoW	-0.05*SC_{EoL}	kg
Steel recycling	treatment of waste reinforcement steel, recycling (Avoided waste)	RoW	-0.95*SC_{EoL}	kg
End of Life - Steel connections			SC_{EoL}	kg

Table 32: End-of-life scenario for steel connections

3 Optipoutre: an optimization tool for beams

3.1 Scope of the analysis

Spans and loadings This study aims to minimize the environmental impact of beams used for buildings and bridges. The span and the structural requirements are not the same for each application. This is why, two different scopes have been determined, one for beams in buildings and the other one for beams for road bridges. The different scopes considered are detailed in Table 33.

Application	Range of spans (m)	Point load (kN)	Distributed load (kN/m)
Bridges	12-30	270	16.2
Buildings	5-12	7	10

Table 33: Scope of the study

The loadings have been determined using Eurocode 1 [71]. The distributed load for a bridge is of $9kN/m^2$ with a coefficient of 0.9 and a spacing of 2m between beams was assumed, which leads to $q_k = 2{*}0.9{*}9 = 16.2kN/m$. The point load is also given such that $Q_k = \alpha_Q Q_k = 0.9{*}300 = 270kN$. It has to be kept in mind that this load has to be placed at the place the most unfavorable, which is for isostatic beams at mid-span.

For building beams, the loadings are different, the category considered is C4 (buildings that can bear places for physical activities such that dancing halls or gyms) as it is constraining and it corresponds to a situation that is common. For this situation, the loadings are $q_k = 5kN/m2$ and $Q_k = 7kN$. A spacing between beams of $2m$ was considered.

An additional permanent loading for both situations was added (to take into account additional permanent loads such as protective barriers for bridges): $g_{k,sup} = 1kN/m$.

Materials and typologies For this study, several materials and typologies have been considered: Precast Beams Prestressed by Adhesion (PBPA), reinforced concrete beams with three different typologies: rectangular beams, I-beams, and optimized beams which will be presented in the next part. Other beams such as timber (solid and glued-laminated) and steel beams were also analyzed.

3.2 The optimization process with Grasshopper

The algorithm of optimization has been implemented for each typology on Grasshopper, a plug-in of Rhino that allows building parametric designs and performing calculations with them. The implementation in Grasshopper works with blocks related to each other, each one having its own purpose (Defining the inputs, visualizing the geometry, performing calculations, etc.). The range of possibilities in Grasshopper is very large. In fact, several open-source plug-ins can be added depending on what has to be achieved. The ones used in this study are the following:

- GHPythonRemote
  This plug-in allows the user to include Python scripts in Grasshopper and to import Python libraries that are useful for the project as numpy, scipy, or others. The main drawback of using Python in Grasshopper is that the version of Python used is v2.7. Thus, recent libraries are no longer compatible with this version, but for usual calculations, it is sufficient.
  The rhinoscriptsyntax library has also been used. It provides tools to draw the beams in a parametric way directly in Python.

- Wallacei [72]
  Wallacei is an open-source plug-in developed by Mohammed Makki during his Ph.D. It performs evolutionary simulations for multi-objective optimizations. The interface is user-friendly and the analysis of the results is possible through some boxes in Grasshopper. The algorithm used within the Wallacei plug-in is the NSGA-II (Non-Dominated Sorting Algorithm), a genetic algorithm whose pseudo-code is the following [73] [74]:

  Initialize parent P_i population (for an arbitrary number of chromosomes)
  Iterate till some n-iterations. On each iteration:

1. *Create offspring Q_i from P_i via crossover mechanism*
2. *Create offspring via mutation mechanism, randomly selecting a pair of parents and exchanging some amount of genes between them*
3. *Optionally creates an offspring via local search mechanism (random finite displacements to some parent's genes)*
4. *Combine P and three groups of Q into one population set*
5. *Evaluation: Calculate the fitness objective for each chromosome in the population*
6. *Selection:*
   - *Find a subset of chromosomes that constitutes a Pareto front*
   - *Calculate crowding (estimate how tightly clustered Pareto chromosomes are using fitness as a criterion)*
   - *Randomly remove some chromosomes from the Pareto front using the crowding index*

After the last iteration, evaluate the fitness of the resulting population and find the final Pareto efficient solution(s).

A Pareto efficient solution is a solution for which no action can be made that will minimize one criterion without making another worse. It is relevant for multi-objective optimizations as the decrease in one indicator studied can lead to an increase of the other. Thus Pareto fronts allow the decision maker to choose the appropriate solution based on whether he wants to prioritize one of the two (or multiple) indicators or have a solution that is good for all of them while not being the optimal one for each of the indicators;

The global workflow for the optimization is drawn in Figure 9.

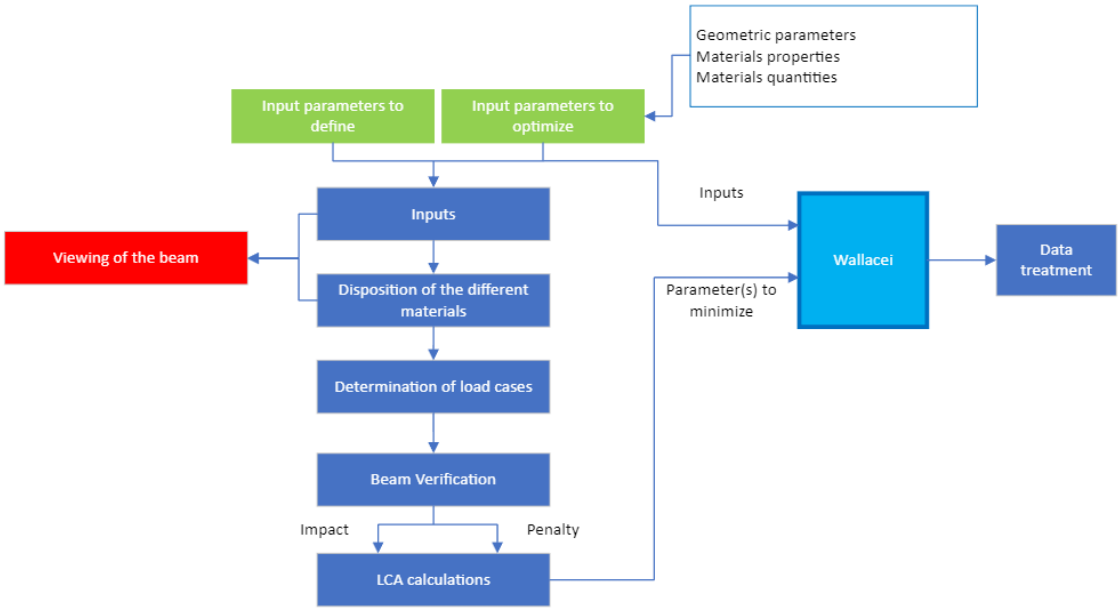

Figure 9: Global workflow of the Grasshopper implementation

Inputs Two types of inputs have to be differentiated: inputs that remain constant during the optimization process and the ones that will be optimized. The ones that are fixed are (for one simulation): the span, the external loadings (the loading due to the self-weight depends on the geometry and is thus calculated at each iteration), the type of scenario chosen for the LCA (optimistic or pessimistic), and some hypotheses for the verification of the beam depending on the typology and type of material.
The parameters that will be optimized are geometric parameters such as the height, width of the section, material properties (type of concrete), and materials quantities (ratio of reinforcement, number of strands, ...).

Disposition of the different materials When considering, for example, the precast beams prestressed by adhesion, it is also required to know the location of each strand to perform the design checks. This is why this step of disposition of the matter is important for composite beams.

Determination of the load cases The load cases are calculated via the loadings defined in 3.1 depending on the situation (Serviceability Limit State (SLS) frequent, quasi-permanent, characteristic, Ultimate Limit State (ULS), and construction phase). The combinations of loadings for all these situations are described in Eurocode 1 [71].

Beam verification After the load cases are defined, the calculations to check whether the beam meet requirements can be performed. This step depends on the material considered and will be described more in detail for each typology later in the report. This step is performed in Python using GHPythonRemote. If the beam does not meet a requirement, a penalty parameter will be added to the LCA score of the beam so that the beam is penalized and will not be chosen by the optimization algorithm [75]. This step will be described in detail for each typology as it depends on the design checks for each material.

LCA calculations With the previous steps, the quantities of all materials are known. The environmental impact of each constituent of the beam is gathered within a Python script. They have been determined upstream with OpenLCA as described in section 2. The environmental indicators can then be determined by multiplying the quantities of each material by the LCA indicator value, and by adding the contribution of the transport, construction phase, and End-of-Life.

Wallacei & Data treatment Each LCA impact indicator, chosen as a function to minimize within the optimization process, is summed up with the penalty factor relative to the indicator. It leads to a number that will be set as input for Wallacei, which will minimize it.
Wallacei takes also as inputs the sliders coming from the changing input parameters so that it can change them during the optimization.
As an output, it can provide any numerical data on the different beams constructed during the optimization. As mentioned before, when performing multi-objective optimizations, Wallacei can display Pareto front solutions. The equations of the optimization can thus be written as below (for a single objective optimization):

$$\begin{cases} \text{Minimize } O + Py_{tot} \\ \text{O being the objective and } Py_{tot} \text{the penalty parameter} \end{cases}$$

3.3 The optimization process with Python

Even if using Rhino has many advantages such as the live overview of the beam during the iterations and many options to produce visuals, it has one main drawback: computation time.
Thus, it was decided at some point to switch all algorithms coded in Grasshopper to scripts in Python. As the blocks in Grasshopper were mainly done using GHPythonRemote, it was not very difficult to copy them directly in Python. The block that required more attention was the one to perform the genetic optimization: Wallacei.
As said before, Wallacei is based on a genetic algorithm called NSGA-II. Luckily, a library called Pymoo has been developed to perform numerous types of optimization including NSGA II. The main difference is that the optimization is done under constraints. It means that instead of calculating a penalty parameter based on the different design checks, it was only needed to inform the algorithm of the different constraints in the form of functions that had to be negative.
For example, if one needs to meet $\sigma \leq f_y$, the function to give to the algorithm becomes $g_1 = \sigma - f_y$. If $g_1 \leq 0$, the requirement is met.
The handling of constraints is performed as explained below [76]. A tournament between two random genes i and j of the population is made. If a multi-objective optimization is performed, the solution i will be kept instead of solution j if one of the three following cases appear:

1. Solution i is feasible and j is not
2. Both solutions are infeasible but solution i has an overall constraint violation that is smaller than j

3. Both solutions are feasible and solution i dominates the other

Another step, that is changed going from Grasshopper to Python, is the visualization of the sections and of the beam. The matplotlib and shapely libraries were used to replace Grasshopper and Rhino. Otherwise, the global workflow remains the same, first defining the input parameters, then performing design checks and LCA calculations.

Now that the global workflow has been described, each typology and material particularity will be discussed in detail during the next sections.

3.4 Precast beams prestressed by adhesion (PBPA)

3.4.1 Design of the beam

Precast Beams Prestressed by Adhesion (PBPA - PRAD in French) are beams in an I-shape (Figure 10) used mostly for bridges, covering of roads, and sometimes as trusses and purlins of industrial frame buildings.

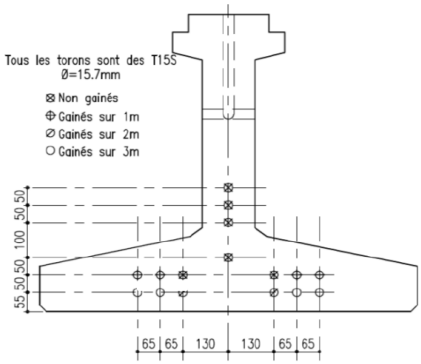

Figure 10: Example of a PBPA used for a flying junction on the high-speed line Tours-Bordeaux [77]

This type of beam can be characterized by:

- Geometric parameters (height and width of all parts of the section: web, heal, and head)
- Number, diameter, and disposition of strands
- Concrete resistance

For the strands, the input is the total area of strands in the cross-section of the beam. A step is then required to know which type of strand to choose and how to place them within the section. This step is described in Figure 11. The strands must remain in the heel of the beam so that the web can be thin so as to spare some concrete. The cover and the horizontal and vertical spacings are fixed within the script. They were all taken equal to $5cm$ based on the standards. Three types of strands were considered (the most used currently): T12.9, T15.2, and T15.7. A_p is the area of one strand, $n_{strands_max}$ is the maximum number of strands that can fit in the heel, $A_{p,max}$ is the maximum area of strands that fit in the heel, and h_{heel} is the height of the heel.

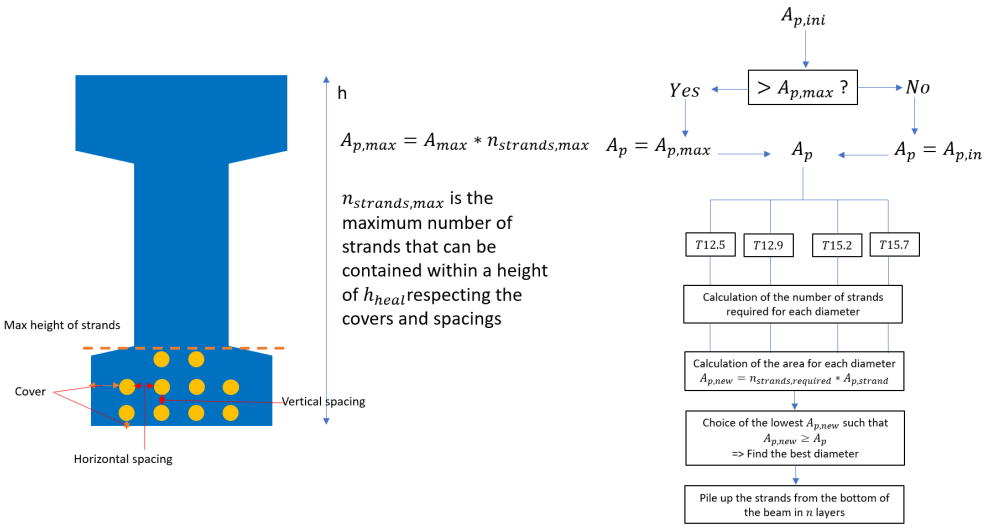

Figure 11: Procedure to place strands within the cross-section

3.4.2 Design checks of the beam

The design checks were done according to Eurocode 2 (EC2) [78], to documents from the CSTB (Centre Scientifique et Technique du Bâtiment) [79], and to classes of the CHEBAP (Centre des Hautes Etudes pour le Beton Armé Précontraint) [80].

Prestress losses When designing a PBPA, the prestress losses at each step of the life of the beam are determined. The initial stress in strands is taken as $\sigma_{max} = 0.95 * fp_{01,k}$, $fp_{01,k} = 0.9 * f_{pk}$ being the elastic limit of prestressing steel and f_{pk} the fracture limit of the prestressing steel. Such values are available for different types of strands in standard tables.
Right after the cables are released, there are losses leading to a prestress constraint of $\sigma_0 = min(0.8f_{pk}, 0.9fp_{01,k})$. Some other losses at this stage have to be considered:

- Loss at anchorage setback:
  $\Delta\sigma_{sl} = E_p \frac{\Delta L}{L_{bench}}$, ΔL being the anchorage setback (taken from the value of the CSTB guide), and E_p the Young's modulus of prestressing steel, $L_{bench} = 18m$
- Relaxation loss on the bench (Appendix D EC2) due to thermal cure: the thermal cure chosen has been taken from a former project of ISC [77]
- Loss due to heat treatment: [EC2 §10.5.2]:
  $\Delta\sigma_\theta = 0.5 * E_p * \alpha_c$, with $\alpha_c = 10^{-5}$ the linear coefficient of thermal expansion
- Calculation of deferred prestressing losses. (EC2 5.46):

$$\sigma_{m,t}(x) = \sigma_{pm0}(x) - \Delta\sigma_{c+s+r}(x)$$

$$\Delta\sigma_{c+s+r} = \frac{\epsilon_{cs} E_p + 0.8 * \Delta\sigma_{pr} + \frac{E_P}{E_{cm}} \phi(t,t_0) \sigma_{c,QP}}{1 + \frac{E_p}{E_{cm}} \frac{A_p}{A_c} (1 + \frac{A_c}{I_c} z_{cp}^2)(1 + 0.8\phi(t,t_0))}$$

with:
- ϵ_{cs} the total value of shrinkage in absolute value
- E_{cm} the Young's modulus of concrete $E_{cm} = 22(\frac{f_{cm}}{10})^{0.3}$ (MPa)
- $\phi(t,t_0)$ the creep coefficient at time t for a loading applied at time t_0
- $\sigma_{c,QP}$ the stress near the rebars in concrete under self-weight, initial prestress, and quasi-permanent loadings
- $\Delta\sigma_{pr}$ the absolute value of stress variation in prestressing steel due to relaxation under quasi-permanent combination
- A_c the concrete cross-section area
- I_c the concrete cross-section inertia
- z_{cp} the distance between the center of gravity of the section and the center of gravity of strands

- A_p the area of one strand

At the serviceability limit state, two characteristic boundary values are used for the prestress force:
$P_{k,sup} = 1.05P_{m,t}(x)$ and $P_{k,inf} = 0.95P_{m,t}(x)$. Other hypotheses such as the construction schedule, and the relative humidity come from the CSTB guide [79].

Design checks for SLS (§7.2 EC2) As the beam is considered isostatic, the bending moment for a combination of forces resulting of a distributed force q and a point load Q is given by:
$M = \frac{qL^2}{8} + \frac{QL}{4}$, L being the span of the beam.
Thus, the compression force in concrete is given by
$\sigma_c = \frac{P}{A_c} + \frac{M-Pe}{I_c} z_{cp}$ and the tension force by $\sigma_{ct} = \frac{P}{A_c} - \frac{M-Pe}{I_c} z_{cp}$, with:
-P the prestress force
-M the bending moment of the beam
-e the eccentricity of the prestress cables

Design checks have to be made at SLS both for concrete and for prestressing steel. With regard to concrete, the following checks must be carried out for the compression stress σ_c:

- $\sigma_c \leq 0.7 f_{ck}(t)$ when releasing the prestress cables
- $\sigma_c \leq 0.6 f_{ck}$ under characteristic loading (for exposure classes XD,XF,XS)
- $\sigma_c \leq 0.45 f_{ck}$ under quasi-permanent loading for a linear creep
- $\sigma_c \leq f_{ctm}$ for uncracked concrete

With regard to prestressing steel:
$\sigma_{pm} \leq 0.8 f_{pk}$ under characteristic loading.

The deflection of the beam has also to be checked, it must not exceed a value of $\frac{l}{250}$, l being the span, both for the instant deflection and the deflection at an infinite time calculated via the creep coefficient $\phi(\infty, t_0)$: $f_\infty = (1 + \phi(\infty, t_0)) f_{inst}$.
As the beam is considered isostatic, the deflection is given for an elastic behavior by:

$$f_{inst} = \frac{M_{QP} L^2}{9.6 * E_c * I_z} - \frac{P_m e L^2}{8 E_c I_z}$$

M_{QP} is the bending moment for the quasi-permanent loading and I_z the inertia of the beam along its bending axis.

Design checks for ULS (§3.6 EC2) At ULS, the compression in concrete can be modeled as a rectangular stress of value ηf_{cd} with a height of λx, x being the height of the compressed zone, and

- $\lambda = \begin{cases} 0.8 & \text{if} f_{ck} \leq 50MPa \\ 0.8 - (f_{ck} - 50)/400 & \text{if } 50 < f_{ck} \leq 90MPa \end{cases}$
- $\eta = \begin{cases} 1 & \text{if} f_{ck} \leq 50MPa \\ 1.0 - (f_{ck} - 50)/200 & \text{if } 50 < f_{ck} \leq 90MPa \end{cases}$

Figure 12 illustrates the strains and stresses in the beam at ULS.

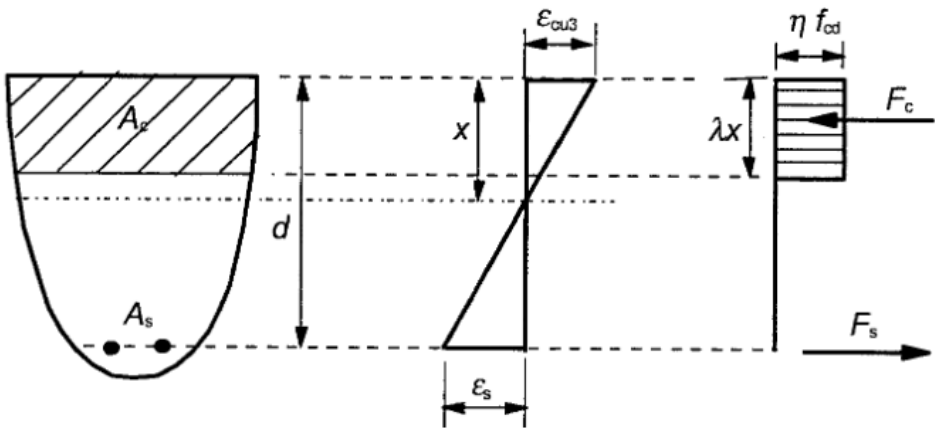

Figure 12: ULS repartition of forces in prestressed concrete [78]

With regard to the prestressing steel, one needs to define the stress-strain relationship. The chosen diagram is the one with a horizontal step. The step value is of $fp_{01k}/1.15$ for prestressing steel (Figure 13);

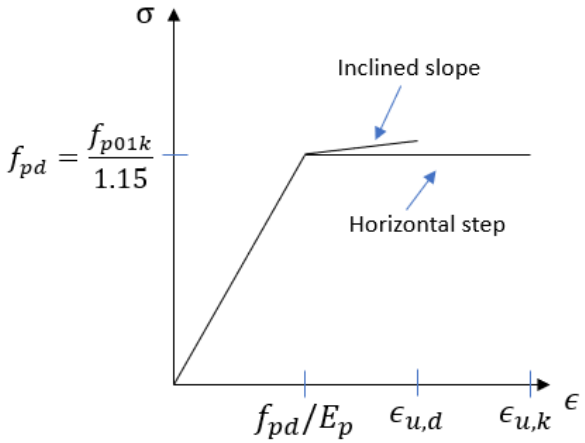

Figure 13: Stress strain relationships for prestressing steel

The balance of the forces on the section leads to the value of x which leads to the value of the resisting moment M_{Rd}:

$$N_{int} = N_{concrete} - N_{prec,supp}P_{m,\infty}$$
$$M_{Rd} = N_{concrete} * (d_p - d_{cog})$$

- d_p is the position of the center of gravity of prestressing steel
- d_{cog} is the center of gravity of the compressed zone

With regard to this, it is possible to check whether $M_{Rd} \geq M_{Ed}$, M_{Ed} is the maximum bending moment in the beam at ULS.

The shear force in the beam must not exceed the resistive shear force ($V_{Rd,max}$) :

$$V_{Rd,max} = \frac{\alpha_{cw} b_{web} z \nu_1 f_{cd}}{tan(\theta) + cotan(\theta)}$$

- $\alpha_{cw} = \begin{cases} 1 + \sigma_{cp,tr}/f_{cd} & \text{if } \sigma_{cp,tr} < 0.25 f_{cd} \\ 2.5 * (1 - \sigma_{cp,tr}/f_{cd}) & \text{if } 0.25 f_{cd} \leq \sigma_{cp,tr} \leq 0.5 f_{cd} \\ 0 & \text{otherwise} \end{cases}$
- $\sigma_{cp,tr} = \frac{N_{ELU}}{b_{web} * h + A_s * 15}$, $N_{ELU} = P_{k,inf,tot}$ and b_{web} the width of the web

- A_s the total area of longitudinal prestressing steel
- θ the strut angle (taken as 30°)
- $\nu_1 = \begin{cases} 0.6 & \text{if } fck \geq 60MPa \\ max(0.9 - f_{ck}/200, 0.5) & \text{otherwise} \end{cases}$

The shearing stress of the webs (σ_1) should not go over a value of $\sigma_1 \leq f_{ctb} = (1-0.8\sigma_3/f_{ck})f_{ctk,005}$,
$\sigma_3 = min(\sigma_c, 0.6f_{ck})$,
$\sigma_1 = VS_1/I_z b_{web}$,
S_1 is the static moment with respect to the bending axis of the zone of the section located above the point considered

3.4.3 Definition of penalty parameters

For each of the conditions that need to be satisfied (ex :$v \leq v_{max}$), a penalty parameter is defined: $Py_i = c_i max(0, \frac{v-v_{max}}{v_{max}})^2$ The c_i parameters are defined such that they give more importance to the conditions that are mostly not satisfied (determined empirically by writing at each iteration of the algorithm, which conditions are not verified).
The different conditions are the following:

- ULS checks:
  - Shear: $Py_{shear} = 10 * max(0, \frac{V_{ELU}-V_{Rd,max}}{V_{Rd,max}})^2$
  - Shearing in the webs: $Py_{shear,w} = max(0, \frac{-f_{ctb}-\sigma_1}{f_{ctb}})^2$
  - Bending resistance: $Py_{bend} = 1000max(0, \frac{M_{Ed}-M_{Rd}}{M_{Rd}})^2$
- SLS checks
  - Short-term deflection: $Py_{def,s} = max(0, \frac{f_{inst}-f_{max}}{f_{max}})^2$
  - Long-term deflection: $Py_{def,inf} = max(0, \frac{f_{inf}-f_{max}}{f_{max}})^2$
  - Compression in concrete under characteristic loading: $Py_{c,compr} = max(0, \frac{\sigma_c-0.6*f_{ck}}{0.6*f_{ck}})^2$
  - Traction in concrete under characteristic loading: $Py_{c,trac} = 100*max(0, \frac{\sigma_{c,ct}-1.5*f_{ctm}}{1.5f_{ctm}})^2$
  - Stress in longitudinal reinforcement under characteristic loading: $Py_{c,rein} = max(0, \frac{\sigma_{pm}-0.8f_{ck}}{0.8f_{ck}})^2$
  - Compression in concrete under quasi-permanent loading: $Py_{QP,compr} = max(0, \frac{\sigma_{c,QP}-0.45f_{ck}}{0.45f_{ck}})^2$
  - Decompression in concrete under frequent loading: $Py_{compr,fr} = max(0, \frac{-f_{ctm}-\sigma_{ct,fr}}{f_{ctm}})^2$

Then all those penalty parameters are summed and multiplied by a penalty factor, which is chosen with a value of 1000:

$$Py_{tot} = 1000 \sum_i Py_i$$

The 1000 value was chosen so that solutions for which design checks are not passed will not be selected by the algorithm while having a value that is not too high to avoid being stuck in a local optimum. This value has been determined via tests where each time it was checked whether it was possible to optimize by hand the solution (meaning that the solution was not the optimal one) or if the solution given at the end did not meet requirements.
It has to be kept in mind that this value of 1000 was designed when optimizing the climate change indicator (short or long-term). If another indicator was optimized, a first simulation was performed to observe the order of magnitude between the value of climate change and the one of the indicator studied so as to divide the value of 1000 by this order of magnitude.

3.4.4 LCA of PBPA

Choice of the studied indicators Based on the procedure described in the LCA section, the indicators chosen for the analysis of PBPA beams are chosen by their amount of participation in the endpoint indicators (human health and ecosystem quality). Three different materials are used for PBPAs: concrete, reinforcing, and prestressing steel. For each one of those materials, the contribution of midpoint to endpoint indicators has been analyzed. From this analysis, six midpoint indicators have been chosen based on a 5% hurdle of participation to at least one of the endpoint indicators for at least one of the materials used for the fabrication of the beam (knowing that there were the same for the six typologies):

- Freshwater ecotoxicity (CTU_e)
- Climate Change, long term ($kgCO_{2,eq}$)
- Particulate Matter formation ($kgPM2.5_{eq}$)
- Water scarcity ($m^3_{world,eq}$)
- Climate change, short term ($kgCO_{2,eq}$)
- Human toxicity cancer (CTU_h)

The two endpoint indicators (human health and ecosystem quality) have also been studied.

As an example, the participation of midpoint indicators in human health and ecosystem quality for C30/37 conventional concrete used for buildings is given in Figure 14.

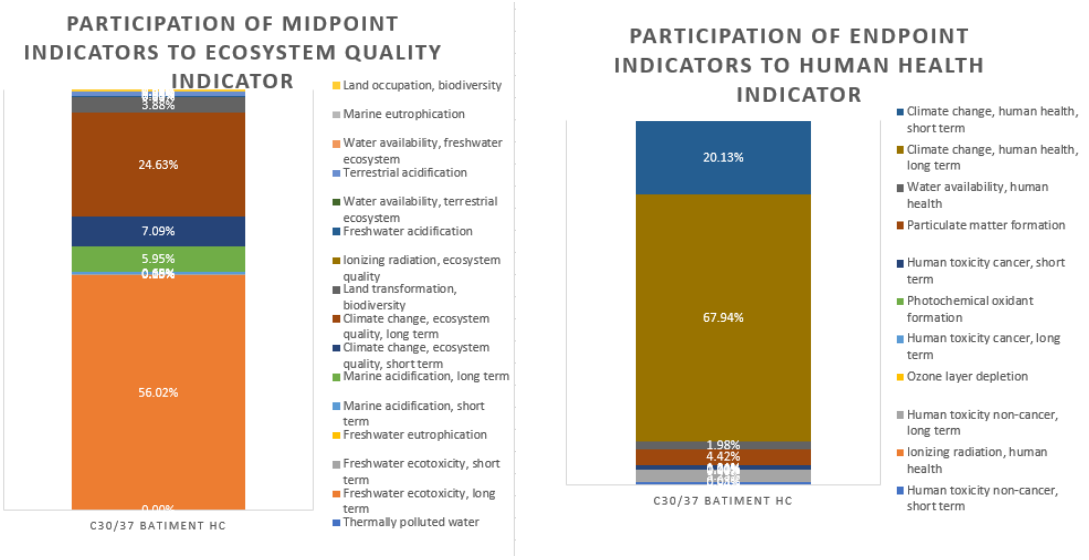

Figure 14: Contribution of midpoint indicators to endpoint indicators for conventional C30/37 concrete

3.5 Reinforced concrete beams

3.5.1 Rectangular beams

Inputs Compared to the PBPAs, rectangular reinforced concrete beams have fewer input parameters as they only require height (h) and width (b) to describe their geometry. The resistance of concrete is also an input to optimize.
The optimistic and pessimistic scenarios can both be implemented (100 or 44% recycled steel and classic or low-carbon concretes).

Design of the section at ULS When designing the concrete section at ULS, several cases are considered according to the three-pivot diagram (Figure 15).

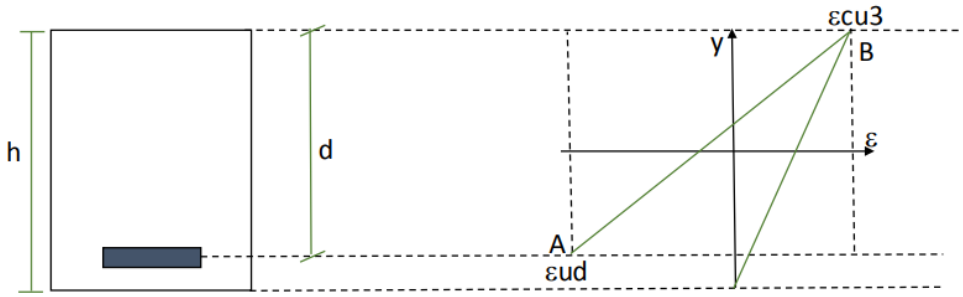

Figure 15: Three-pivot diagram [81]

At ULS, it is supposed that the diagram of strains passes through one of the pivots (A or B in flexion, C in compression), ϵ_{ud}, and ϵ_{cu3} being defined as for PBPA. When it passes through point A, it means that steel works at its best ($\epsilon_s = \epsilon_{ud}$), through point B, that concrete works at its best ($\epsilon_s = \epsilon_{cu3}$), and through point C that the entire section is under compression.
In this case, the simplified rectangular diagram is also used as for PBPAs (Figure 12).
The first limit case is when there is a pivot both at points A and B. When noting $\mu = \frac{M}{bd^2\eta f_{cd}}$ the scaled moment and $\alpha = \frac{x}{d}$, d being the distance from the reinforcing bar's center of gravity to the top of the section and x the distance to the neutral axis to the top of the section, we have three cases:

- If $M < M_{AB}$ or $\alpha < \alpha_{AB}$ or $\mu < \mu_{AB}$: pivot at A
- If $M = M_{AB}$ or $\alpha = \alpha_{AB}$ or $\mu = \mu_{AB}$: pivot at A and B
- If $M > M_{AB}$ or $\alpha > \alpha_{AB}$ or $\mu > \mu_{AB}$: pivot at B

,with $\alpha_{AB} = \frac{\epsilon_{cu3}}{\epsilon_{cu3}+\epsilon_{ud}}$ and $\mu_{AB} = \frac{M_{AB}}{bd^2\eta f_{cd}}$.

In this study, the compressed steels in the upper part of the section are not considered to participate in the resistance but are nevertheless taken into account in the LCA. If concrete works at its best and steels are at their elastic limit (BE diagram): $\mu_{BE} = \frac{M_{BE}}{bd^2\eta f_{cd}}$ $\alpha_{BE} = \frac{\epsilon_{cu3}}{\epsilon_{cu3}+\epsilon_{se}}$. Then if $\mu > \mu_{BE}$ or $\alpha > \alpha_{BE}$ or $M > M_{BE}$, the solution must be penalized because the bending moment is too high. The stress-strain diagram that has been considered for steel is the one of Figure 16 with a factor $k = 1.08$.

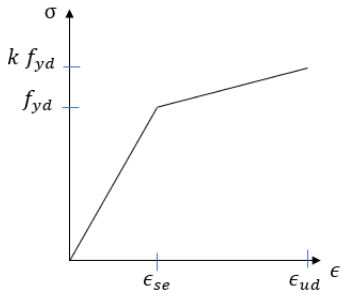

Figure 16: Stress-strain relationship for steel [81]

The required section of longitudinal reinforcement A_s is determined via the following procedure: A first guess of a value of d is made $d = 0.9h$, with this value and the value of the bending moment, it is possible to have access to the value of x. Then three cases have to be investigated:

- If $x < x_{AB}$: pivot at A : $A_s = \frac{\lambda b\eta f_{cd} x}{k f_{yd}}$
- If $x_{AB} < x < x_{BE}$: pivot at B: $A_s = \frac{\lambda d\eta f_{cd} x}{\sigma_s}$, σ_s can be found via the stress-strain diagram for steel after having computed ϵ_s
- If $x > x_{BE}$, the solution is penalized

Then, the required total area of steel is translated in terms of layers and rebars of a certain diameter. It leads to a new value of d. Until the value of d is different from the one at the beginning of this process, the procedure is repeated, to design with a value of d that is accurate. In general, three iterations are enough.

The process to translate the total required reinforcement area in bars and layers is described in Figure 17. The rules to create an appropriate layout are the following:

- There should not be only one bar in the section
- The same diameter is used for the rebars in the same layer
- Rebars of a layer have diameters that are at least equal to the ones of the layer below
- The layout is symmetric

- A rebar of an upper layer is always placed above another rebar

The two layers of reinforcing steel are superimposed directly on top of each other, with the third layer at a distance of 5 cm from the layer below.

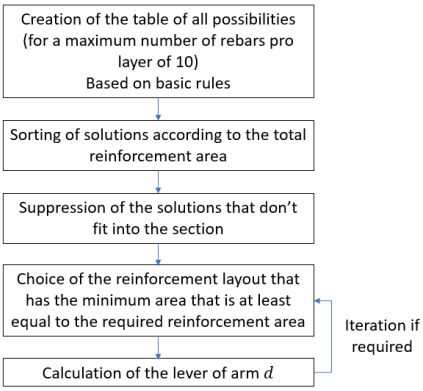

Figure 17: Procedure to choose the reinforcement layout

Once the longitudinal reinforcement layout has been chosen, the shear reinforcement layout has also to be defined.
The maximum shear in the section is V_{Ed} and the maximum resisting shear force of the section is

$$V_{Rd,max} = \frac{\alpha_{cw} b z \nu_1 f_{cd}}{tan(\theta) + cotan(\theta)}$$

with:
$\alpha_{cw} = 1$
θ the inclination angle of the struts varying from 22 to 45°
$\nu_1 = \begin{cases} 0.6 & \text{if } f_{ck} < 60MPa \\ min(0.9 - f_{ck}/200, 0.5) & \text{otherwise} \end{cases}$
z is the lever arm of the longitudinal reinforcement $z \approx 0.9d$

So as to minimize the volume of shear reinforcement, the angle θ should be as low as possible. The test $V_{Ed} \leq V_{Rd,max}$ is done first for $\theta = 22°$, if this does not work, a higher value of θ is used by steps of 2°. If at the end of the process, θ is larger than 45°, then the shear force is too high, which means that the solution has to be penalized.
Once θ has been found, the number of struts in the beam can be found. For each strut i, the shear force is computed. If $V_{Ed,i} > V_{Rd,c}$ (the design shear resistance of the member without reinforcement), then a shear reinforcement layout is defined with an area of:

$$A_{sw} = \frac{V_{Ed}}{z f_{yd}} tan(\theta)$$

$V_{Rd,c} = max(C_{Rd,c} k_{tr} (1000 \rho_1 f_{ck})^{1/3} bd, \nu_{min} db)$
$C_{rd,c} = \frac{0.18}{\gamma_c}$
$\rho_1 = min(0.02, \frac{A_s}{bd})$
$k_{tr} = min(1 + (200/d)^{0.5}, 2)$, d is in mm
$\nu_{min} = 0.035 k_{tr}^{2/3} \sqrt{f_{ck}}$

Otherwise, ($V_{Ed,i} \leq V_{Rd,c}$), only nominal transverse reinforcements are placed $\rho_{min} = \frac{0.08\sqrt{f_{ck}}}{f_{yk}}$
Once the required area is defined, the spacing, number, and diameter of shear reinforcement need to be defined. A maximum spacing is first chosen: $s_{l,max} = 0.75d$. If for this spacing a number of ties in the section with a certain diameter is found, this layout is chosen, if not, a shorter spacing is chosen and the process iterates till a convenient spacing is found. The spacing is then modified to become a multiple of the length of the strut by choosing a spacing that is smaller than the one found before to ensure the shear resistance. The number of ties in the section depends on the longitudinal rebars, as there can be only one vertical rebar per longitudinal rebar and a minimum of two transversal rebar has been taken as there are always two rebars in the upper part of the section.

Design of the section at SLS Now that the reinforcement layout is known, one needs to check whether it passes also the SLS design checks. The hypothesis is made that both concrete and steel are in their elastic domain at SLS.
The ratio $\alpha_e = \frac{E_s}{E_c}$ is fixed at a value of 15, which is a safe value often considered bu engineers.
The diagram of stresses and strains is described in Figure 18.

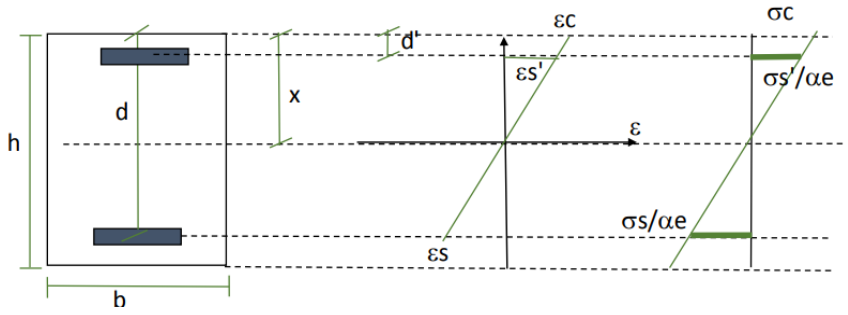

Figure 18: Stresses and strains along the height of the section at SLS [81]

For the SLS, the reinforcement in the upper part of the section is also not considered. The neutral axis position x needs once again to be determined as it is not the same at the ULS. The equation to determine it is :

$$b\frac{x^2}{2} + \alpha_e A_s x - \alpha_e d A_s = 0$$

The stresses of the section are determined via the relations:

$$\sigma_c = \frac{M}{\alpha_e A_s (d-x)^2 + b\frac{x^3}{3}} x$$

$$\sigma_s = \alpha_e (d-x)\frac{\sigma_c}{x}$$

The different design checks that need to be performed are the following:

- $\sigma_s \leq 0.8 f_{yk}$
- $\sigma_c \leq 0.6 f_{ck}$

If the two conditions are met, then the SLS checks are completed. If $\sigma_c \leq 0.6 f_{ck}$ and $\sigma_s > 0.8 f_{yk}$, it is possible to increase the total amount of reinforcing steel:

$$A_s = \frac{bx^2}{\alpha_e (d-x)}$$

Once again iterations are required in order to be sure that the d used for the formula above is the one of the exact reinforcement layout. If $\sigma_c > 0.6 f_{ck}$ the solution will be penalized, the section can not meet requirements without considering upper reinforcing bars.

The opening of cracks should also be controlled. Clause 7.3.3 (101) of Eurocode 2 is used as a simplified method. The maximum opening of cracks is defined depending on the exposure class ($w_{max} = 0.4mm$ for building beams and $w_{max} = 0.3mm$ for bridge beams). The stress in the reinforcement bars (in MPa) must be inferior to a value that is 1000 times the maximum opening crack (in mm).

$$\sigma_s(MPa) > 1000 w_{max}(mm)$$

The deflection of the beam under quasi-permanent loading is limited. A simplified method was used (§7.4.2 EC2). If the ratio $\frac{l}{h}$ is higher than a maximum value $\frac{l}{h}_{max}$, then it means that the deflection of the beam is too high.

$$(\frac{l}{h})_{max} = \begin{cases} K(11 + 1.5\sqrt{f_{ck}}\frac{\rho_0}{\rho} + 3.2\sqrt{f_{ck}}(\frac{\rho_0}{\rho} - 1)^{3/2}) & \text{if } \rho \leq \rho_0 \\ K(11 + 1.5\sqrt{f_{ck}}\frac{\rho_0}{\rho - \rho'} + \frac{1}{12}\sqrt{f_{ck}}\sqrt{\frac{\rho'}{\rho_0}}) & \text{otherwise} \end{cases}$$

- K is a coefficient taking into account the structural system considered
- $\rho_0 = 10^{-3}\sqrt{f_{ck}}$ is the reference ratio of reinforcement
- ρ is the maximum ratio of longitudinal traction reinforcement in the beam
- ρ' is the maximum ratio of longitudinal compression reinforcement in the beam

Penalty parameters Design checks are similar to the ones for prestressed beams

- ULS checks:
  - Flexion: Need of rebars in compression or too many rebars required: $Penalty_{flex} = 100 * max(0, \frac{\mu - \mu_{BE}}{\mu_{BE}})^2$
  - Shear: Too much stress in the struts: $Penalty_{tr} = 10 * max(0, \frac{\theta - \pi/4}{\pi/4})^2$
- SLS checks
  - Flexion: Too much compression in concrete $Penalty_{compr} = 10 * max(0, \frac{\sigma_c - 0.6 * f_{ck}}{0.6 f_{ck}})^2$
  - Openings of cracks too high either for characteristic, frequent and quasi-permanent load case: $Penalty_{crack} = 500 max(0, \frac{\sigma_s - 1000 * w_{max}}{1000 * w_{max}})^2$
  - Deflection too high: $Penalty_{def} = 10 max(0, \frac{\frac{l}{h} - \frac{l}{h}_{max}}{\frac{l}{h}_{max}})^2$

Other considerations The reinforcement calculated before is the one required for the maximum bending moment (at mid-section). This amount of steel is not required for the entire length of the beam. Thus, when multiple layers are considered, the upper one is removed and the maximum bending moment M_i for this new section of steel is calculated. Then, the abscissa of the point where $M = M_i$ is calculated. It is then possible to remove the upper layer at this specific point. If there are three layers, the same process is used to remove the second layer. This process is called bar-stopping.

The calculation of the total volume of steel includes the anchorages of the rebars as well as the overlap of the rebars. In fact, the maximum length of rebars is 12m (the maximum length that trucks can move on the road). So for beams longer than 12m, two or more rebars are required so as to be modeled as one single bar along the entire length of the beam. An overlap is necessary to ensure the transfer of forces between the different bars. This one is the following:
$l_{overlap} = max(0.3 * 1.15 * l_{brqd}, 10\phi_{max}, 200)mm$,
$l_{bqrd} = \frac{\phi_{max}}{4 f_{bd}} f_{yd}$
$f_{bd} = 2.25 \nu_1 \nu_2 f_{ctd}$,
$\nu_1 = 1$
$\nu_2 = \begin{cases} 1 & \text{if } \phi_{max} \leq 32mm \\ (132 - \phi_{max})/100 & \text{otherwise} \end{cases}$
ϕ_{max} being the maximum diameter of the rebars.
The anchorage length of the rebar is of $l_{anch} = max(0.3 l_{bqrd}, 10\phi_{max}, 100)mm$

LCA As for PBPAs, concrete and steel are the two main and only components of reinforced concrete beams. Therefore, the choice of indicators is the same as for PBPAs.

3.5.2 I-shaped beams

Specific features The inputs of I-beams are the same as for PBPA (geometric parameters, resistance of concrete) except the fact that the amount of reinforcing steel is calculated within the workflow whereas for PBPA the amount of prestressing steel was an input.
I-beams design checks are very similar to rectangular beams. The differences rely on the fact that when calculating the area of concrete under compression, one needs to consider that the width of the section varies with the height. An effective width of the compressed zone of the beam is defined depending on the height of the compressed zone. It is calculated as the average value of the width along the height of the compressed zone x. It is calculated as such, with h_{head} and b_{head} the height and width of the head of the beam and d_{head} the height of the upper inclined part of the beam:

$$b_{eff} = \begin{cases} b_{head} & \text{if } x < h_{head} \\ \frac{b_{head} h_{head} + (x - h_{head}) b_{head} - (x - h_{head})^2 (b_{head} - bame)(2 d_{head})}{x} & \text{if } h_{head} < x < h_{head} + d_{head} \\ \frac{b_{head} h_{head} + (x - h_{head} - d_{head}) b_{web} + d_{head} b_{head} - d_{head} (b_{head} - b_{web})/2}{x} & \text{otherwise} \end{cases}$$

3.5.3 Optimized beams

Optimal height of the struts This part is based on the work of S. Maitenaz during his Ph.D. [11]. His work stems from the statement that only part of the concrete beams contribute to its structural capacity, and that it is possible to keep only the struts and the concrete around the ties and leave the rest hollow using a "truss-analogy" method.

Two resisting forces appear in EC2, the design value of the shear force which can be sustained by the shear reinforcements $V_{Rd,s}$, and to the design value of the maximum shear force which can be sustained by the strut in compression $V_{Rd,max}$

$$V_{Rd,s} = \frac{A_{sw}}{s} z f_{yd} cot\theta$$

$$V_{Rd,max} = \alpha_{cw} b_w z \nu_1 f_{cd} \frac{cot\theta}{1 + cot^2\theta}$$

In order to identify the height of the strut in the expression of $V_{Rd,max}$ above, it is possible to use trigonometric formulas, as $h_{strut} = zsin\theta$ as can be seen in Figure 19.

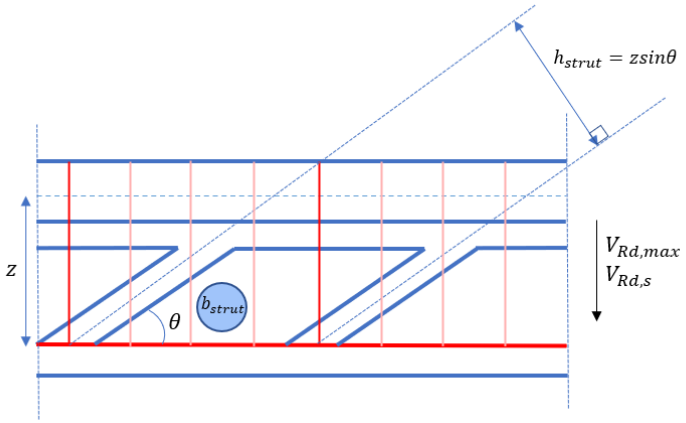

Figure 19: Relation between the height of the strut, its inclination and the lever of arm [11]

Thus,

$$V_{Rd,max} = \alpha_{cw} \nu_1 f_{cd} b_{strut} h_{strut} sin\theta$$

One still needs to check whether $V_{Rd,max} \geq V_{Ed}$. As it is the only constraint concerning this quantity, it is thus possible to optimize the matter while meeting this requirement. Two optimization parameters are at hand: the height and width of the strut. As in this study the width of the strut b_{strut} does not change along the beam, only the optimization of the height of the strut is considered. After some calculations, the optimal height of the strut was found as:

$$h_{strut} = zsin\theta \frac{V_{Ed}}{V_{Rd,max}}$$

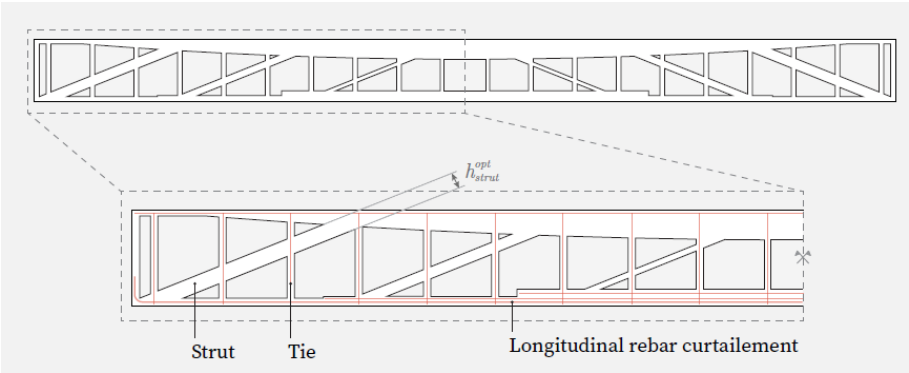

Figure 20: Optimal height of the strut [11]

Optimal transversal reinforcement To minimize the amount of concrete used for the beam, the transversal rebars need to be as far apart as possible. The minimum shear reinforcement required is:

$$A_{sw,min} = s\frac{V_{Ed}}{z f_{yd} cot\theta}$$

The maximum distance between two shear reinforcement rebars is of $s_{l,max} = 0.75d$. Thus, the procedure to find the appropriate transversal reinforcement layout is the following:

1. Try the largest value of s and the lowest diameter of the rebars ϕ with a single tie in the section (with one or two branches depending on the longitudinal layout)
2. If the solution does not meet requirements, the diameter of the bars is increased
3. If it still does not work with the largest diameter, the number of rebars in the section is increased (if possible), and the procedure is repeated
4. If for the largest diameter of rebars and the maximum number of rebars in the section, it does not meet requirements, s is reduced by steps of $5cm$.

The shear reinforcement layout should also meet the following requirements:

- Each longitudinal rebar is in contact with one shear rebar and reciprocally
- The spacing between two transversal rebars s_l should be at least equal to $10cm$ regarding the feasibility for the construction
- The distance s_t between two bars in the same plan should meet $s_t \leq min(0.75d, 0.6)$ (Eurocode)
- The spacing s_l takes values multiples of $5cm$ for the sake of simplicity on the construction site

3.6 Timber beams

As timber is an isotropic material, it is defined by characteristic mechanical properties along its different axes (0 and 90° in relation to the fibers axis):

- $f_{m,0k}$, the bending resistance
- $f_{t,0k}$, the axial traction resistance
- $f_{t,90k}$, the transversal traction resistance
- $f_{c,0k}$, the axial compression resistance
- $f_{c,90k}$, the transversal compression resistance

The modulus of elasticity and the shear modulus are also defined along axes at 0 or 90 degrees to the wood fibers. Those properties differ regarding the type of timber considered (glued laminated or solid timber) and the resistance class.

For solid timber, a resistance class of C24 was chosen, and for glued laminated timber, the choice was left to the user of the optimization tool to pick either a GL24h or a GL28h. These values were considered as they are the most used for timber constructions both for buildings and civil engineering works.

Each design resistance value is calculated as :

$$R_d = R_k \frac{k_{mod}}{\gamma_m}$$

k_{mod} is a factor depending on the type of action (permanent, long term, etc.) and of the service class of the element that depends on the temperature and the humidity of the surroundings.
γ_m is equal to 1.25 for glued laminated timber and 1.3 for solid timber.

At the ULS, the different design checks are the following:

- Traction along the direction of the fibers: $\sigma_{t,0,d} \leq f_{t,0d}$
- Compression along the direction of the fibers: $\sigma_{c,0,d} \leq f_{c,0d}$
- Compression perpendicular to the direction of the fibers (mainly at the supports): $\sigma_{c,90d} \leq f_{c,90d}$
- Bending without risk of spillage $\frac{\sigma_{m,y,d}}{f_{m,y,d}} + k_m \frac{\sigma_{m,z,d}}{f_{m,z,d}} \leq 1$ and $k_m \frac{\sigma_{m,y,d}}{f_{m,y,d}} + \frac{\sigma_{m,z,d}}{f_{m,z,d}} \leq 1$, $k_m = 0.7$ for rectangular sections
- Shear resistance with an effective width taking into account cracks $b_{eff} = k_{cr} b$, k_{cr} depending on the service class and the type of timber

At the SLS, the design checks are the following:

- The instant deflection should be less than $l/300$, l being the span
- The long-term deflection should be less than $l/150$

3.7 Steel beams

Steel beams are available from a European catalog [82] and are described by their mechanical properties such as the inertia along the two axes of bending, the area, the linear density, etc. The profiles considered for this study are chosen among the following: IPE, IPN, HEA, HEB, HP, HD, and HL.

The steel resistance is determined using the steel grade. Only S355-grade steel was considered. Its resistance is of $f_y = 355MPa$ for a width of the web $t_w \leq 40mm$, and $f_y = 335MPa$ otherwise.

After having chosen a steel profile, its class is determined. The classes vary from 1 to 4, with class 1 being the highest-performance class.
The class is defined both for the web and the flanges. The lowest-performing class of the two is considered to describe the entire section. The term d corresponds to the height of the web, $c = (b - t_w)/2$ with b the width of the profile, t_w to the width of the web, and t_f to the thickness of the flanges as can be seen in Figure 21.

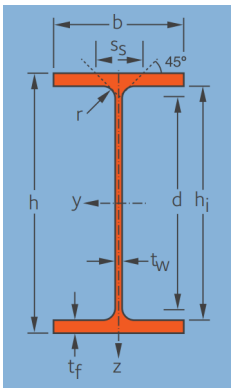

Figure 21: Dimensions of steel I- or H-sections [82]

Class 1 sections can reach their plastic strength without the risk of local buckling and have a high rotation capacity that can form a plastic hinge. $\frac{d}{t_w} \leq 72\epsilon$, $\frac{c}{t_f} \leq 9\epsilon$

Class 2 sections can also reach plastic strength without the risk of local buckling, but have limited rotational capacity. $\frac{d}{t_w} \leq 83\epsilon$, $\frac{c}{t_f} \leq 10\epsilon$

Class 3 sections can reach their elastic strength in extreme fiber, but not their plastic strength, due to the risk of local buckling. $\frac{d}{t_w} \leq 124\epsilon$, $\frac{c}{t_f} \leq 14\epsilon$

Class 4 sections cannot reach their elastic strength due to the risk of local buckling. $\frac{d}{t_w} > 124\epsilon$, $\frac{c}{t_f} > 14\epsilon$

With $\epsilon = \sqrt{\frac{235}{f_y}}$, f_y being in MPa.

Class 4 sections are usually avoided as they cause problems for the design of steel beams. Thus, class 4 sections were deleted from the catalog considered.

Design at ULS The resisting shear of the sections is given as:

$$V_{plRd} = \frac{A_{vz} f_y}{\sqrt{3}\gamma_{M0}}$$

γ_{M0} is the security factor for ULS $\gamma_{M0} = 1$.
A_{vz} is the shear area and is given in the catalog.
The following verification needs to be considered: $V_{Ed} \leq V_{plRd}$.
Furthermore, if $V_{Ed} > \frac{1}{2}V_{plRd}$, the resisting bending of the section is multiplied by a factor $\rho = (\frac{2V_{Ed}}{V_{plRd}} - 1)^2$, otherwise $\rho = 1$.
Considering the resisting bending, the design check is $M_{Ed} \leq M_{Rd}$, M_{Rd} depending on the section's class.

$$M_{Rd} = \begin{cases} \rho f_y \frac{W_{pl,y}}{\gamma_{M0}} & \text{for Classes 1 and 2} \\ \rho f_y \frac{W_{el,y}}{\gamma_{M0}} & \text{for Class 3} \end{cases}$$

$W_{el,y}$ and $W_{pl,y}$ are the elastic and plastic bending moduli of inertia.

Furthermore, if the section considered is an I section, which is the case for all the sections considered, M_{Rd} becomes:

$$M_{Rd} = min(M_{Rd}, (W_{pl,y} - \frac{\rho A_w^2}{4t_w})\frac{f_y}{\gamma_{M0}})$$

A_w is the area of the web.

The ULS design checks also include the checks considering Lateral Torsional Buckling (LTB) with the calculation of a maximum bending M_{bRd}.

$$M_{bRd} = \chi_{LT}\beta_w W_{pl,y}\frac{f_y}{\gamma_{M1}}$$

$$\chi_{LT} = min(1, \frac{1}{\Psi_{LT} + \sqrt{\Psi_{LT}^2 - \bar{\lambda}_{LT}^2}})$$

$$\Psi_{LT} = \frac{1}{2}(1 + \alpha_{LT}(\bar{\lambda}_{LT} - 0.2) + \bar{\lambda}_{LT}^2)$$

$$\bar{\lambda}_{LT} = \sqrt{\beta_w} W_{pl,y}\frac{f_y}{M_{cr}}$$

$$M_{cr} = C_1\pi^2\frac{EI_z}{L^2}(\sqrt{(C_2 z_g)^2 + \frac{I_w}{I_z} + \frac{L^2 G I_t}{\pi^2 E I_z}} - C_2 z_g)$$

$$\alpha_{LT} = \begin{cases} 0.21 & \text{for rolled I sections and } \frac{h}{b} \leq 2 \\ 0.34 & \text{for rolled I sections and } \frac{h}{b} > 2 \\ 0.49 & \text{for welded I sections and } \frac{h}{b} \leq 2 \\ 0.76 & \text{otherwise} \end{cases}$$

$$\beta_w = \begin{cases} 1 & \text{for Classes 1 and 2} \\ \frac{W_{el,y}}{W_{pl,y}} & \text{for Class 3} \end{cases}$$

γ_{M1} is the security coefficient for LTB

$$\gamma_{M1} = \begin{cases} 1 & \text{for buildings} \\ 1.1 & \text{for bridges} \end{cases}$$

As seen in the formulas above, calculating the critical bending requires calculating the values of C_1, C_2, and z_g. C_1 and C_2 are constants depending on the loading and support types of the beam.
For an isostatic beam under uniform loading $C_1 = 1.13$ and $C_2 = 0.46$. For an isostatic beam

under point load at mid-span, $C_1 = 1.35$, and $C_2 = 0.55$. As the load considered in this study is a combination of both, C_1 and C_2 are calculated as a weighted sum of the two load cases [83].

$$C_i = \frac{M_u C_{i,u} + M_p C_{i,p}}{M_u + M_p}$$

The letter p stands for punctual loading and u for uniform loading, M_p is the bending at mid-span under punctual loading and M_u is the bending at mid-span under uniform loading.
z_g stands for the distance between the force's point of application to the section's shear center. In this study, the self-weight is applied at the shear center ($z_g = 0$) but the additional loads are applied on the top of the section ($z_g = \frac{h}{2}$). A similar weighted sum was used to calculate an average z_g based on the bendings caused by each loading type.

The calculations of M_{cr} for different load cases have been compared to the results of the LT-Beam software [84] and the differences obtained were of the order of 0.3%, which validates the relations used for C_1, C_2 and z_g.

The lateral torsional buckling effect was only considered for building applications as for bridges, this effect will not be limiting. In fact, bracings are often installed to counteract this effect. The amount of connections taken into account in the LCA calculations includes those bracings.

Core shear buckling is a phenomenon that can appear for slender beams and needs to be considered for the design. The beam was considered with no transversal stiffeners. For this type of beam, the core shear buckling has to be checked when $\frac{b}{t_w} \leq \frac{72\epsilon}{\eta}$, $\eta = 1.2$ for S355 steel. If this condition is not met, an additional check is made:

$$V_{Ed} \leq V_{bw,Rd} + V_{bf,Rd} = \chi_w A_w \frac{f_y}{\sqrt{3}\gamma_{M1}} + V_{bf,Rd}$$

A_w is the area of the web, $V_{bw,Rd}$ is the participation of the web to the resistance and $V_{bf,Rd}$ the one of the flanges and the uprights.
χ_w is determined via the calculation of the critical shear τ_{cr}, given by:

$$\tau_{cr} = k_\tau \sigma_E = k_\tau \frac{\pi^2 E}{12(1-\nu^2)} (\frac{t_w}{b})^2$$

b is the height of the section ($b = h_w$)
a is the distance between two transversal stiffeners (in this study $a = L$)
α is defined as the ratio of a over b $\alpha = \frac{a}{b}$
Then, it is possible to have access to k_τ

$$k_\tau = \begin{cases} 4 + \frac{5.34}{\alpha^2} & \text{if } \alpha \leq 1 \\ 5.34 + \frac{4}{\alpha^2} & \text{if } \alpha > 1 \end{cases}$$

This critical shear leads to the value of $\bar{\lambda}_w = \sqrt{\frac{f_y}{\tau_{cr}\sqrt{3}}}$ what leads to the value of χ_w. For a non-rigid end post, the relation is the following:

$$\chi_w = \begin{cases} \eta & \text{if } \bar{\lambda}_w < \frac{0.83}{\eta} \\ \frac{0.83}{\bar{\lambda}_w} & \text{otherwise} \end{cases}$$

On the other side, $V_{bf,Rd}$ is calculated via these relations:
$V_{bf,Rd} = \frac{b_f t_f^2 f_{yf}}{c\gamma_{M1}}(1 - (\frac{M_{Ed}}{M_{f,Rd}})^2)$, if $M_{Ed} \leq M_{f,Rd}$, otherwise $V_{bf,Rd} = 0$.
$c = L(0.25 + 1.6 * \frac{M_p l,f}{M_{pl,w}})$
with $M_{pl,f} = \frac{b_f t_f^2 f_{yf}}{4}$ the plastic hinge of the flange,
$M_{pl,w} = \frac{t_w h_w^2 f_{yw}}{4}$ the plastic bending of the web, and
$M_{f,Rd} = b_f t_f (h - t_f) \frac{f_y}{\gamma_{M0}}$ the resisting bending of the flanges alone.

If $V_{Ed} \leq V_{bf,Rd} + V_{bw,Rd}$, but $V_{Ed} \geq 0.5 V_{bw,Rd}$ or $V_{Ed} \leq V_{bw,Rd}$ and $M_{Ed} > M_{f,Rd}$ then the interaction of shear and bending has also to be checked. The following inequality has to be satisfied:

$$\bar{\eta}_1 + (1 - \frac{M_{f,Rd}}{M_{pl,rd}})(2\bar{\eta}_3 - 1)^2 \leq 1$$

with $\bar{\eta}_1 = \frac{M_{Ed}}{M_{pl,rd}}$
and $\bar{\eta}_3 = \frac{V_{Ed}}{V_{bw,Rd}}$

SLS design checks The deflection of the beam is limited to a certain value in order to ensure the serviceability of the building or bridge. In both cases, the maximum deflection was taken as $\frac{L}{250}$, L being the span of the beam. The calculation of the deflection is made using the elastic relations of deflections and loadings.

In the case of bridge applications, other checks are required. Under characteristic loading, the maximum stress and shear stress should remain under a certain value: $\sigma_{Ed} \leq \frac{f_y}{\gamma_{M,ser}}$ and $\tau_{Ed} \leq \frac{f_y}{\sqrt{3}\gamma_{M,ser}}$ with $\gamma_{M,ser} = 1$.

Under repeated loadings, the web deforms slightly out of plane and comes back to its initial position. This phenomenon is called web breathing and can cause cracks at the joint between the flanges and the web. As in this case study, transversal stiffeners are not considered, it is possible to neglect this effect if:

$$\frac{h_w}{t_w} \leq min(30 + 4L, 300), L \geq 20$$

Otherwise, under frequent loading, the following inequality has to be satisfied:

$$\sqrt{(\frac{\sigma_{x,Ed,ser}}{\sigma_{cr}})^2 + (1.1\frac{\tau_{x,Ed,ser}}{\tau_{cr}})^2} \leq 1.1$$

$\sigma_{cr} = k_\sigma \sigma_E$, with $\sigma_E = 190000(\frac{t_w}{h_w})^2 MPa$ and $k_\sigma = 0.85$ $\tau_{cr} = k_\tau \sigma_E$

Based on the requirements defined above, penalty functions have been defined in the same way as for the other typologies to ensure that the beam satisfies all the design checks once the optimization and performed.

3.8 Calculation of prices

As price is still in most applications what is determinant in the choice of a solution compared to another, it has been calculated and provided as information for each type of beam.
Price data was collected from professionals in the sector (Vinci subsidiary employees, suppliers) or from available catalogs (Polyvert, unit time catalog). The list of this data is provided in Appendix 3. Some data have been kept confidential, as they are taken from internal Vinci documents. These prices should be treated with caution, as they are averaged over data that is highly case-dependent and therefore not 100% reliable.

4 Presentation of the results

4.1 Performance of the algorithm

Setting of Wallacei As mentioned in a previous part of the report, Wallacei is based on a genetic algorithm. In order to set aside beams that do not meet requirements, a penalty factor was used.
$Penalty_{tot} = \frac{c}{2} \sum_i c_i Penalty_i$
Each of the individual penalty factors c_i was empirically determined based on which criteria was the least fulfilled for different types of beams. For example, if the bending resistance at ULS was the most constraining criterion for PBPA, the corresponding c_i was higher than the c_i of other criteria. Still, the global penalty factor c needs to be determined.
A factor c that is too low would lead to solutions that do not meet design requirements. Otherwise, if c is too high, the algorithm would struggle to cover a large range of solutions and take more time to converge.

Furthermore, different parameters define how the algorithm works:

- Number of generations and population per generation: they define the number of iterations, the more there is, the longer the simulation is but the more optimal it is as well
- Mutation probability: the percentage of mutations taking place in the generation (recommended value of $1/n$, n being the number of parameters to determine)

- Crossover probability: the percentage of solutions in the generation that will reproduce for the next generation (recommended value of 0.9)
- Crossover and mutation distribution index: a high distribution index gives more probability for solutions near the parent and a small one creates more offspring around the parent for children solutions (recommended values of 20 and 20)

After many simulations to understand the impact of each one of these parameters, the recommended values were kept as they seemed to perform better for a given number of iterations.

Computation time and complexity The number of iterations in Wallacei is defined both by the number of generations and the generation size. It was observed in the simulations that the results were exactly the same when the total number of iterations was the same and when the recommended parameters were chosen. For example, a simulation of 30 generations with 30 individuals (30x30=900 iterations) was giving the same results as a simulation of 15 generations with 60 individuals (15x60=900 iterations).
The higher the number of iterations, the more optimal the result. Still having too many iterations leads to longer computation time. Thus, simulations were performed to identify the number of iterations leading to accurate results with the least computation time. It was found that 600 iterations were enough in most cases.

The computation time varied from one typology to the other. The PBPA algorithm is quite fast with simulations during approximately 3 minutes.
For reinforced concrete typologies, it was longer because to find the appropriate reinforcement layout, a sort and a search in the table of all possibilities of reinforcement layouts was performed which is time-consuming. This led to simulations of approximately 30 minutes. For steel and timber typologies, it was quicker with simulations lasting approximately 5mins.

NSGA II in Pymoo As said previously in the report, not only Rhino has been used for the simulations but also Python with the Pymoo library. The Pymoo library enables optimizations to be performed using (among others) genetic algorithms such as NSGA II. The main advantage of using Pymoo is that it is much faster. In fact, even for simulations requiring a considerable number of calculations such as the ones for reinforced concrete solutions, the simulations were not lasting more than 3 minutes.
The same algorithm parameters as the ones from Wallacei can also be chosen by the user. It was chosen to keep the parameters that were by default in Wallacei so as to proceed to similar simulations. The results obtained via the two different methods were in fact very similar.

4.2 Sensitivity analysis

As detailed in the LCA part of this report, different scenarios have been considered to see the influence of the LCA hypotheses on the final results.
For each typology, four comparisons between LCA scenarios were carried out:

- Building scenario (Span=8m):
  - Optimization of the Human Health (HH) impact indicator
  - Optimization of the Ecosystem Quality (EQ) impact indicator
- Bridge scenario (Span=20m):
  - Optimization of the Human Health (HH) impact indicator
  - Optimization of the Ecosystem Quality (EQ) impact indicator

The two spans were chosen based on the most common spans in buildings and bridges according to the experience of ISC employees. The choice of optimizing according to the two endpoint indicators of Impact World + is based on the fact that endpoint indicators account for the impacts of all midpoint indicators based on their importance in damage to human health and ecosystem quality. Still, as the Global Warming Potential indicator (in $kgCO_{2,eq}$) is the most commonly used impact, it was given as information for all of the optimizations.

4.2.1 PBPA beams

As a recall, the different LCA scenarios for PBPAs are the following:

- Use of Conventional or Low-Carbon concrete
- Prestressing steel coming from Italy or the Netherlands
- Reinforcing steel made of 44% or 100% of scrap steel

The results of the sensitivity analysis on these parameters are shown in Figures 22 and 23.

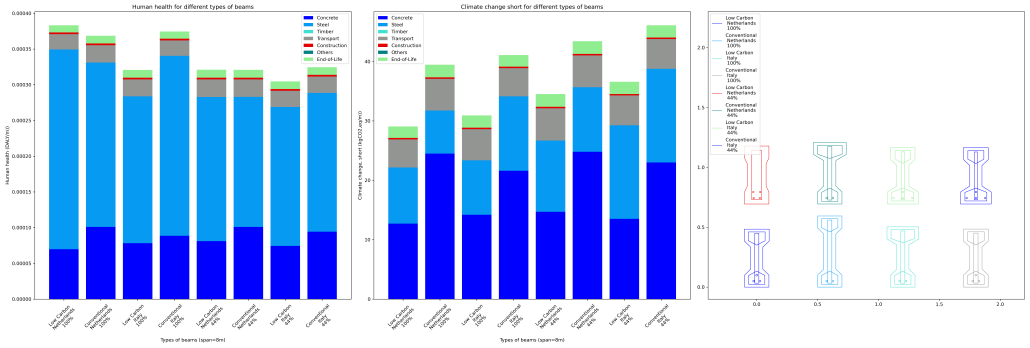

(a) Span 8m - Human Health Optimization

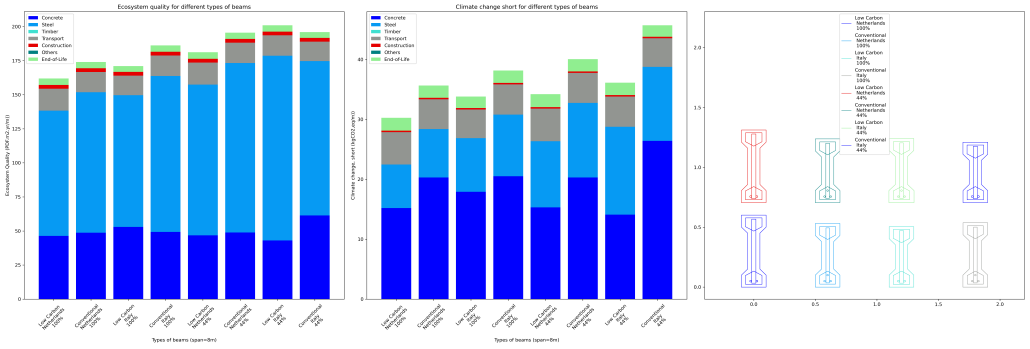

(b) Span 8m - Ecosystem Quality Optimization

Figure 22: Sensitivity Analysis of PBPAs - Span 8m

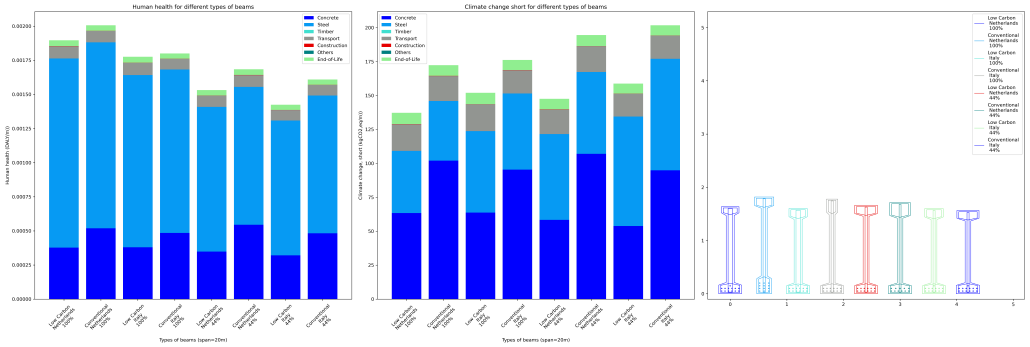

(a) Span 20m - Human Health Optimization

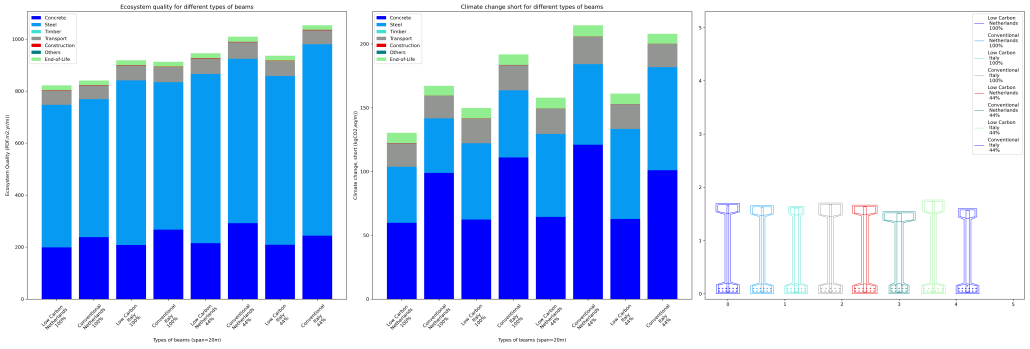

(b) Span 20m - Ecosystem Quality Optimization

Figure 23: Sensitivity Analysis of PBPAs - Span 20m

The first analysis that can be performed in regard to the results is that optimizing the HH or EQ indicator does not lead to the same results. In fact, the best case scenario for Human Health is when using low-carbon concrete with reinforcing steel coming at 44% from secondary steel and prestressing steel from Italy. On the contrary, for EQ the best scenario is when using low-carbon concrete with reinforcing steel coming entirely from secondary steel and with prestressing steel from the Netherlands. EQ follows the same logic in terms of best-case and worst-case scenarios as the Climate Change Short (CCS) impact indicator. Low-carbon concrete is better than conventional concrete for both indicators, but for steel, the manufacture of steel from scrap is worse in terms of human health compared to the production with primary steel. It is the opposite for EQ and CCS impact indicators.
Thus, depending on the scenario, optimizing with the HH or the EQ impact indicator does not lead to the same geometry of the beam.
For example, when considering a scenario with conventional concrete, prestressing steel from Italy, and reinforcing steel made of 44% scrap, optimizing HH will lead to a typology with more prestressing and reinforcing steel and less concrete than the optimal beam relative to the EQ indicator.
Still, this effect is not as visible as it would have been expected. In fact, in Ecoinvent steel is considered not to degrade in soils and water. So, its impact is very high for both human health and ecosystem quality as some part of it is landfilled. This leads to geometries with only a few rebars and a large amount of concrete. If the indicator that is optimized is climate change, the results would be different as the fact that steel does not degrade is not taken into account for CO_2 emissions. The effect of using more concrete than steel when using low-carbon concrete instead of conventional concrete for a given steel would then be more visible. These considerations also apply to reinforced concrete beams.

Furthermore, what is interesting is that when going from conventional to low-carbon concrete, the optimal beam tends to use less steel and more concrete, because the gain in environmental impact is greater when reducing as much as possible the amount of steel. This is why, all other parameters equal, low-carbon concrete beams tend in general to be higher.
Steel accounts for a very large share of CCS when optimizing the HH impact indicator. Concrete is thus less represented. It is more balanced when optimizing the EQ impact indicator, the share is near the 50-50 ratio for CCS that is common for such beams.

4.2.2 Reinforced concrete rectangular beams

As a recall, the different LCA scenarios for reinforced concrete rectangular beams are the following:

- Use of Conventional or Low-Carbon concrete
- Reinforcing steel made of 44% or 100% of scrap steel
- Beam precast off-site or in-situ

The results of the sensitivity analysis for this type of beam are shown in Figures 24 and 25.

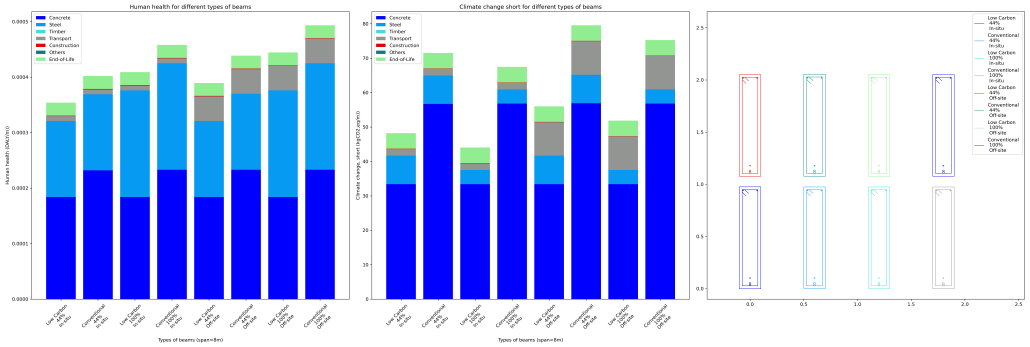

(a) Span 8m - Human Health Optimization

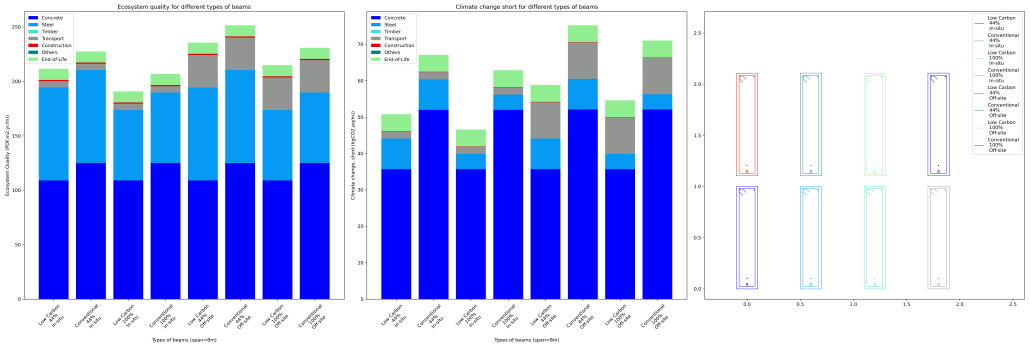

(b) Span 8m - Ecosystem Quality Optimization

Figure 24: Sensitivity Analysis of RC rectangular beams - Span 8m

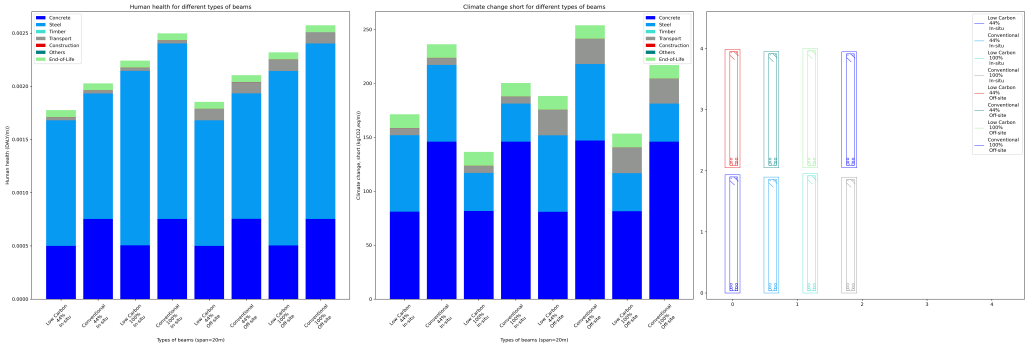

(a) Span 20m - Human Health Optimization

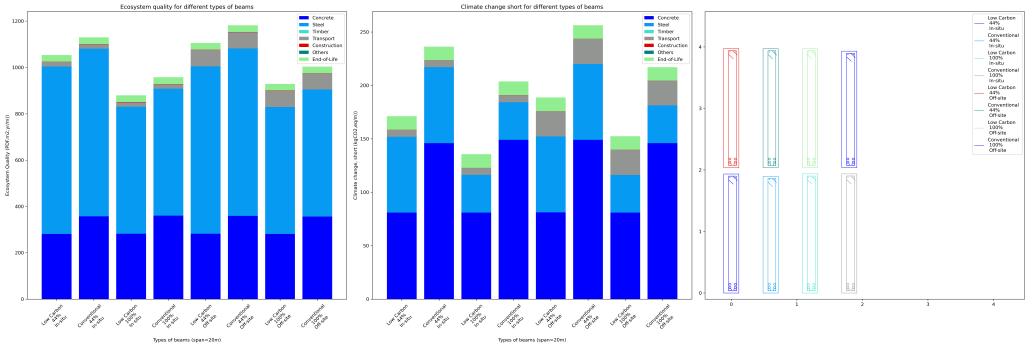

(b) Span 20m - Ecosystem Quality Optimization

Figure 25: Sensitivity Analysis of RC rectangular beams - Span 20m

The results presented above confirm the trends that were identified before for PBPAs. It is interesting to see that the beams coming out of the optimization process tend to be very thin and slender (especially for a span of 20m). In fact, when considering RC beams, the thickness of the beam does not provide much resistance compared to the height of the beam. Still, two-meter-high beams can be a nuisance on the construction site. This fact was not considered in this study but it is very simple to change the boundaries of the geometry parameters in the optimization tool so as to prevent this aspect. For the two spans considered, the minimum thickness of 20cm was selected by the algorithm.
It can also be seen that for HH, building the beam in situ or off-site does not change much the results. It has greater importance for the EQ impact indicator, as manufacturing off-site leads to more impacts due to transport.

4.2.3 Reinforced concrete I-beams

As a recall, the different LCA scenarios for reinforced concrete I-beams are the following:

- Use of Conventional or Low-Carbon concrete
- Reinforcing steel made of 44% or 100% of scrap steel

The beams were assumed to be always precast off-site.
The results of the sensitivity analysis for this type of beam are shown in Figures 26 and 27.

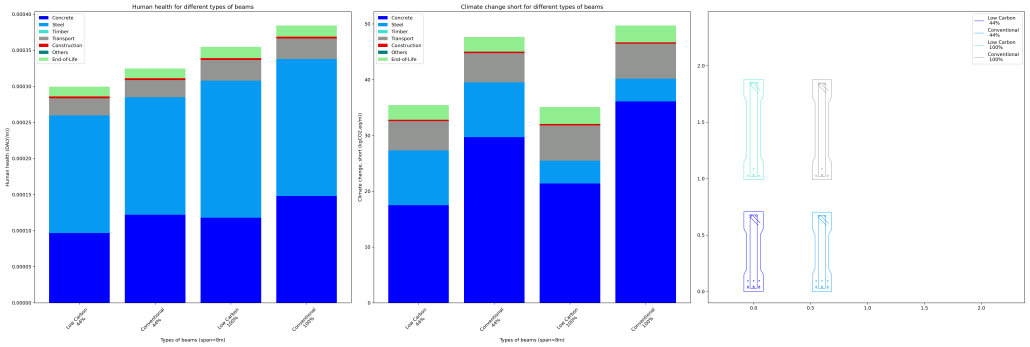

(a) Span 8m - Human Health Optimization

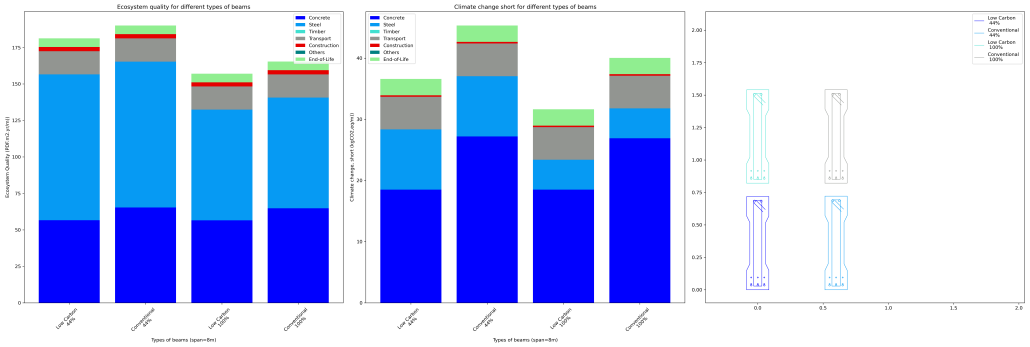

(b) Span 8m - Ecosystem Quality Optimization

Figure 26: Sensitivity Analysis of RC I-beams - Span 8m

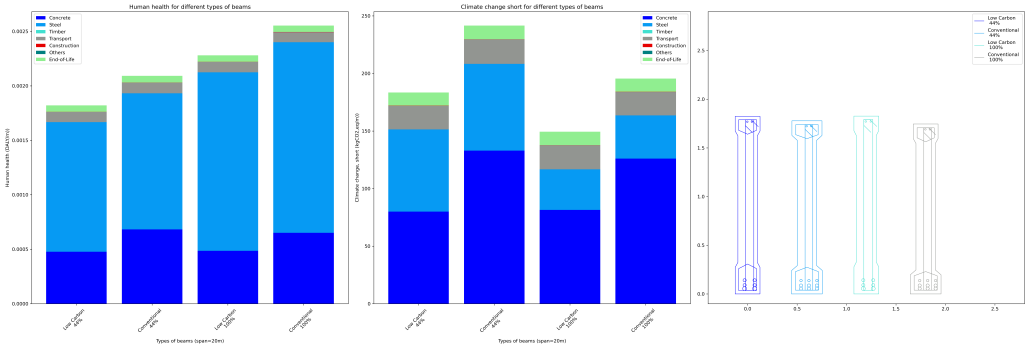

(a) Span 20m - Human Health Optimization

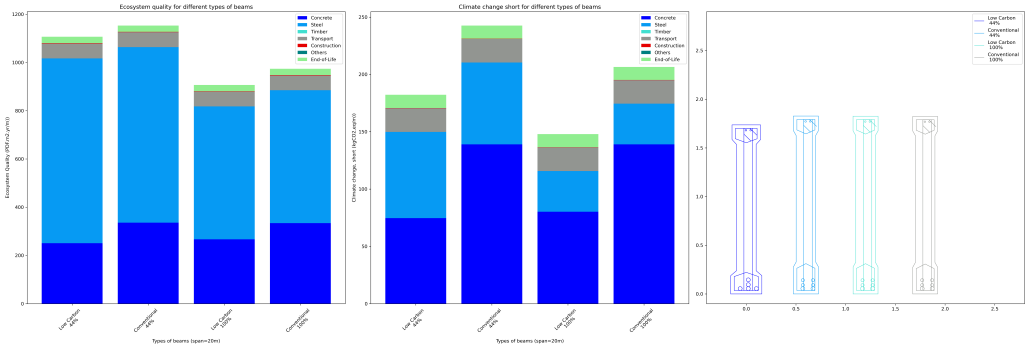

(b) Span 20m - Ecosystem Quality Optimization

Figure 27: Sensitivity Analysis of RC I-beams - Span 20m

As before for PBPAs and RC rectangular beams, the best and worst scenario is different when optimizing HH or EQ. The beams tend to be very slender (the minimum thickness for the web is reached by the algorithm or not very far from it). The end-of-life and transport account for a share that is not negligible when looking at CCS. An order of magnitude of 10% for each is common, and that is what can be observed here.

4.2.4 Optimized reinforced concrete beams

As a recall, the different LCA scenarios for optimized reinforced concrete beams are the following:

- Use of Conventional or Low-Carbon concrete
- Reinforcing steel made of 44% or 100% of scrap steel
- Manufacture in-situ or off-site

The beams were assumed to be always precast off-site.
The results of the sensitivity analysis for this type of beam are shown in Figures 28 and 29.

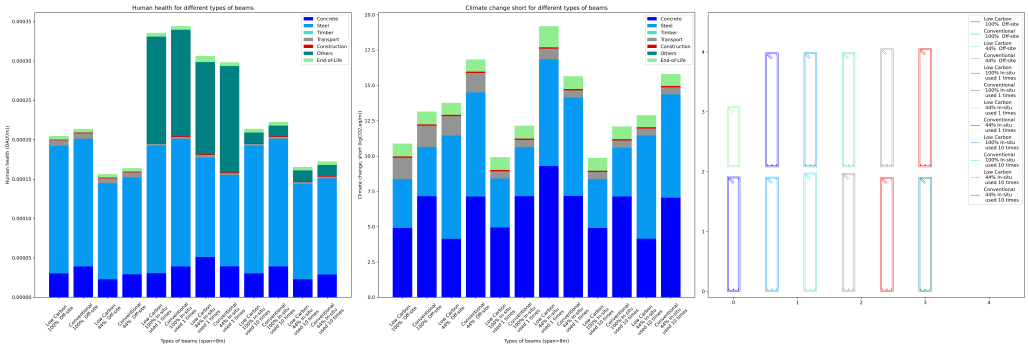

(a) Span 8m - Human Health Optimization

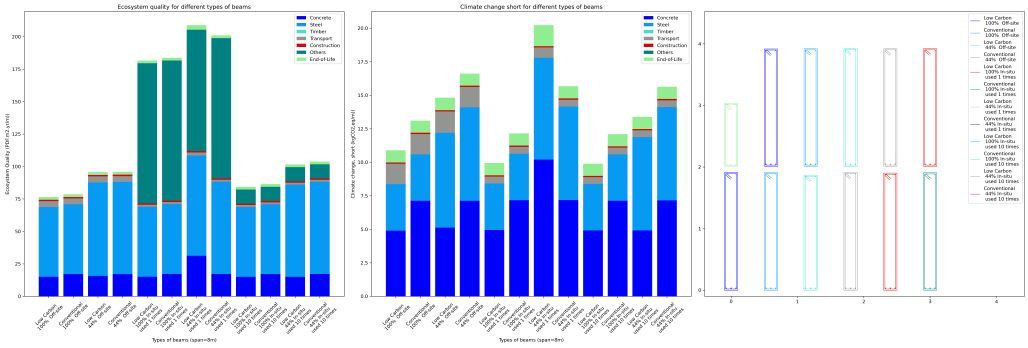

(b) Span 8m - Ecosystem Quality Optimization

Figure 28: Sensitivity Analysis of optimized RC beams - Span 8m

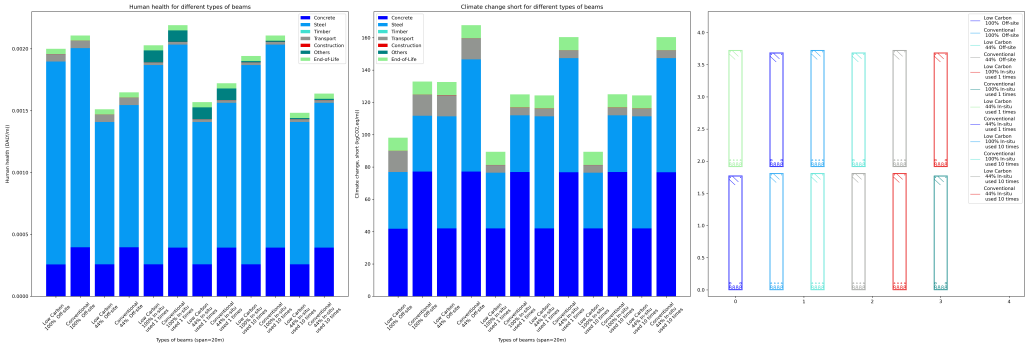

(a) Span 20m - Human Health Optimization

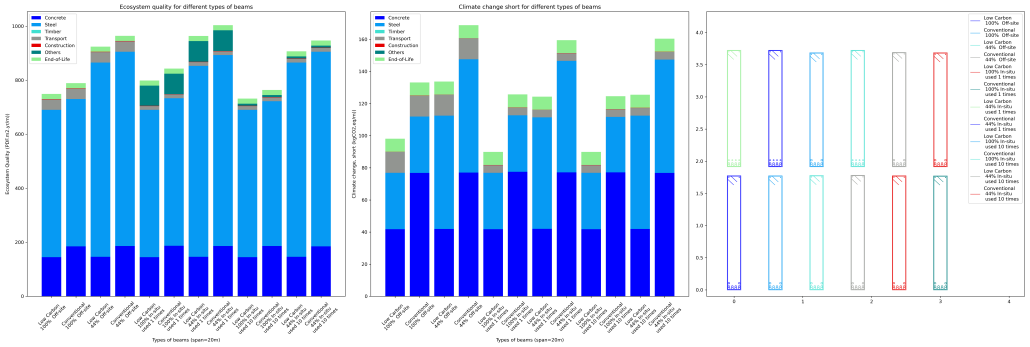

(b) Span 20m - Ecosystem Quality Optimization

Figure 29: Sensitivity Analysis of optimized RC beams - Span 20m

One feature of these results is immediately obvious concerning the "Others" category which stands for the timber formworks used to create the holes inside the beam when the beam is precast on site. For small beams such as the ones with a span of 8m, this impact can be really high due to the low rate of re-use of the formworks and the high density of holes inside the beam. This impact is more hidden by the ones of steel and concrete when considering higher spans.
It is interesting to notice that even for small spans the algorithm tends to choose beams that are very slender. In fact, this is not as for conventional reinforced concrete beams where the matter is everywhere inside the beam, here the sizes of the holes in the beam depend on its geometry. Thus it seems that increasing significantly the height of the beam tends to minimize the amount of concrete while avoiding reinforcing bars via the inertia that is also high.

Even if the sections look similar for an 8 or 20m span beam, it has to be kept in mind that the holes in the beam will be smaller when the span increases at the same time as the loads.
It can also be noticed that one beam for the 8m span is completely different compared to the others. This can be due to the fact that with the holes, two solutions very different in terms of section correspond to similar amounts of concrete and steel.
It can also be seen that for bridge applications (span of 20m), manufacturing the beam off-site or in-situ does not change significantly the results as the fabrication of the formworks used in situ compensates approximately for the additional transport for off-site fabrication.

4.2.5 Timber beams

As a recall, the different LCA scenarios for timber beams are the following:

- Glued laminated (GL24h or GL28h) timber or solid timber (dried at 10 or 20%)
- Ratio of steel connections

The results of the sensitivity analysis for this type of beam are shown in Figures 30 and 31.

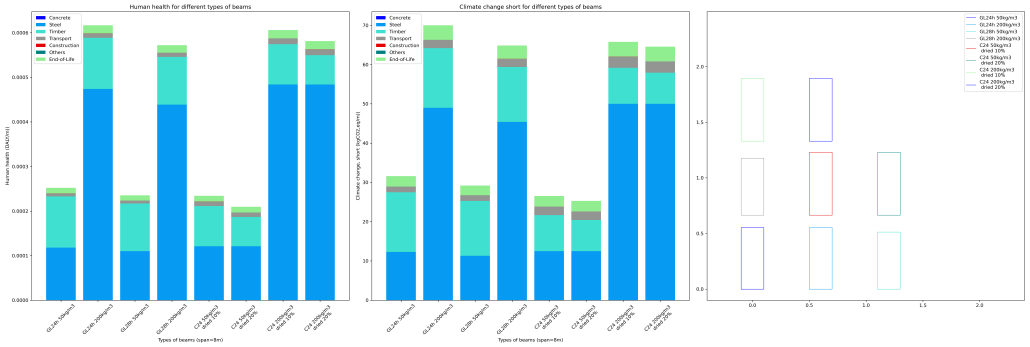

(a) Span 8m - Human Health Optimization

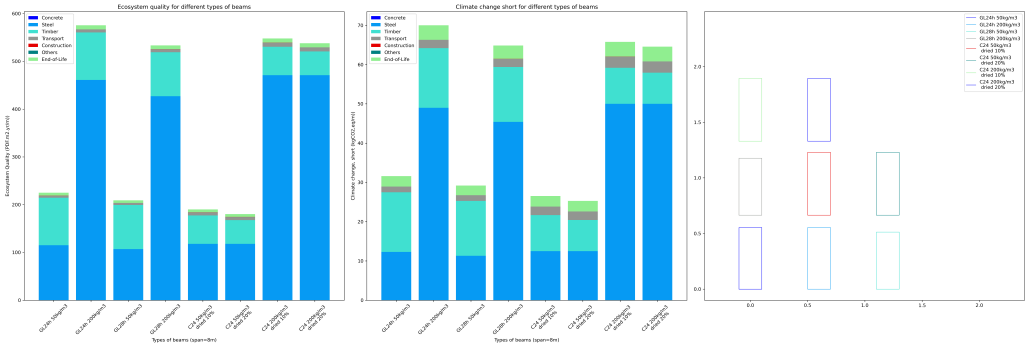

(b) Span 8m - Ecosystem Quality Optimization

Figure 30: Sensitivity Analysis of timber beams - Span 8m

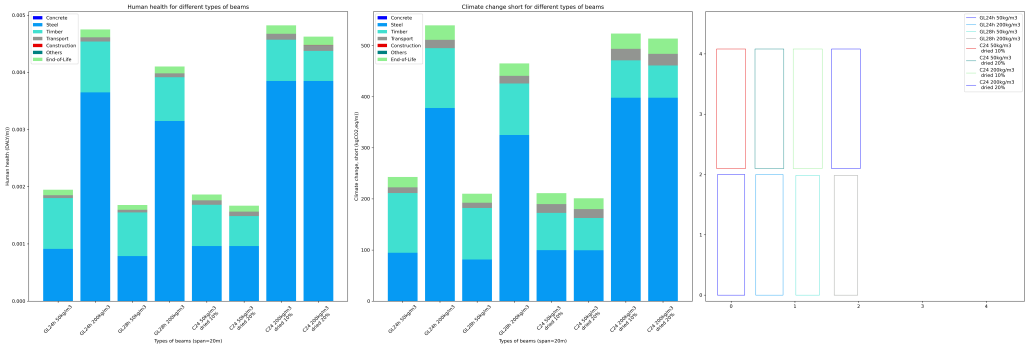

(a) Span 20m - Human Health Optimization

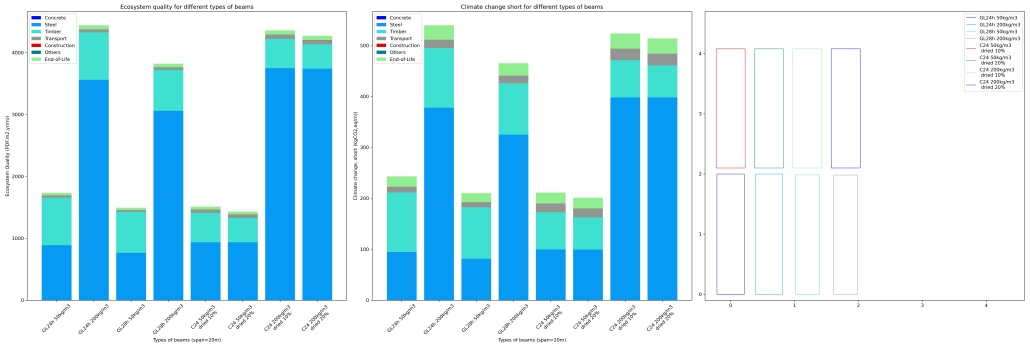

(b) Span 20m - Ecosystem Quality Optimization

Figure 31: Sensitivity Analysis of timber beams - Span 20m

First, compared to the beams described above, timber is not a composite material, thus optimizing for HH or EQ leads to exactly the same sections, the objective being in fact to minimize the entire volume of timber. This is why the graphs look very similar for both indicators and spans. What can be seen directly is that the majority of the impact of the entire beam is due to the steel connections, and about 75% for a high ratio of connections. Even if the timber has a low impact compared to concrete, the fact that steel connections are used to bind the beams and columns

leads to impacts that are very significant.
Furthermore, it can be seen that going from GL24h to GL28h leads to a smaller section (which makes sense as GL28h has better mechanical performances) but as the same LCA process was considered for both, using GL28 is, of course, less impacting than using GL24h. For both spans, it is clearly visible that the solid timber section is bigger than the GL24h one that is bigger than the GL28h.
The drying percentage of timber has a significant impact on the timber impact (approximately 15-30% for both indicators). Still, in the overall calculations, as steel is also taken into account, it does not influence that much the final results (approximately 2-5% for both indicators).
In this case, it can also be seen that the beams are as slender as possible: for a span of 8m the minimum width was chosen by the algorithm, and for a span of 20m, the minimum width for a maximum height of 2m was chosen.

4.2.6 Steel beams

As a recall, the different LCA scenarios for steel beams are the following:

- Percentage of scrap steel used for manufacturing the steel beam (70 or 100%)
- Ratio of connections used for bridge applications (5 or 15%)

The results of the sensitivity analysis for this type of beam are shown in Figures 32 and 33.

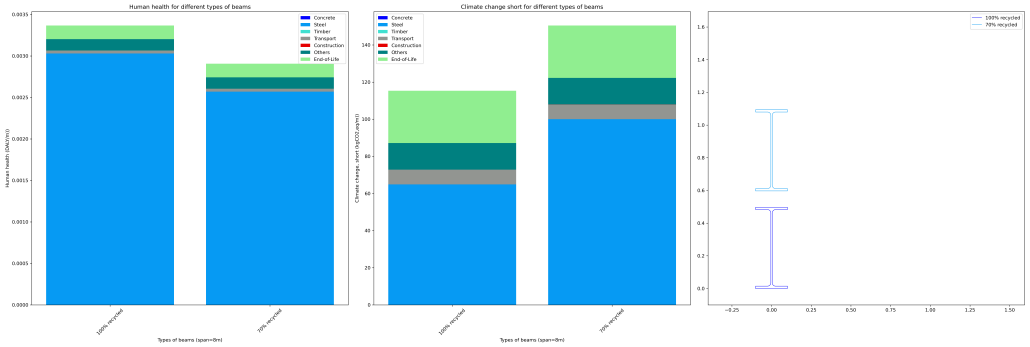

(a) Span 8m - Human Health Optimization

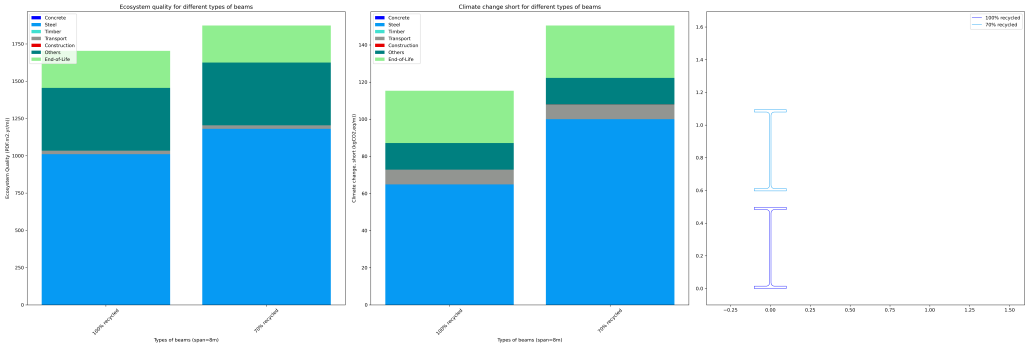

(b) Span 8m - Ecosystem Quality Optimization

Figure 32: Sensitivity Analysis of steel beams - Span 8m

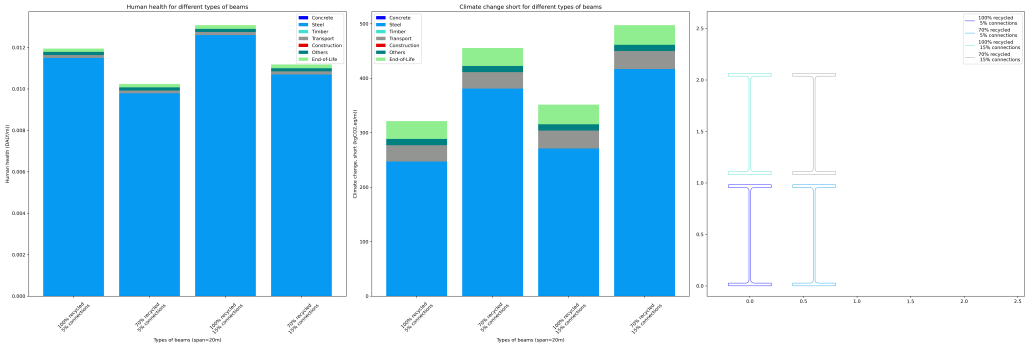

(a) Span 20m - Human Health Optimization

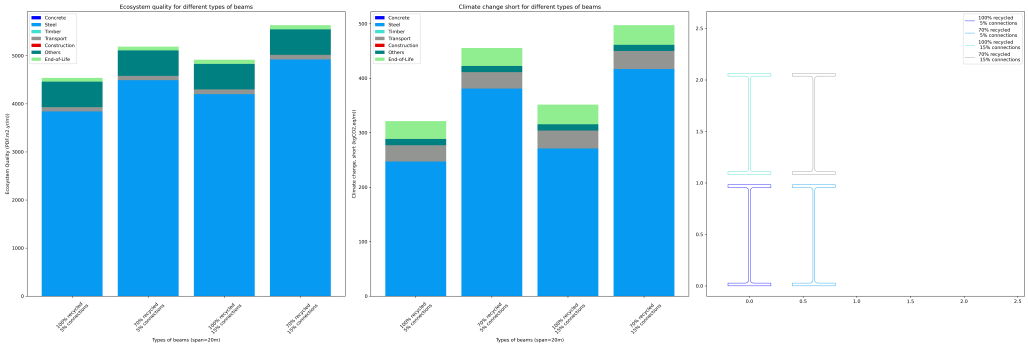

(b) Span 20m - Ecosystem Quality Optimization

Figure 33: Sensitivity Analysis of steel beams - Span 20m

As for prestressing and reinforcing steel, steel beams do not perform similarly for the two end-point indicators depending on the percentage of scrap used for manufacturing the steel. Secondary steel is better for EQ but not for HH. Still, in all cases the goal of the algorithm is to reduce as much as possible the steel's volume, thus it leads to the same profiles to optimize either with the HH or EQ impact indicators or for the different LCA scenarios.
As the same type of steel was used for both the steel beam and the connectors, increasing the ratio of the connections by 10% leads to an increase of the global impact of 10%.

4.2.7 Conclusion on the sensibility analysis

What can be seen with the sensitivity analysis performed before is that, depending on the material and typology chosen, the results can differ heavily depending on the LCA scenario chosen. Thus, choosing the appropriate LCA hypotheses when using the optimization tool is a mandatory step. If not done properly, the results can be distorted.
For typologies involving steel, the choice of the impact indicator has a large influence on what is chosen as the best scenario. Even if currently, the impact indicator the most used is the climate change one, it has to be kept in mind that this is not the only one and that by choosing only this one, some conclusions could be missed. This is why the multi-criteria approach of LCA is important.

4.3 Comparison of the different typologies

4.3.1 Variation of the results depending on the span

So as to give an idea of how each of the typologies performs environmentally with the span, simulations have been performed for the best-case and worst-case scenarios for the indicators of Human Health and Ecosystem Quality to see the range of results for each typology with the span.

First, the best-case and worst-case scenarios for each of the typologies and for the two indicators have been identified based on the results presented in the section above. They are presented in Table 34. The abbreviations used in the Table stand for:

- LCC: Low-carbon concrete
- CC: Conventional concrete
- 44-70 or 100%: Percentage of recycled steel in the steel mix

- IS: In-situ fabrication
- OS: Off-site fabrication
- It: Prestressing steel production in Italy
- N: Prestressing steel production in the Netherlands
- 1x: Re-use only 1 time of the timber formworks
- dried 10% or 20%: drying percentage of solid wood
- 50-200kg/m^3 amount of steel connections
- 5-15%: ratio of steel connections (for bridge applications, otherwise for buildings it is fixed at 3%)

Typology	Best-Case		Worst-Case	
	HH	EQ	HH	EQ
RC rectangular	LCC 44% IS	LCC 100% IS	CC 100% OS	CC 44% OS
RC I	LCC 44%	LCC 100%	CC 100%	C 44%
RC opt	LCC 44% OS	LCC 100% OS	CC 100% IS 1x	CC 44% IS 1x
PBPA	LCC It 44%	LCC N 100%	CC N 100%	CC It 44%
Timber	ST dried 20% 50kg/m^3	ST dried 20% 50kg/m^3	GL24h 200kg/m^3	GL24h 200kg/m^3
Steel	70% (5%)	100% (5%)	100% (15%)	70% (15%)

Table 34: Best-case and worst-case scenarios for the different impact indicators and typologies

For spans lower than 12m, the load cases are the ones for buildings, and for spans higher than 12m, the loadings are the ones for bridges, thus two different graphs were drawn depending on where a bridge or a building application was considered.

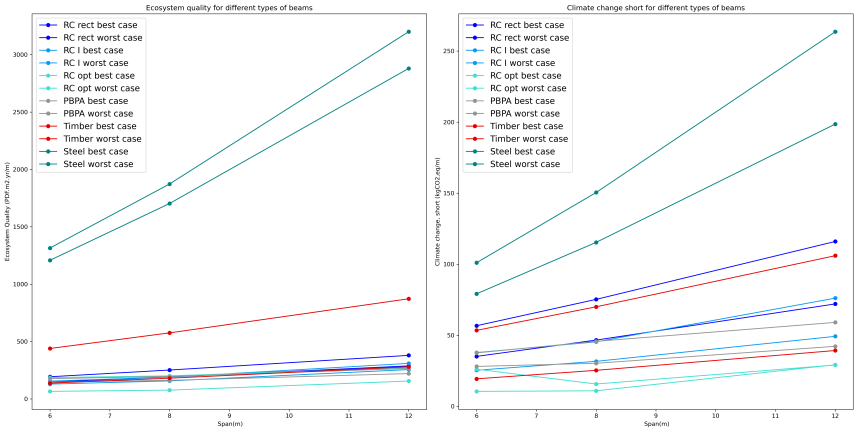

(a) Building scenario - Ecosystem Quality

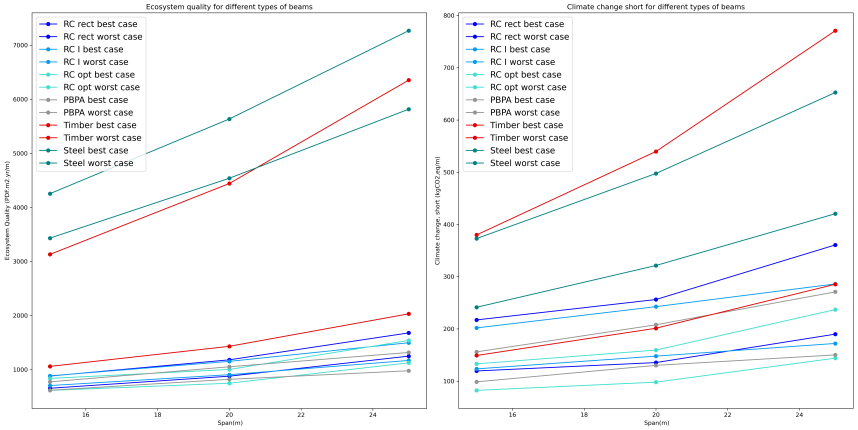

(b) Bridge scenario - Ecosystem Quality

Figure 34: Comparison of beams along the span - Ecosystem Quality

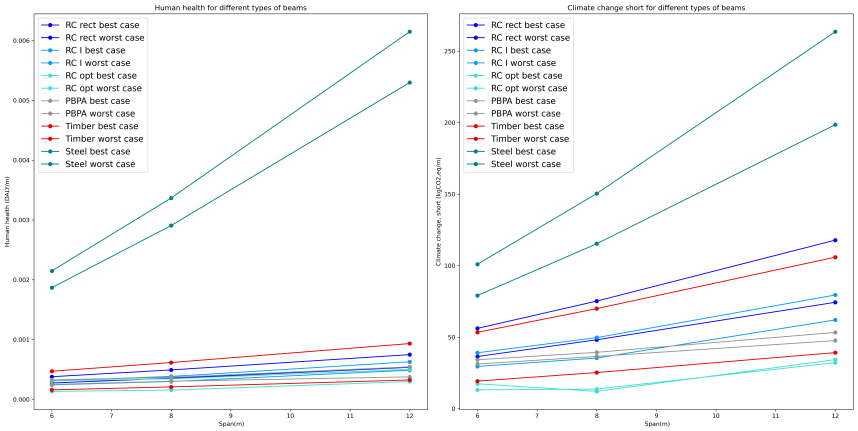

(a) Building scenario - Human Health

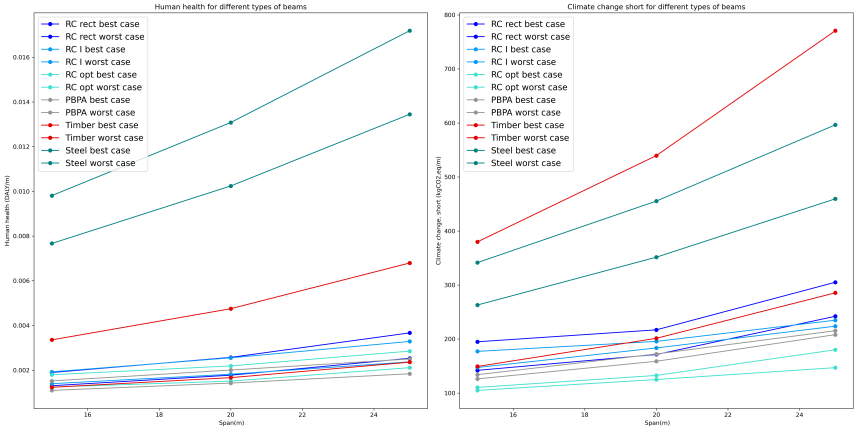

(b) Bridge scenario - Human Health

Figure 35: Comparison of beams along the span - Human Health

The first thing that stands out in the graphs from Figure 34 and 35 is that steel is quite always the worst typology for both HH and EQ (and CSS). In fact, even if the volume of steel is low compared to the volume of concrete used for the same application for RC typologies, its impact is very high for both indicators. The gain in weight with a steel beam does not balance this high impact.
This high impact of steel can also explain the results for timber beams. In fact, as timber is not very resistant, a high volume of it is used especially for bridge applications. Thus, when considering a high ratio of steel connections, it greatly reduces the environmental performance of timber beams. This is why in worst-case applications with a ratio of $200 kg/m^3$ of steel connections, the timber beams can be even worse than the steel beams. For building applications with shorter spans, the conclusion is more balanced as less steel is used and the worst-case timber becomes better than the best-case steel and is more in the range of results of the other typologies.

When comparing the other typologies with one another, it can be seen that the ranking remains quite always the same for both indicators and both applications: RC optimized beams perform better than PBPA beams that perform better than RC I-beams that perform better than RC rectangular beams. Still, as the variability of the results depending on the LCA hypotheses is quite high, choosing the worst-case scenario of the best beam and the best one of the second or third-best beam can change the ranking. As discussed before, timber beams are a good option for building applications in the best-case scenario with a low ratio of steel connections, but for EQ in the bridge scenario, even the best-case LCA scenario does not perform well compared to the other typologies.
Furthermore, it can be seen that for bridge applications, PBPAs can be a very good alternative to RC-optimized beams as their impact is comparable for best-case scenarios for both indicators (even better for some spans). For building applications, their interest is lower.

Another interesting observation is that for all typologies the scaled impacts increase with the span. It means that from the point of view of the beams only, it is better to use more beams of shorter spans than one longer beam. Of course, when considering the entire structure, some additional columns will have to be added that can change the global LCA results if more beams are used instead of one. This observation is understandable, as the maximum bending moment is proportional to the square of the span, which increases the impact measured per meter of the span as the span increases. More material is required to support these loads.

4.3.2 Choice of the optimal beam

To have more details about the results presented before, two fixed spans were considered (8 and 20m), one for building applications and the other for bridge applications. The different impacts are given as a percentage relative to the reinforced concrete rectangular beam impact. The price is also given (as a green line) as information. The price data should be treated with caution as it has been based on averaged data or on only some estimates of costs. For example, the price rockets up for optimized RC beams prefabricated in situ, for which the formworks are used only one time. The formworks' price is in fact really high as it is custom-made and the process is not industrialized.
The comparison is made for the two spans but also for the two indicators studied: HH and EQ (best and worst-case scenarios). The indication of the prices and the one of the climate change short impact are also added. The results are presented in Tables 36, 37, 38 and 39.

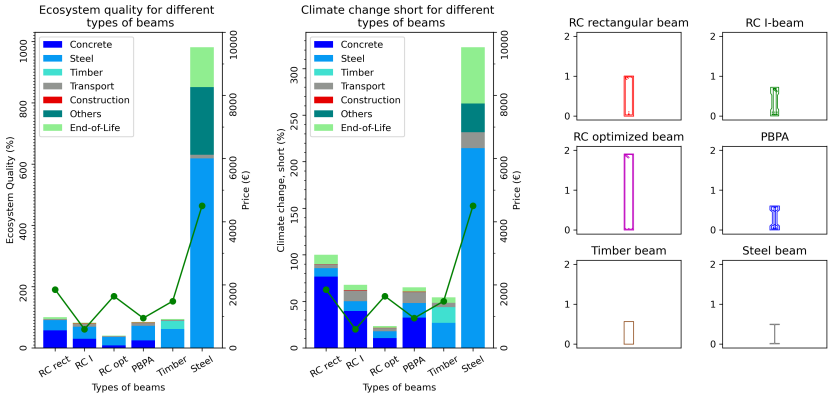

(a) Span 8m - Best-case - Ecosystem Quality

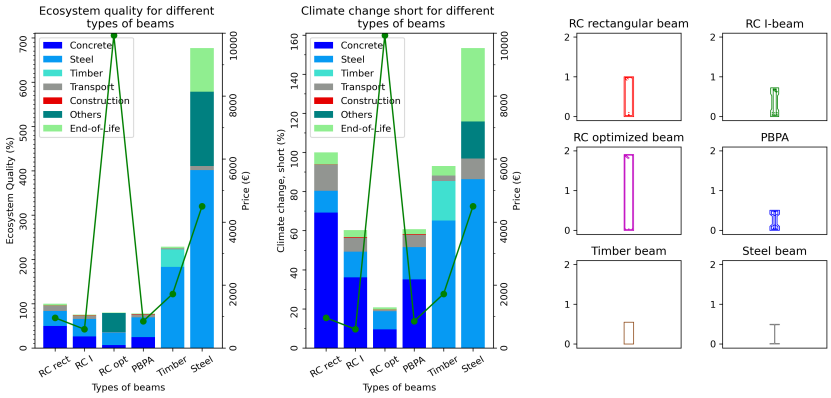

(b) Span 8m - Worst-case - Ecosystem Quality

Figure 36: EQ optimization in best and worst-case for a span of 8m

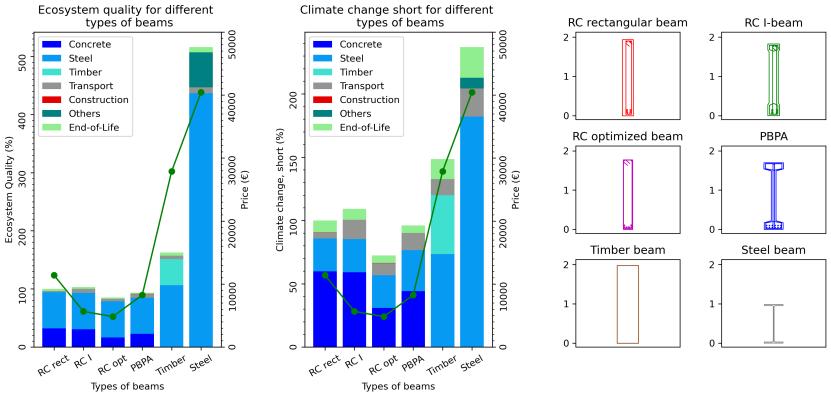

(a) Span 20m - Best-case - Ecosystem Quality

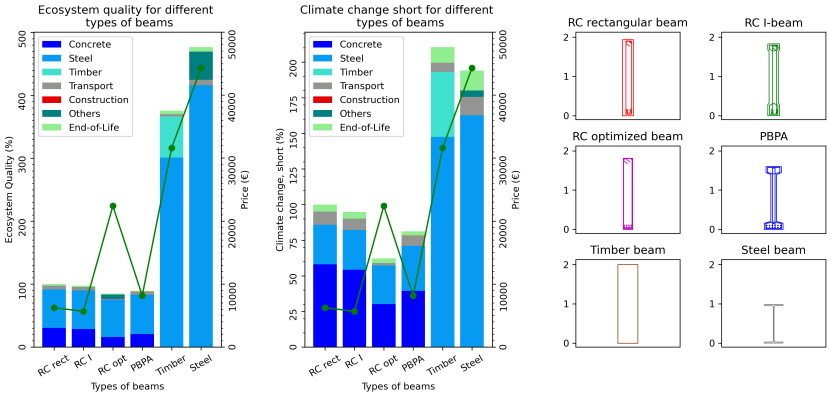

(b) Span 20m - Worst-case - Ecosystem Quality

Figure 37: EQ optimization in best and worst-case for a span of 20m

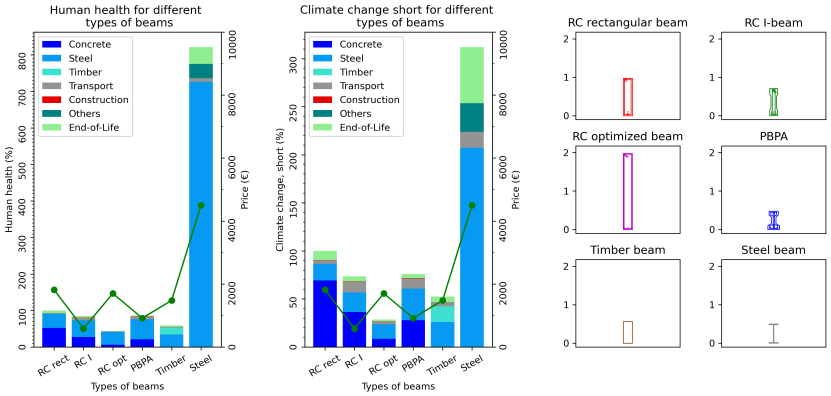

(a) Span 8m - Best-case - Human Health

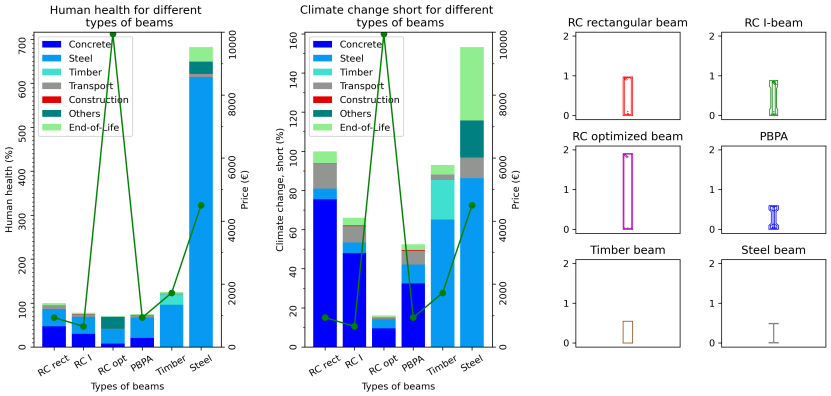

(b) Span 8m - Worst-case - Human Health

Figure 38: HH optimization in best and worst-case for a span of 8m

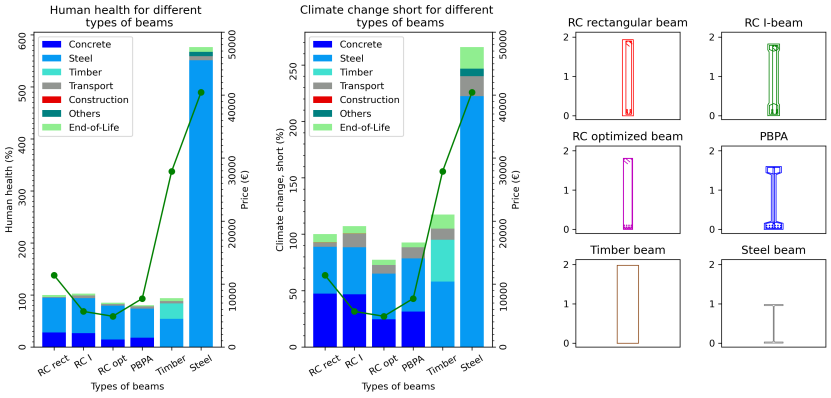

(a) Span 20m - Best-case - Human Health

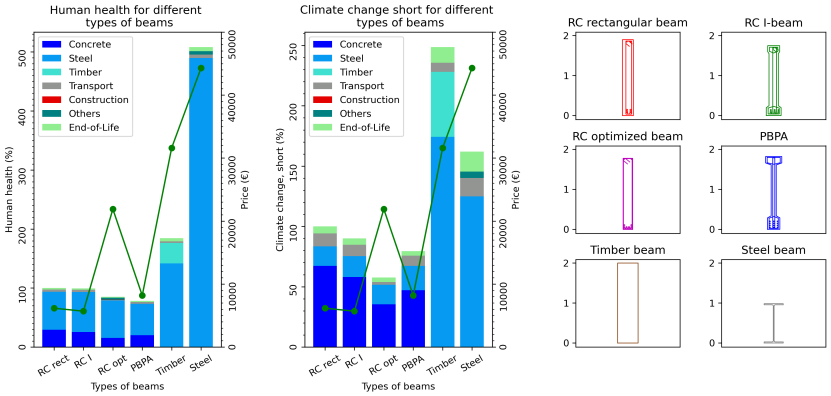

(b) Span 20m - Worst-case - Human Health

Figure 39: HH optimization in best and worst-case for a span of 20m

The conclusions that can be drawn from these graphs are similar to the ones described in the section before.
It can be seen that for all typologies, for both EQ and HH, steel accounts quite always for the major part of the impact, both for best-case and worst-case LCA scenarios. It is very different when looking at the climate change indicator. For short spans and for reinforced concrete or prestressed beams, concrete accounts for the major part. For bridge applications, the ratio becomes more of the order of 50-50 between steel and concrete for EQ and varies between 50-50 and 30-70 for HH. In all cases, it can also be seen here that steel beams are the worst options environmentally and economically (except for a span of 8m when RC-optimized beams prefabricated in situ are very expensive). Timber beams are interesting economically only when a low ratio of connections is used and for a short span.
For all typologies, impact indicators, and scenarios, the on-site installation has an impact that is negligible ("Construction" category in red). The end-of-life participation in the global impact depends significantly on the impact indicator considered. In fact for HH and EQ, the participation is very low but for climate change, it is more of the order of 10%. The results for transport are very similar: not very impacting for HH and EQ but more for the CCS impact indicator.

4.4 Pareto Fronts

When performing multi-objective optimizations, it is useful to know the increase of an objective when reducing the other. The Pareto fronts display allows to observe such information. Pareto front solutions are non-dominated solutions of the optimization, meaning that for these solutions it is not possible to decrease an objective without increasing at least one of the others.
For this study, it was interesting to identify the additional cost of reducing the LCA impact studied. This is why multi-objective optimizations were performed with one objective being the price of the beam and the other the impact indicator studied (HH or EQ). Four different graphs were drawn, all for a rectangular reinforced concrete beam and for all LCA scenarios available for spans of 8 and 20 meters and for the HH or EQ impact indicators. The results are presented in Figures 40,

41 42 and 43. The abbreviations are the same as the table before.

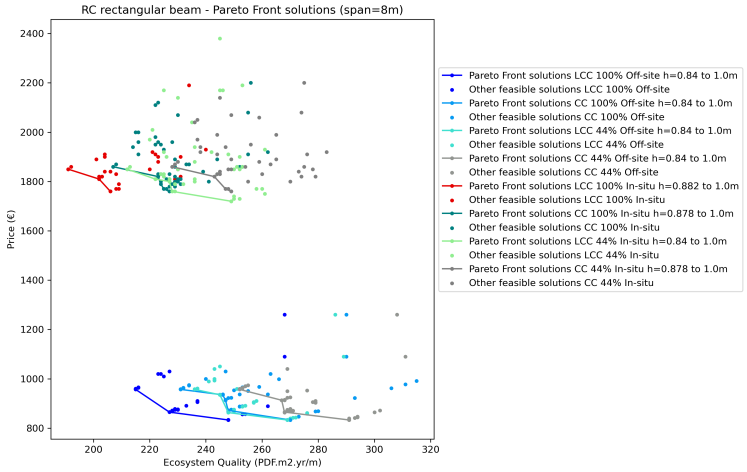

Figure 40: Pareto Front - Span 8m - Ecosystem Quality

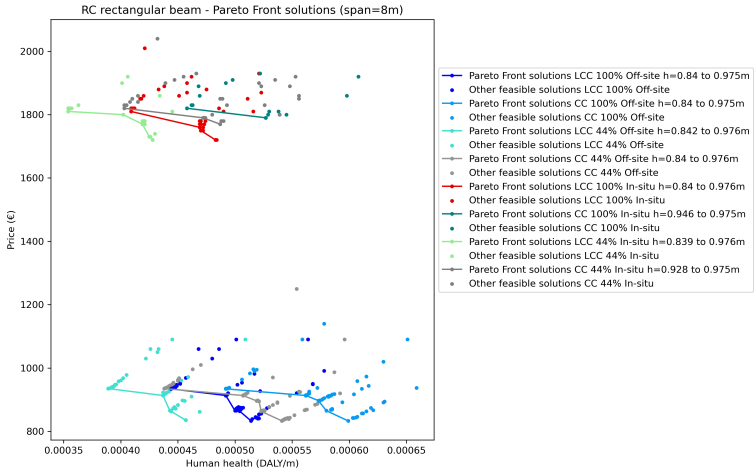

Figure 41: Pareto Front - Span 8m - Human Health

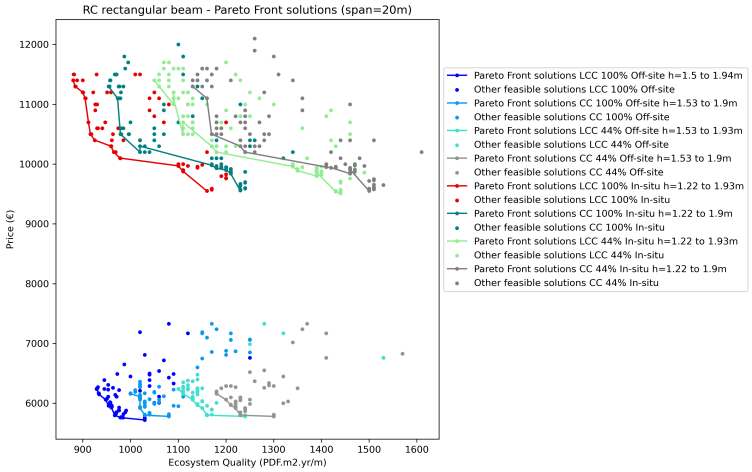

Figure 42: Pareto Front - Span 20m - Ecosystem Quality

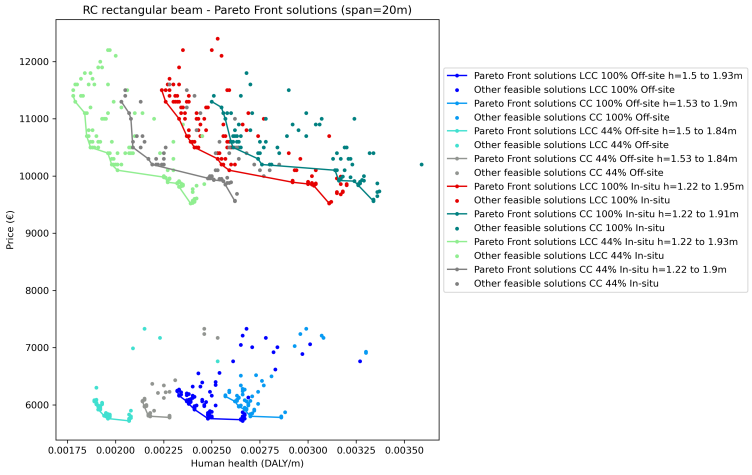

Figure 43: Pareto Front - Span 20m - Human Health

These results highlight the fact that the in-situ fabrication is maybe more expensive but allows the reduction of the impact considered by 10 to 20% for small spans. The interest in producing the beam on-site is smaller for longer spans. It can also be seen that changing the LCA scenario does not change much the shape of the Pareto Front, it only shifts it in the graph space.
It has also been observed that the different points in the Pareto Front correspond to different values of concrete resistance, the higher the price, (and smaller the impact), the lower the resistance. It means that having concrete that is less resistant will decrease, in most scenarios, the impact while increasing the price. It means that the higher impact of a more resistant concrete is not balanced by the amount of concrete saved. For the cost, it is then more interesting to use high-resisting concrete but not for environmental considerations.

4.5 Limitations of the study

The results of this study are based on several assumptions, including those used in the LCA calculations. Those hypotheses are based mainly on averaged data from use cases in France but might not be representative of a specific construction site that will be considered when using the tool. Thus, when using the Optipoutre tool, it is of interest to look more in detail at the hypotheses to make them more in correlation with the use case for which the tool will be used. In particular, it is possible to know, for a given construction site, what will be the transport distances from the different providers, and it will be then possible to change them directly in the tool.

As for this study, no particular construction site was considered, the transport distances values are averaged and might not represent well one particular use case. The results might then differ from the ones that were presented above. In fact, it has been seen in the sensitivity analysis that big differences occur when considering different LCA scenarios for the different typologies of beams.

Price data either come from internal data from the VINCI group that are reliable or from a single estimation of costs that are only representative of a single use case and might not well represent other use cases. For example, for optimized reinforced concrete beams, it has been seen that the price for timber formworks made the price of the entire beam soar. It might not be very representative of reality as the price of the formworks was based on only one estimate of costs made for custom-made formworks with no industrialization process. Thus, prices will have to be changed based on the use case studied. With new projects and more experience, it will also be possible to add more prices in the database to be more representative of the project considered. The prices are based on the French market and are not representative of other markets.

As has been seen in the results presented before, optimized reinforced concrete beams seem to be a good option when trying to reduce the environmental impact of the beams. Still, these beams are optimized at their best, meaning that sometimes even for small spans the best beam in terms of impact is one that is really high and might not be implemented on-site as it requires too much space. Furthermore, the trusses are not reinforced with steel bars as they are in compression and in theory do not require reinforcement. Still, it is not common to consider non-reinforced concrete in a beam, and it is possible that this may not be accepted by the prime contractor. Reinforcing trusses will lead to thicker trusses as a layer of concrete cover is required on each side of the reinforcing bars. For small spans, for which the trusses are thin, the optimized beams might then not be the optimal solution compared for example to timber beams or PBPAs.

This study focuses on isostatic beams and not on the entire structure of the bridge or of the building. It is possible that choosing an isostatic beam instead of a hyperstatic one might lead to increasing the environmental impact somewhere else in the structure. This tool is then limited in its range as it focuses on only one primary element of structures and not on the structure as a whole.

4.6 Perspectives and Future Work

As said before, the first step in improving the developed tool is to take into consideration other constraints that are not just based on the Eurocode theory but also on on-site feasibility and construction site particularities. For example, for short-span beams, it would be possible to limit the height of the beam according to the maximum that can be implemented on-site.
Moreover, to ease the use of the tool, a graphic interface can be as well implemented to make the tool accessible to anyone, especially for engineers of the design office. Currently, the tool is made of several Python scripts that work well independently (one for each combination of material/typology). Gathering the different scripts in one and adding an interface to set the inputs of the scripts would be a mandatory step if the tool has to be used by people unfamiliar with Python. The output will be one graph comparing each beam typology and giving the dimensions of each with additional information (reinforcement layout for example).

Furthermore, this study is the first step in a more global approach to optimizing structures as a whole. First, this tool could be derived for other structural elements such as columns, slabs, and walls. Then the objective would be to couple those elementary tools with other tools to build an algorithm able for example to compare different types of grids for a given building in order to optimize the global footprint of the building including beams, columns, slabs, foundations, etc. A tool for grid optimization has already been developed within ISC and creating a bridge between the two (or more to come) algorithms is a way of improving significantly the environmental performances of structures.

Conclusion

The construction sector is one with the highest emissions in the world. In the current global context of climate change, it is of the utmost importance to reduce the environmental impact of this sector as much as possible. Today's engineers do notnecessarily have the right tools to identify the levers for improvement and make the right choices in environmental terms. The adoption of good practices begins with the identification of these good practices. Optipoutre is an optimization tool capable of finding the right shape for each type of beam and comparing optimal beams with each other to select the best from an environmental point of view. For a simple structural element, it aims to identify the levers for action that can significantly reduce the environmental impact of a beam with a given span and load.

The results showed that there could be a factor of 10 between the best and worst solution for a given case study for the impact indicators of ecosystem quality and human health. If steel beams are set aside, the factor is closer to 2, which is still very significant. Choosing the right beam, therefore, means, for a given structural element, reducing the chosen environmental impact by up to 50%. Even if this reduction is only for beams and is not representative of the entire reduction that is achieved at the scale of a bridge or building, it is still a first step in the process of building better structures.

References

[1] Banu Sizirici, Yohanna Fseha, Chung-Suk Cho, Ibrahim Yildiz, and Young-Ji Byon. A Review of Carbon Footprint Reduction in Construction Industry, from Design to Operation. *Materials*, 14(20):6094, October 2021.

[2] David J M Flower and Jay G Sanjayan. Green house gas emissions due to concrete manufacture. *Green House Gas Emissions*, 2007.

[3] John Orr, Michał P. Drewniok, Ian Walker, Tim Ibell, Alexander Copping, and Stephen Emmitt. Minimising energy in construction: Practitioners' views on material efficiency. *Resources, Conservation and Recycling*, 140:125–136, January 2019.

[4] Lina Bouhaya, Robert Le Roy, and Adélaïde Feraille-Fresnet. Simplified Environmental Study on Innovative Bridge Structure. *Environmental Science & Technology*, 43(6):2066–2071, March 2009.

[5] Johanne Hammervold, Marte Reenaas, Helge Brattebø, and Ph D Student. Environmental Life Cycle Assessment of Bridges.

[6] A. Zeitz, C.T. Griffin, and P. Dusicka. Comparing the embodied carbon and energy of a mass timber structure system to typical steel and concrete alternatives for parking garages. *Energy and Buildings*, 199:126–133, September 2019.

[7] Inkwan Paik and Seunguk Na. Comparison of Environmental Impact of Three Different Slab Systems for Life Cycle Assessment of a Commercial Building in South Korea. *Applied Sciences*, 10(20):7278, October 2020.

[8] José V. Martí, Tatiana García-Segura, and Víctor Yepes. Structural design of precast-prestressed concrete U-beam road bridges based on embodied energy. *Journal of Cleaner Production*, 120:231–240, May 2016.

[9] J. Fernandez-Ceniceros, R. Fernandez-Martinez, E. Fraile-Garcia, and F.J. Martinez-de Pison. Decision support model for one-way floor slab design: A sustainable approach. *Automation in Construction*, 35:460–470, November 2013.

[10] Byung Kwan Oh, Branko Glisic, Seol Ho Lee, Tongjun Cho, and Hyo Seon Park. Comprehensive investigation of embodied carbon emissions, costs, design parameters, and serviceability in optimum green construction of two-way slabs in buildings. *Journal of Cleaner Production*, 222:111–128, June 2019.

[11] Sébastien Maitenaz. Optimisation and Digital Fabrication of Concrete Structures. 2022.

[12] DongHun Yeo and Rene D. Gabbai. Sustainable design of reinforced concrete structures through embodied energy optimization. *Energy and Buildings*, 43(8):2028–2033, August 2011.

[13] G. Habert and N. Roussel. Study of two concrete mix-design strategies to reach carbon mitigation objectives. *Cement and Concrete Composites*, 31(6):397–402, July 2009.

[14] Dane Miller, Jeung-Hwan Doh, and Mitchell Mulvey. Concrete slab comparison and embodied energy optimisation for alternate design and construction techniques. *Construction and Building Materials*, 80:329–338, April 2015.

[15] Rasmus Rempling, Alexandre Mathern, David Tarazona Ramos, and Santiago Luis Fernández. Automatic structural design by a set-based parametric design method. *Automation in Construction*, 108:102936, December 2019.

[16] Olivier Jolliet, Myriam Saadé, and Pierre Crettaz. *Analyse du cycle de vie: comprendre et réaliser un écobilan.* PPUR Presses polytechniques, 2010. Google-Books-ID: g9S55CklsOoC.

[17] Matthias Finkbeiner, Atsushi Inaba, Reginald Tan, Kim Christiansen, and Hans-Jürgen Klüppel. The New International Standards for Life Cycle Assessment: ISO 14040 and ISO 14044. *The International Journal of Life Cycle Assessment*, 11(2):80–85, March 2006.

[18] Thomas Kägi, Fredy Dinkel, Rolf Frischknecht, Sebastien Humbert, Jacob Lindberg, Steven De Mester, Tommie Ponsioen, Serenella Sala, and Urs Walter Schenker. Session "Midpoint, endpoint or single score for decision-making?"—SETAC Europe 25th Annual Meeting, May 5th, 2015. *Int J Life Cycle Assess*, 2016.

[19] European committee for standarsiation . NF EN 15804 - Contribution des ouvrages de construction au développement durable - Déclarations environnementales sur les produits, 2019.

[20] INIES, URL: https://www.inies.fr/inies-et-ses-donnees/fdes-produits-de-construction/.

[21] AFGC. Données d'impact pour les Ouvrages de Génie Civil (DIOGEN), URL : http://www.diogen.fr/.

[22] Ecoinvent, URL: https://ecoinvent.org/.

[23] Ya Hong Dong and S Thomas Ng. Comparing the midpoint and endpoint approaches based on ReCiPe—a study of commercial buildings in Hong Kong. *Int J Life Cycle Assess*, 2014.

[24] M A J Huijbregts, Z J N Steinmann, P M F Elshout, G Stam, F Verones, M D M Vieira, A Hollander, M Zijp, and R van Zelm. ReCiPe 2016 v1.1 A harmonized life cycle impact assessment method at midpoint and endpoint level. 2016.

[25] Cécile Bulle, Manuele Margni, Laure Patouillard, Anne-Marie Boulay, Guillaume Bourgault, Vincent De Bruille, Viêt Cao, Michael Hauschild, Andrew Henderson, Sebastien Humbert, Sormeh Kashef-Haghighi, Anna Kounina, Alexis Laurent, Annie Levasseur, Gladys Liard, Ralph K. Rosenbaum, Pierre-Olivier Roy, Shanna Shaked, Peter Fantke, and Olivier Jolliet. IMPACT World+: a globally regionalized life cycle impact assessment method. *The International Journal of Life Cycle Assessment*, 24(9):1653–1674, September 2019.

[26] Koliann Mam. Exploration structurelle et environnementale des ouvrages en bois de grande portée.

[27] Cong Chen. *Une étude des bétons de construction classiques et alternatifs par la méthode d'analyse du cycle de vie*. These de doctorat, Troyes, January 2009.

[28] Philip Van den Heede. Durability and Sustainability of Concrete with High Volumes of Fly Ash, 2014.

[29] Snežana Marinković, Jelena Dragaš, Ivan Ignjatović, and Nikola Tošić. Environmental assessment of green concretes for structural use. *Journal of Cleaner Production*, 154:633–649, June 2017.

[30] DHUP. La Direction de l'Habitat, de l'Urbanisme et des Paysages (DHUP) | immobilier-etat.gouv.fr.

[31] M. Collepardi, S. Collepardi, U. Skarp, and R. Troli. Optimization of Silica Fume, Fly Ash and Amorphous Nano-Silica in Superplasticized High-Performance Concretes, 2004.

[32] G. Habert, J.B. d'Espinose de Lacaillerie, and N. Roussel. An environmental evaluation of geopolymer based concrete production: reviewing current research trends. *Journal of Cleaner Production*, 19(11):1229–1238, July 2011.

[33] Elisabete R. Teixeira, Ricardo Mateus, Aires F. Camões, Luís Bragança, and Fernando G. Branco. Comparative environmental life-cycle analysis of concretes using biomass and coal fly ashes as partial cement replacement material. *Journal of Cleaner Production*, 112:2221–2230, January 2016.

[34] C. Chen, G. Habert, Y. Bouzidi, A. Jullien, and A. Ventura. LCA allocation procedure used as an incitative method for waste recycling: An application to mineral additions in concrete. *Resources, Conservation and Recycling*, 54(12):1231–1240, October 2010.

[35] US Geological Survey. Mineral Commodity Summaries. Technical report, 2021.

[36] Matthias Dreveton. Conception Environnementale Des Structures. MA thesis, 2020.

[37] Henan Superior. Silica fume price per kg, September 2018. Section: Blogs.

[38] Argus, URL: https://www.argusmedia.com/metals-platform/metal/minor-and-specialty-metals-silicon.

[39] ArcelorMittal. Fact Book 2021, 2021.

[40] Selectra. KELWATT, URL: https://www.kelwatt.fr/.

[41] HSA Material. Quel est le prix par tonne de poudre de microsilice?, July 2022.

[42] BORAL. Flyash slides for investors, May 2018.

[43] MineralInfo.

[44] Worldsteel Association. Life cycle inventory study - 2017 data release, 2017.

[45] Per Fidjestøl and Magne Dåstøl. The History of Silica Fume in Concrete- from Novelty to Key Ingredient in High Performance Concrete.

[46] American Concrete Institute. ACI Committee.

[47] Alessandro Arrigoni, Daman K. Panesar, Mel Duhamel, Tamar Opher, Shoshanna Saxe, I. Daniel Posen, and Heather L. MacLean. Life cycle greenhouse gas emissions of concrete containing supplementary cementitious materials: cut-off vs. substitution. *Journal of Cleaner Production*, 263:121465, August 2020.

[48] Patricia Bredy Tuffe. Condesil "Béton...L'addition s'il vous plaît !!" AFGC, 2018.

[49] COMITE NATIONAL ROUTIER. Enquête longue distance - 2021, September 2022.

[50] CTICM. FDES poutrelle en acier utilisée comme élement d'ossature. 2022.

[51] Carbone 4 and Le hub des prescripteurs bas carbone. Brief filière - Béton - Les messages clés.

[52] VINCI. Exegy, solutions béton bas carbone.

[53] Chiappini. Email exchange with Mr Chiappini (Arcelor Mittal), 2021.

[54] Pascal Xicluna. La gestion durable de la forêt publique, une stratégie française, 2018.

[55] Anne Ventura. Conceptual issue of the dynamic GWP indicator and solution. *The International Journal of Life Cycle Assessment*, 2022.

[56] Geoffrey Guest, Francesco Cherubini, and Anders Hammer Stromman. The role of forest residues in the accounting for the global warming potential of bioenergy. *GCB Bioenergy*, 2012.

[57] Guillaume Habert. Conférence AFGC - ACV dynamique - Du bâtiment au stock bâti, 2021.

[58] ArcelorMittal. FDES Structures en acier ArcelorMittal XCarb™ de sources recyclées et renouvelables. 2022.

[59] Bauforumstahl e. V. EPD Bauforumstahl Beams and Profiles. 2018.

[60] Duferdofin. EPD Duferdofin Steel beams and angels. 2019.

[61] Özkan. EPD Özkan Steel Trading Construction steel. 2021.

[62] Siderurgica Balboa. EPD Siderurgica Balboa profiles sections. 2020.

[63] WOST SA. EPD WOST SA Hot rolled Steel Profiles. 2022.

[64] CELSA Barcelona. EPD Steel beams and steel merchant bars (100% renewable electricity).

[65] Julien Anticorrosion and Peintures Maestria. Caractéristiques Techniques EPODUX ZINC 62-208.

[66] CERIB. FDES Poutrelle en béton armé, masse d'acier 2,7 - 4,8 KG. 2021.

[67] CERIB. FDES Poutrelle en béton armé, masse d'acier 2,7 KG. 2021.

[68] PATRICK GUIRAUD. Infociments - La carbonatation, un phénomène naturel bénéfique pour le béton.

[69] FNB. FDES– Elément porteur résineux en bois de France. 2021.

[70] CERIB. FDES - Poutrelle en béton précontraint.

[71] Eurocode 1 - Action sur les structures.

[72] Diego Navarro-Mateu, Mohammed Makki, and Ana Cocho-Bermejo. Urban-Tissue Optimization through Evolutionary Computation. 2018.

[73] Kalyanmoy Deb, Samir Agrawal, Amrit Pratap, and T Meyarivan. A Fast Elitist Non-dominated Sorting Genetic Algorithm for Multi-objective Optimization: NSGA-II. In G. Goos, J. Hartmanis, J. van Leeuwen, Marc Schoenauer, Kalyanmoy Deb, Günther Rudolph, Xin Yao, Evelyne Lutton, Juan Julian Merelo, and Hans-Paul Schwefel, editors, *Parallel Problem Solving from Nature PPSN VI*, volume 1917, pages 849–858. Springer Berlin Heidelberg, Berlin, Heidelberg, 2000. Series Title: Lecture Notes in Computer Science.

[74] Pham Ngo Gia Bao, Tram Loi Quan, Quan Thanh Tho, and Akhil Garg. NSGA II implementation in Python.

[75] Universitat Autnoma de Barcelona UAB. Algorithm for constrained optimization.

[76] K. Deb, A. Pratap, S. Agarwal, and T. Meyarivan. A fast and elitist multiobjective genetic algorithm: NSGA-II. *IEEE Transactions on Evolutionary Computation*, 6(2):182–197, April 2002.

[77] ISC. Poutres PRAD - LGV SEA Tours Bordeaux.

[78] Eurocode 2 Calcul des structures en béton.

[79] CSTB and CERIB. Dimensionnement des éléments en béton précontraint par fils adhérents.

[80] Centre hautes études du béton armé et précontraint . Flexion à l'état limite ulitme, 2005.

[81] Jacqueline Saliba. Cours de Béton armé 2022, Université de Bordeaux.

[82] ArcellorMittal. Profilés et Aciers Marchands.

[83] Maxime Lebastard. Métal é Tech, Le fer savoir du CTICM, Déversement élastique des poutres-consoles, 2021.

[84] CTICM. LTBeam Software Version : 1.0.11.

5 Appendices

5.1 Appendix 1: Concrete mixes

C20/25 for buildings

Conventional Scenario

Ingredient	Amount (kg/m^3)
CEM I 52.5	259
Limestone Filler	40
Blast Furnace Slag	0
Sand	867
Aggregates	910
Water	170
Superfluidifier	3.54

Low-carbon Scenario

Ingredient	Amount (kg/m^3)
CEM I 52.5	137
Limestone Filler	40
Blast Furnace Slag	137
Sand	863
Aggregates	906
Water	170
Superfluidifier	3.61

C25/30 for buildings

Conventional Scenario

Ingredient	Amount (kg/m^3)
CEM I 52.5	275
Limestone Filler	100
Blast Furnace Slag	0
Sand	880
Aggregates	970
Water	178
Superfluidifier	0

Low-carbon Scenario

Ingredient	Amount (kg/m^3)
CEM I 52.5	145
Limestone Filler	100
Blast Furnace Slag	145
Sand	880
Aggregates	970
Water	178
Superfluidifier	0

C30/37 for buildings

Conventional Scenario

Ingredient	Amount (kg/m^3)
CEM I 52.5	300
Limestone Filler	0
Blast Furnace Slag	0
Sand	852
Aggregates	920
Water	170
Superfluidifier	3.79

Low-carbon Scenario

Ingredient	Amount (kg/m^3)
CEM I 52.5	109
Limestone Filler	0
Blast Furnace Slag	221
Sand	858
Aggregates	901
Water	170
Superfluidifier	3.3

C30/37 for bridges

Conventional Scenario

Ingredient	Amount (kg/m^3)
CEM I 52.5	360
Limestone Filler	0
Blast Furnace Slag	0
Sand	840
Aggregates	881
Water	175
Superfluidifier	3

Low-carbon Scenario

Ingredient	Amount (kg/m^3)
CEM I 52.5	126
Limestone Filler	0
Blast Furnace Slag	234
Sand	844
Aggregates	886
Water	175
Superfluidifier	2.88

C35/45 for buildings

Conventional Scenario

Ingredient	Amount (kg/m^3)
CEM I 52.5	320
Limestone Filler	40
Blast Furnace Slag	0
Sand	837
Aggregates	878
Water	170
Superfluidifier	4.52

Low-carbon Scenario

Ingredient	Amount (kg/m^3)
CEM I 52.5	168
Limestone Filler	40
Blast Furnace Slag	168
Sand	837
Aggregates	878
Water	170
Superfluidifier	4.52

C35/45 for bridges

Conventional Scenario

Ingredient	Amount (kg/m^3)
CEM I 52.5	360
Limestone Filler	0
Blast Furnace Slag	0
Sand	840
Aggregates	881
Water	175
Superfluidifier	3

Low-carbon Scenario

Ingredient	Amount (kg/m^3)
CEM I 52.5	126
Limestone Filler	0
Blast Furnace Slag	234
Sand	844
Aggregates	886
Water	175
Superfluidifier	2.88

C40/50 for buildings

Conventional Scenario

Ingredient	Amount (kg/m^3)
CEM I 52.5	350
Limestone Filler	0
Blast Furnace Slag	0
Sand	853
Aggregates	895
Water	165
Superfluidifier	4.33

Low-carbon Scenario

Ingredient	Amount (kg/m^3)
CEM I 52.5	184
Limestone Filler	0
Blast Furnace Slag	184
Sand	848
Aggregates	891
Water	165
Superfluidifier	4.42

C40/50 for bridges

Conventional Scenario

Ingredient	Amount (kg/m^3)
CEM I 52.5	360
Limestone Filler	0
Blast Furnace Slag	0
Sand	845
Aggregates	886
Water	170
Superfluidifier	3.75

Low-carbon Scenario

Ingredient	Amount (kg/m^3)
CEM I 52.5	144
Limestone Filler	0
Blast Furnace Slag	216
Sand	837
Aggregates	904
Water	170
Superfluidifier	3.6

C50/60 for buildings

Conventional Scenario

Ingredient	Amount (kg/m^3)
CEM I 52.5	380
Limestone Filler	30
Blast Furnace Slag	0
Sand	840
Aggregates	955
Water	172
Superfluidifier	0

Low-carbon Scenario

Ingredient	Amount (kg/m^3)
CEM I 52.5	200
Limestone Filler	30
Blast Furnace Slag	200
Sand	840
Aggregates	955
Water	172
Superfluidifier	0

C50/60 for bridges

Conventional Scenario

Ingredient	Amount (kg/m^3)
CEM I 52.5	390
Limestone Filler	0
Blast Furnace Slag	0
Sand	832
Aggregates	904
Water	170
Superfluidifier	3.6

Low-carbon Scenario

Ingredient	Amount (kg/m^3)
CEM I 52.5	156
Limestone Filler	0
Blast Furnace Slag	234
Sand	825
Aggregates	891
Water	170
Superfluidifier	3.51

C60/75 for buildings

Conventional Scenario

Ingredient	Amount (kg/m^3)
CEM I 52.5	437
Limestone Filler	50
Blast Furnace Slag	0
Sand	790
Aggregates	800
Water	175
Superfluidifier	6.5

Low-carbon Scenario

Ingredient	Amount (kg/m^3)
CEM I 52.5	230
Limestone Filler	50
Blast Furnace Slag	230
Sand	790
Aggregates	800
Water	175
Superfluidifier	6.5

C60/75 for bridges

Conventional Scenario

Ingredient	Amount (kg/m^3)
CEM I 52.5	410
Limestone Filler	0
Blast Furnace Slag	0
Sand	816
Aggregates	882
Water	165
Superfluidifier	5.13

Low-carbon Scenario

Ingredient	Amount (kg/m^3)
CEM I 52.5	164
Limestone Filler	0
Blast Furnace Slag	246
Sand	822
Aggregates	888
Water	165
Superfluidifier	4.92

5.2 Appendix 2: LCA scopes for each type of beam

PBPA

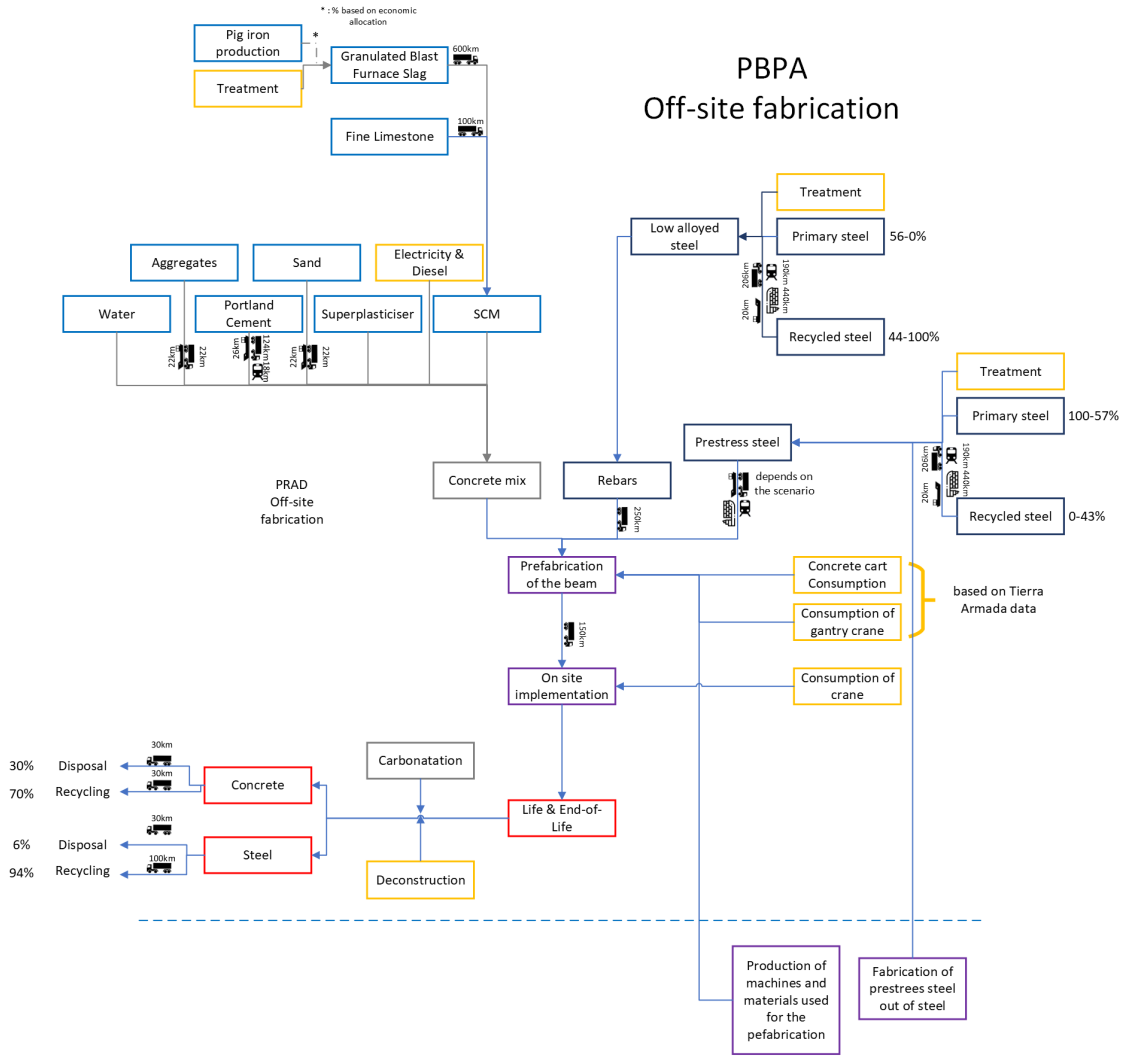

Figure 44: LCA Scope for PBPAs

Reinforced concrete rectangular beams

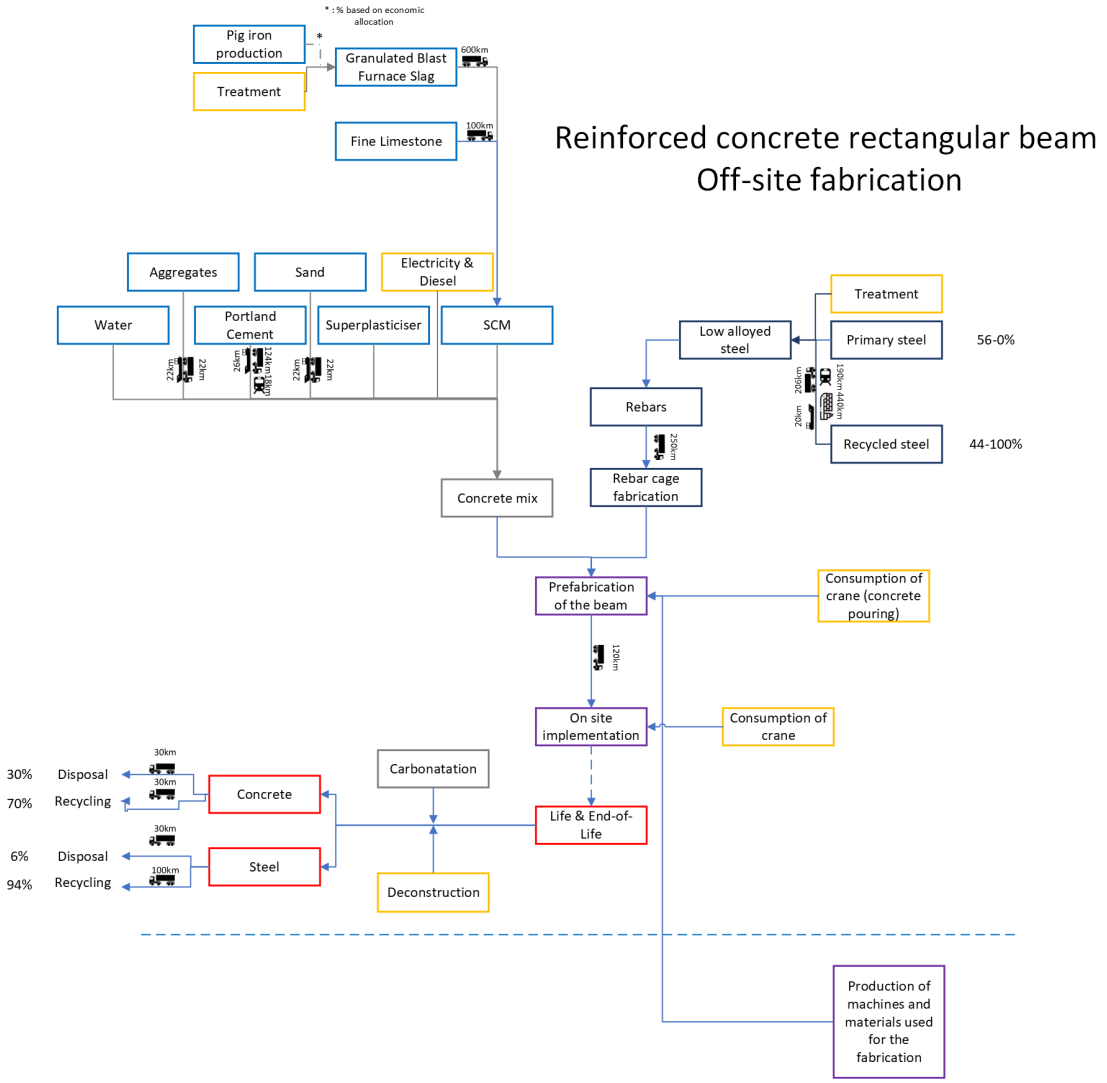

Figure 45: LCA Scope for rectangular reinforced concrete beams built off-site

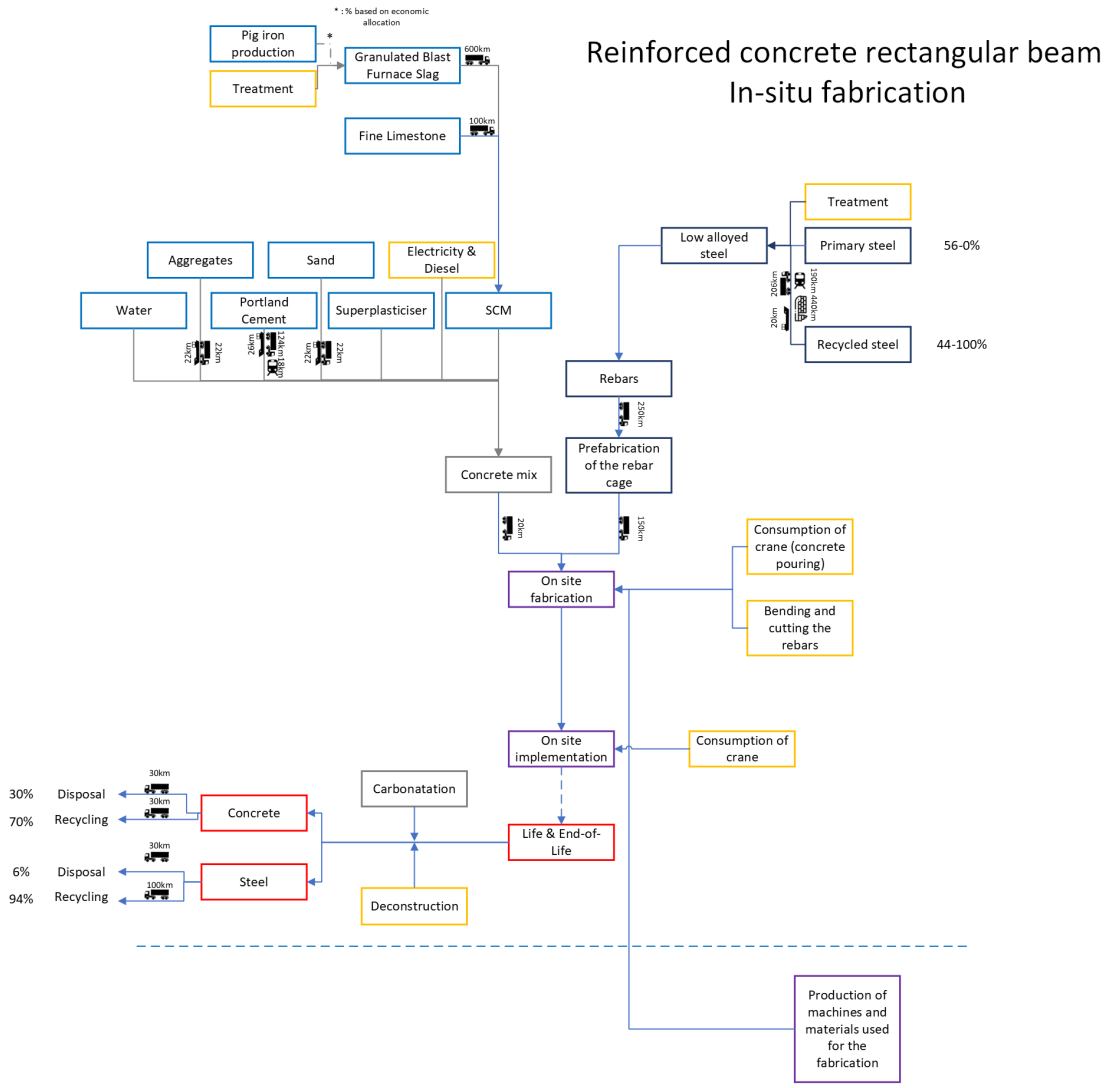

Figure 46: LCA Scope for rectangular reinforced concrete beams built in-situ

Reinforced concrete I-beam

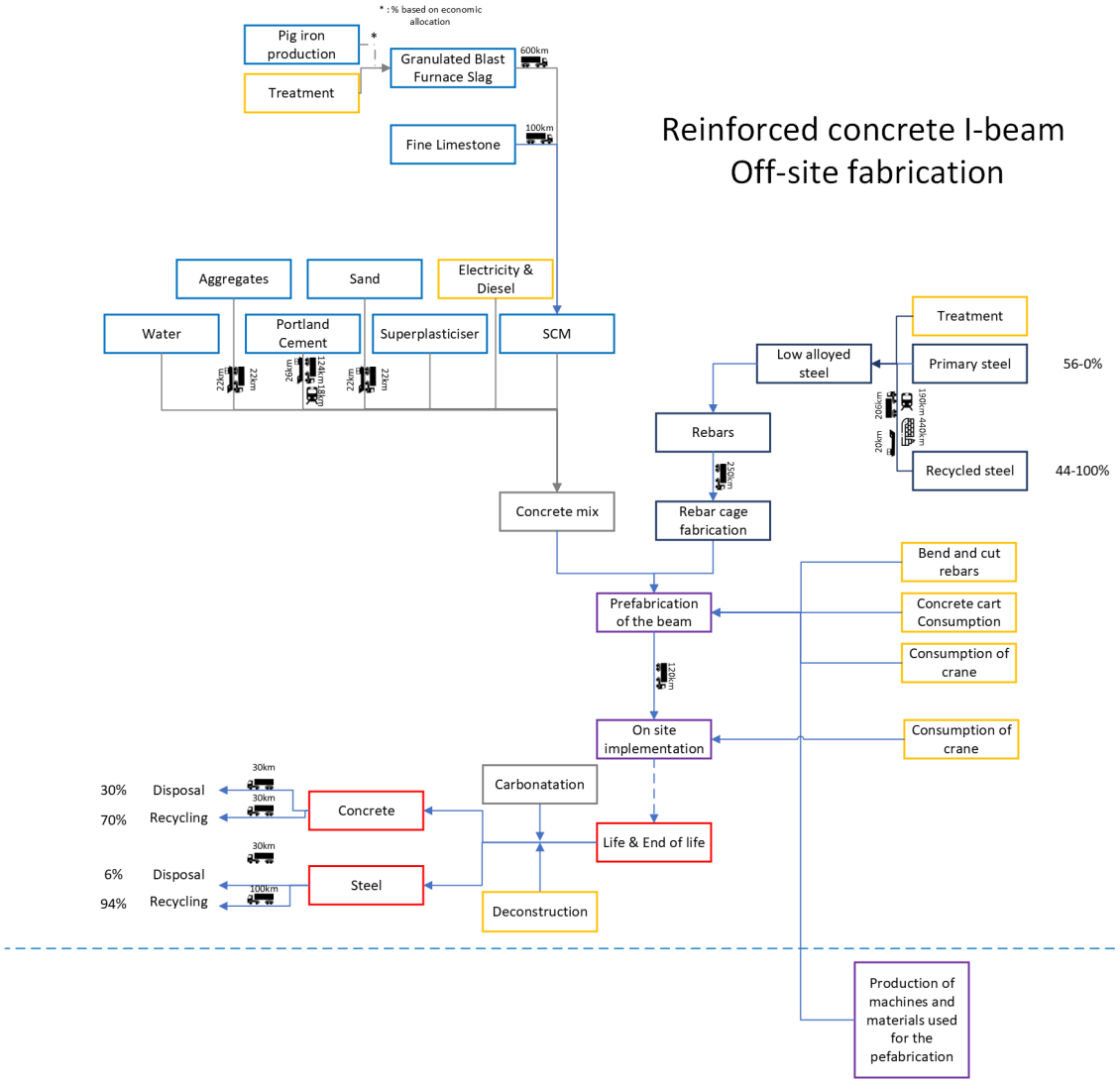

Figure 47: LCA Scope for reinforced concrete I-beams built in-situ

Timber beams

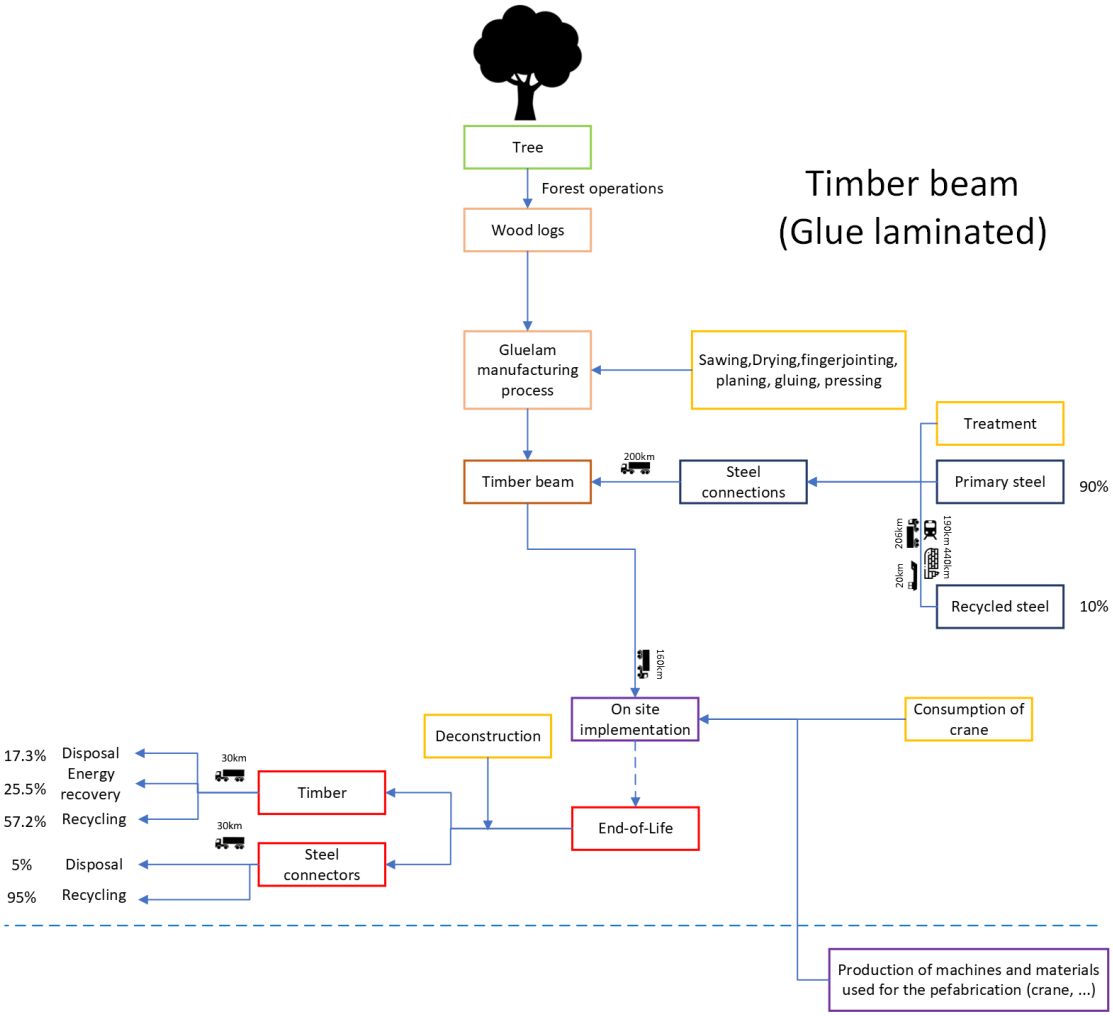

Figure 48: LCA Scope for glued laminated timber beams

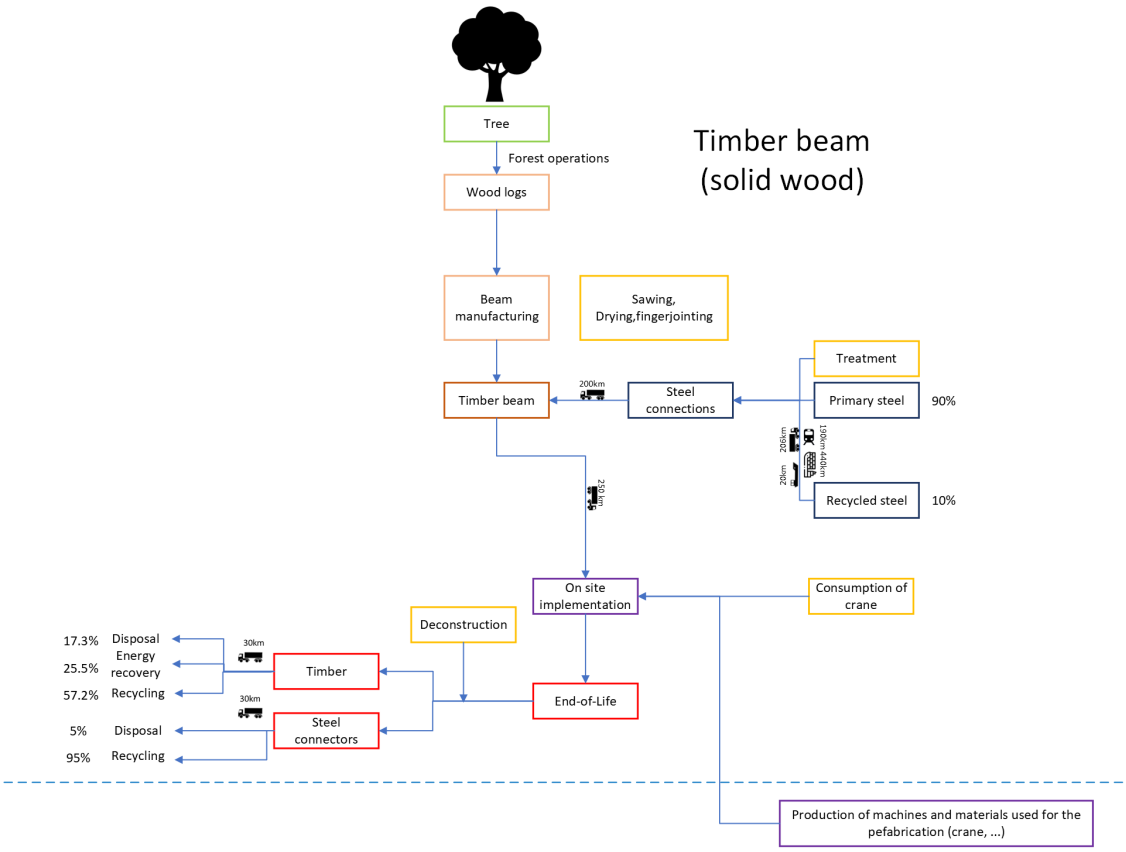

Figure 49: LCA Scope for solid timber beams

Steel beam

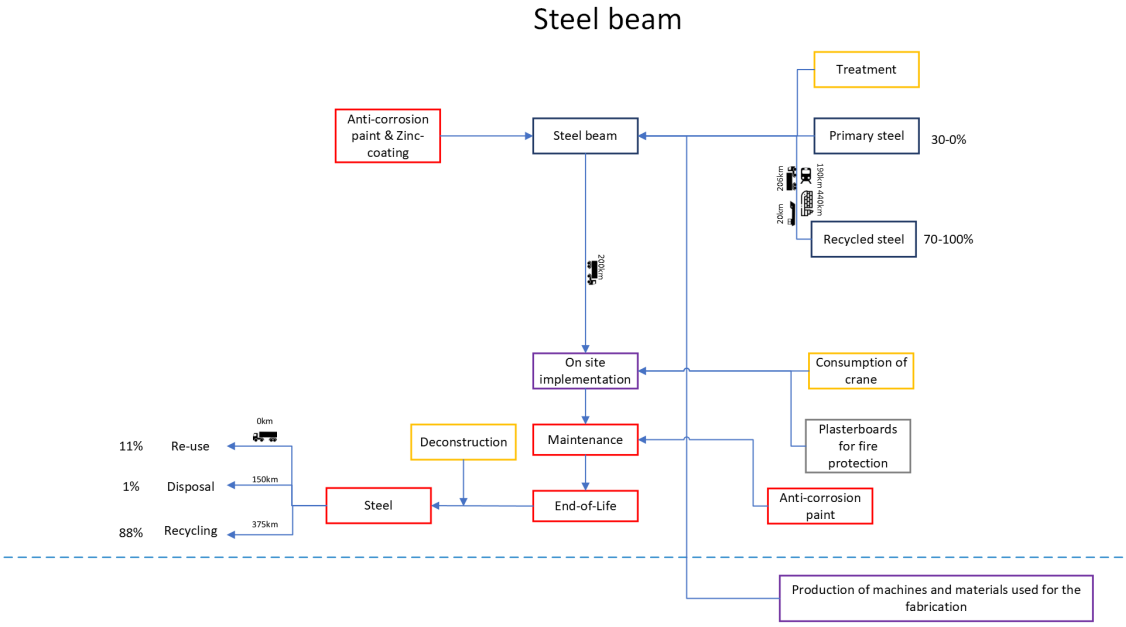

Figure 50: LCA Scope for steel beams

5.3 Appendix 3: Price data

The data common to all beams taking into account the on-site installation is detailed in the table below:

Process	Quantity	Unit	Source
Installation	1	$h/beam$	Unit time catalog
Crane rental	4500	€/month	Solumat
Crane operation time	0.16	$h/beam$	Polyvert
Crane operator time	0.16	$h/beam$	Polyvert
Labor price for building applications	40	€/h	Bateg
Labor price for bridge applications	48	€/h	Vinci

PBPA

In addition to the processes described above, the following are to be added. No data was found concerning the price of steel and concrete for the various existing types (in terms of strength or diameter). A single average value was therefore considered for a use case with C35/45 concrete and T15 strands. Transport is included in the price of concrete and steel.

Process	Quantity	Unit	Source
Concrete price	1034	€/m^3	Matière® estimate of costs
Prestressing steel price	2.62	€/kg	Matière® estimate of costs
Passive steel price	2.88	€/kg	Matière® estimate of costs
Keying	1	$h/beam$	Unit time catalog

Reinforced Concrete beams (rectangular and in I-shape)

For reinforced concrete beams, both the steel and concrete prices come from internal data of Vinci that is confidential. The concrete price depends on the application (building or bridge), on the resistance class, and on the scenario (normal or low-carbon concrete). Regarding steel, the price depends on the diameter of the rebars considered.

The first table described the prices used for the on-site prefabrication and the second one for the external prefabrication.

Process	Quantity	Unit	Source
Concrete prices	-	€/m^3	Vinci catalog
Steel prices	-	€/kg	Vinci catalog
Formworks installation	2	h/m^2	Unit time catalog
Concrete Pouring	1.5	h/m^3	Unit time catalog
Rebars installation	10	h/t	Unit time catalog
Formworks rental L<8m b<0.7m	25	€/month	Solumat
Formworks rental L<8m b>0.7m	27.96	€/month	Solumat
Formwork extension rental 4m b<0.7m	15.4	€/month	Solumat
Formwork extension rental 4m b>0.7m	17.11	€/month	Solumat
Prefabrication time	0.5	day/beam	BATEG
Shoring	1	h/beam	Unit time catalog
Keying	1	h/beam	Unit time catalog
Screed	0.05	h/m of edge	Unit time catalog

Process	Quantity	Unit	Source
Beam concrete purchase (transport included)	490	€/m^3	Vinci project
Beam steel purchase	2	€/kg	Vinci project
Keying	1	h/beam	Unit time catalog

Reinforced Optimized Concrete beams

For optimized beams prefabricated on-site, additional prices corresponding to the formworks and labor for the holes need to be considered.

Process	Quantity	Unit	Source
Timber formworks purchase	28000	€/m^3	Vinci project
Timber formworks transport	24.25	€/m^3/km	Vinci project
Labor for timber formworks installation	0.05	h/hole	Vinci project

No other additional expenses are considered for the external prefabrication scenario.

Steel beams

Steel beams are considered to be delivered with zinc coating and anti-corrosion paint directly. Furthermore, transport is included in the price. For building applications, the price for plasterboards and their installation is added to the calculations, and for bridge applications, the painting price is considered.
It can happen that the price of the beam differs according to the type of profile, but no data has been found for these different types, thus a single value has been considered.
It was also assumed that the price of the connections was the same as the one of the beam itself (in €/kg).

Process	Quantity	Unit	Source
Steel beam purchase	6.5	€/kg	ArcelorMittal estimate of costs
Paint	2.4	€/kg	ArcelorMittal estimate of costs
Plasterboards purchase	5	€/m^2	Vinci expert
Plasterboards installation	15	€/m^2	Vinci expert

Timber beams

The price of timber beams depends on the type of beam that is used. As three types of timber are considered(GL24h, GL28h and solid timber), three different prices are attributed to them.

Process	Quantity	Unit	Source
Solid timber beam purchase	1300	€/m^3_{timber}	Vinci expert
GL24h timber beam purchase	1600	€/m^3_{timber}	Vinci expert
GL28h timber beam purchase	1760	€/m^3_{timber}	Vinci expert
Beam transport	70	€/m^3	Vinci expert
Steel connectors purchase	175	€/m^3_{timber}	Vinci expert